/MODELING AND SIMULATION OF A CONTINUOUS FLUIDIZED-BED DRYER/

by

YIMING CHEN

B.E. ChE. Zhejiang University, Hangzhou, China. 1982

A MASTER'S THESIS

submitted in partial fulfillment of the

requirements for the degree

MASTER OF SCIENCE

Department of Chemical Engineering

KANSAS STATE UNIVERSITY

Manhattan, Kansas

1986

Approved by:

J. S. Lee
Major Professor

L. T. Fan
Co-Major Professor

TABLE OF CONTENTS

 Page

LISTS OF TABLES

LISTS OF FIGURES

Page

CHAPTER II LITERATURE REVIEW

ACKNOWLEGEMENTS

I wish to acknowledge my co-advisers, Dr. F. S. Lai and Dr. L. T. Fan, for their invaluable guidance throughout the course of this work. Their enthusiasm and helpful criticism have been a constant source of inspiration. I also wish to acknowledge the financial support provided by the U.S. Grain Marketing Research Laboratory.

CHAPTER I

INTRODUCTION

Fluidized-bed drying is one of the modern methods for drying. In comparison with the conventional packed-bed or moving-bed dryers, fluidized-bed dryers possess the following significant features:

1. Drying gas is locally mixed intensively during its passage through the bed; consequently, the rate of mass and heat transfer between gas and solids are high.
2. This extremely rapid heat transfer enables relatively high inlet gas temperature to be used.
3. The time of drying is relatively short.

Because of its numerous advantages, fluidized-bed drying has been increasingly applied in diverse industries in either the batch or continuous mode. While batch fluidized bed dryers are often used when the production scale is small or products are heat sensitive, continuous fluidized-bed dryers are extensively used in processes closely integrated with continuous production without intermediate storage. Besides, the cost of drying per unit mass of product is relatively small.

Although the theory of fluidization has developed rapidly in the last two decades, this development is not amply reflected in the study and practice of fluidized-bed drying. Conventional models for a fluidized-bed dryer are mainly based on the overall mass and energy balances around the entire dryer. In addition to these mass and energy balances, the models for a continuous fluidized-bed dryer commonly impose assumptions that

1. The bed temperature is uniform.
2. The outlet streams are in thermal and concentration equilibrium.

3. The fluid-mechanistic behavior of the drying gas is homogeneous; in other words, the drying gas is not partitioned into different phases of the fluidized bed, such as emulsion and bubble phases.

Hence, all these models involve postulates which are not adequately representative of the complicated phenomena occuring in a fluidized bed dryer. This inevitably limits their range of applicability.

The overall objective of this work is to derive a fairly rigorous mechanistic model for a continuous fluidized-bed dryer based on the information generated through an extensive and critical review of the available literature on this and the related subjects. In addition to this introductory chapter, this thesis contains three other chapters. An extensive and expositional review of the fluidized-bed drying is presented in Chapter II. It covers the classification of fluidized-bed dryers, phenomena of fluidization, transport processes in a fluidized-bed dryer, drying characteristics of the solids, and modeling of fluidized-bed dryers. Chapter III is concerned with modeling and simulation of a continuous fluidized-bed dryer. The model, based on the two-phase theory of fluidization, delineates the intricate transport processes in the dryer. The proposed model, in essence, is a significant amendment and extension of a comprehensive mechanistic model which is available for a continuous fluidized-bed dryer. Conclusions and recommendations are given in the final chapter.

CHAPTER II

LITERATURE REVIEW

INTRODUCTION

This chapter presents an extensive and expositional review of the published works on the various aspects of the fluidized-bed drying. The review covers the classification of fluidized-bed dryers, phenomena of fluidization, transport processes in a fluidized-bed dryer, drying characteristics of the solids and modeling of fluidized-bed dryers.

CLASSIFICATION OF FLUIDIZED-BED DRYERS

Fluidized bed dryers can be classified mainly according to the following criteria (see Tables 1 and 2)

1. Operating Mode. Fluidized-bed dryers can be operated either in batch or continuous fashion. The latter can be further classified based on staging modes (single stage or multiple-stage). Both batch and continuous operations are often subgrouped according to the types of devices employed in facilitating fluidization (for example, vibrating or rotating devices, or it can be of conventional stationary fluidized bed without any external devices).

2. Structural and Mechanical Features. Fluidized-bed dryers can also be classified on the basis of their geometry and bed depth. The bed can be of constant or variable cross-sectional area in the axial direction, with cross-section being rectangular or circular. The bed depth can be deep or shallow.

A fluidized bed can be formed by synthesizing through various combinations of these two criteria according to varying objectives. An example can be a continuous, multi-stage, deep cylindrical-tapered fluidized bed for drying (Brit. Chem. Eng., 1961). In this review, we shall present several

examples of each category. For additional examples, readers are refered to the references listed in Tables 1 and 2.

Single-stage dryers

The best known dryers in this category are cylindrical ones (Fig. 1). Their main advantages are simplicity in construction and operation, ease in maintenance, low cost and the possibility of complete automation. Among disadvantages must be included the relatively large unevenness of drying in comparison with other types of fluidized-bed dryers, and convection of fine particles of the dried material. To increase the uniformity of drying, some dryers are built in a slightly conical form, with a tapered angle of 30-40° (Fig. 2). The ratio of the cross section diameter of the upper part of the chamber to the lower varies within the range of 10:1 to 50:1.

Multi-stage dryers

Multi-stage dryers are used mainly where, due to the sensitivity of the dried material to relatively long exposure to elevated temperatures, the drying temperature must be low, and, at the same time, where a final low moisture content in the material is required. A two-stage dryer with back-mixing/plug-flow bed (Fig. 3) is suitable for products that initially release their moisture readily and later have a drying curve of decreasing drying rate. These stages are so arranged that the product flow in the counter-current mode to the drying gases, thereby reducing considerably space requirements and construction costs as well as energy consumption. Another example of multi-stage dryers is given in Fig. 4.

Centrifugal-bed dryers

The centrifugal fluidized bed allows table, smooth fluidization for large irregular particles of low bulk density at air velocities well above those required for pneumatic transport. High velocities of air flowing in the radial direction permit intensive heat transfer at relatively low temperatures. Thus, this type of dryers (Fig. 5) can be used for initial moisture reduction of sticky, high moisture and heat sensitive materials.

Vibrated-hed dryers

Some products to be dried have very wide particle size distrihutions and others consist of rather large, oddly-shaped particles or agglomerates. To dry such products, mechanical assistance is required to suspend the particles in the drying gas. This can be accomplished by vibrating a fluidized-bed (Fig. 6). A vibro-fluidized bed can be obtained in apparatus of different construction by means of vibration of the drying chamber, the bottom or baffles of the bed, and also by using special vibrating devices inserted directly into the drying chamber. It has been shown (Slenov and Mikhailov, 1972) that drying in the vibrated fluidized bed significantly intensifies the drying process; the drying rate is increased several folds with the effect of vibration; and sticking of the particles is avoided.

PHENOMENA OF FLUIDIZATION

When a fluid flows upward through a bed of solid particles at a relatively low flow rate, the particles remain immobile or fixed. As the flow rate of the fluid increases, the drag force acting on the particles will also increase until a point is eventually reached where the drag force is equal to the gravitational force holding the particles within the bed. At this point, the particles will begin to move apart, becoming suspended in the flowing fluid, and the bed will expand upwards. Under this condition, the frictional force between a particle and fluid counterbalances the effective weight of the particle, and the bed is considered to be in the state of minimum or incipient fluidization. If the flow rate of the fluid is increased further, the movement of particles is intensified, and bubbling and channeling of the fluid are observed. Such a bed is called a dense-phase fluidized bed, bubbling fluidized bed or, simply, fluidized bed. A still higher fluid velocity results in the solid particles being transported out of the bed with the flowing fluid. A bed under such a condition is termed a lean-phase fluidized bed or, simply, entrained bed. Recycling of these carried-away particles by means of a mechanical device, e.g., a cyclone, to the bottom of the bed will give rise to the so-called "fast fluidization" regime, characterized by a high degree of particle turbulence. This is true especially for the gas-solid system with fine particles since their terminal velocity is relatively low.

For a liquid-solid system with particles of moderate size and density or gas-solid system with fine and light particles, an increase in the flow rate of fluid above the minimum fluidization velocity tends to cause the bed to expand smoothly without the formation of bubbles. Such a phenomenon is called bubbleless or particulate fluidization. Nevertheless, liquid bubbles

can form if the solid particles are large and heavy (e.g., relatively large tungsten particles fluidized by water).

Bubbles in a hubbling hed have been observed to coalesce and grow in size. If the bubble diameter approaches to that of the bed, it will be in the slugging regime; however, this topic is outside the scope of the present review.

A fluidized bed system has numerous advantages over the fixed or moving bed system. These include intensive or rapid local mixing of solids, thereby inducing a uniform bed cnndition and high rates of heat or mass transfer between the particles and fluid or between the wall and the bed. On the other hand, the fluidized bed system has some undesirable characteristics. For example, the extensive macroscopic mixing of solids leads to their nonuniform residence time distribution; this tends to lower the quality of the solid product, and also reduces the overall potential for heat transfer, mass transport or chemical reaction involving the solids as reactants. Furthermore, the existence of buhbles renders gas-solid contact inefficient.

Extensive research has heen undertaken tn facilitate our understanding of the behavior of fluidized beds. The volume of puhlications on this and related subjects is enormous. To survey comprehensively these publicatinns is almost an impossible task; thus, only those relevent to the present work, which deals exclusively with gas-solid systems, are reviewed.

Pressure Drop and Minimum Fluidizing Velocity

Columnar hed. Fluidization is initiated when the pressure drop through the bed becomes equal to the total effective weight of solids. In other words (see, e.g., Kunni and Levenspiel, 1969),

$$(-\Delta P)_{mf} = (1-\epsilon_{mf})(\rho_s-\rho_f)H_{mf}g \qquad (1)$$

The superficial velocity of fluid at minimum fluidization, U_{mf}, appears in numerous correlations relating various variables and parameters defining the state of fluidization; therefore, its accurate estimation or prediction is important. While numerous methods have been proposed for estimating U_{mf}, the most widely employed one is that obtained by equating the pressure drop expression for the fluidized bed to that for the fixed bed proposed by Ergun (1952); it is

$$\frac{\rho_f(\rho_s-\rho_f)gd_p^3}{\mu^3} = \left\{\frac{1.75}{\phi_s\epsilon_{mf}^3}\right\} Re_{mf}^2 + \left\{\frac{150(1-\epsilon_{mf})}{\phi_s^2\epsilon_{mf}^3}\right\} Re_{mf} \qquad (2)$$

where

$$Re_{mf} = \frac{d_p U_{mf}\rho_f}{\mu} \qquad (3)$$

If information on shape factor, ϕ_s, and the incipient fluidized bed voidage, ϵ_{mf}, is not available, eqn. (2) can be approximated by (Wen and Yu, 1966)

$$Re_{mf} = [(33.7)^2 + 0.0408\,\frac{\rho_f(\rho_s-\rho_f)gd_p^3}{\mu^2}]^{1/2} - 33.7 \qquad (4)$$

Tapered bed. As stated at the outset of this section, under the condition of incipient fluidization, the total forces exerted on a solid particle by the fluidizing medium equals its total effective weight. For a columnar bed, the cross-sectional area is uniform along the axial direction. If it is assumed that packed bed of solids prior to the onset of fluidization is essentially uniform, we can consider the balance between the overal frictional and gravitational forces exerted on the entire bed in determining the minimum fluidization condition. For a tapered bed, however, the pressure

drop through a given increment varies along the axial direction in which the cross-sectional area of the bed increases. Thus, the overall pressure drop through the entire bed height should be evaluated by applying eqn. (2) to a section of the bed with a differential height and integrating the resultant equation from the bottom to the top of the bed (Fig. 7). The final expression takes the form (Shi et al., 1984)

$$(\Delta p)_{mf} = \phi_1 U_o h_o \ln\left[\frac{H+h_o}{h_o}\right] + \phi_2 U_o^2 h_o \left[\frac{H}{H+h_o}\right] \tag{5}$$

where

$$\phi_1 = \frac{150(1-\epsilon_{mf})^2}{\epsilon_{mf}^3} \frac{\mu}{(\phi_s d_p)^2} \tag{6}$$

and

$$\phi_2 = \frac{1.75(1-\epsilon_{mf})}{\epsilon_{mf}^3} \frac{\rho_f}{(\phi_s d_p)} \tag{7}$$

It has been shown that the above expression reduces to that for the columnar bed when the apex angle becomes negligibly small. Correspondingly, the minimum fluidization velocity is evaluated as

$$\phi_1 U_{mf} \ell_o WH + \phi_2 U_{mf} \ell_o h_o W \ln\left[\frac{H+h_o}{h_o}\right]$$

$$= 0.5(1-\epsilon_{mf})(\rho_s-\rho_f)\ell_o WH\left[\frac{H+2h_o}{h_o}\right] g \tag{8}$$

Centrifugal bed. In a centrifugal fluidized bed, particles are fluidized in the centrifugal field. The bed usually consists of a cylindrical basket which rotates about its axis of symmetry. The rotation of the axis causes the particles in the basket to form an annular region at the circumference of the basket. Fluid is injected inward through the porous

surface of the basket wall. When the rotational speed of the basket is fixed, the pressure drop through a centrifugal packed bed increases as the fluid velocity increases, and at a certain velocity, the particle at the free board surface of the bed will begin to fluidize. At this instance, the pressure drop through the bed reaches a maximum and corresponding fluid velocity reaches a critical fluidization velocity.

Fan et al. (1985) have proposed a mechanistic model for determining the incipient fluidization conditions in a centrifugal fluidized bed. Unlike many other models (see, e.g., Levy et al., 1978; Kroger et al., 1979) it takes into account the centrifugal acceleration and the curvature effect of the cylindrical fluidized bed. According to this model, the pressure drop through a packed bed in the centrifugal field with a differential thickness of dr can be expressed in terms of the sum of the drag force as correlated by Ergun (1952) and the centrifugal and dynamic force experienced by it (Fig. 8). The maximum pressure drop through this confined volume element is evaluated by equating the product of the pressure drop through it and the radial area with the effective weight of the particles contained in it. Integrating over the radius of the bed yields the overall maximum pressure drop across the entire bed. It has been derived as

$$(-\Delta P)_{max} = \phi_1 U_{oc} r_o \ln \frac{r_o}{r_i} + \phi_2 U_{oc}^2 r_o^2 \left(\frac{1}{r_i} - \frac{1}{r_o}\right) + \frac{\rho_f \omega^2}{2}(r_o^2 - r_i^2) + \frac{\rho_f U_{oc}^2 r_o^2}{2}\left(\frac{1}{r_i^2} - \frac{1}{r_o^2}\right) \quad (9)$$

The corresponding critical fluidizing velocity, U_{oc} is evaluated through

$$[\phi_2 r_o^2 \ln \frac{r_o}{r_i} + \rho_f r_o^2 (\frac{1}{r_i} - \frac{1}{r_o})]U_{oc}^2 + \phi_1 r_o (r_o - r_i) U_{oc}$$

$$- \frac{\omega^2}{3} [(1-\epsilon_{mf})(\rho_s - \rho_f) - \rho_f](r_o^3 - r_i^3)$$

$$= 0 \qquad (10)$$

The estimated minimum fluidization velocities are in good agreement with the experimental data.

Vibrated bed. The vibrated fluidized bed consists essentially of a vibrating screen through which air is forced from a plenum beneath it. Suppose that the horizontal screen is subject to vibrations of amplitude α and angular frequency ω. If the vibrational acceleration $\alpha\omega^2$ is less than that due to gravity g, the solids will remain in contact with the screen. However as vibrational intensity increases ($\alpha\omega^2/g>1$) a point will be reached where the bed begins to detach itself from the screen and move freely under the influence of gravity. This state is defined as that of incipient vibrofluidization. The incipient vibrofluidization velocity U_{mv} can be significantly lower than the minimum fluidizing velocity $(U_{mf})_s$ of the corresponding static bed. A theoretical expression for $U_{mv}/(U_{mf})_s$ has been derived by means of force and momentum balances (Jinescu, 1971)

$$\frac{U_{mv}}{(U_{mf})_s} = 1 - (\frac{1+k}{2\pi j})(\frac{\alpha\omega^2}{g}) \qquad (11)$$

In this expression, k is a collision elasticity factor which must be determined experimentally. It approaches zero for fine particles and unity for coarse particles. The factor j, which is a small integer, is given by

$$j = \frac{(t_a + t_d)}{t_p} \qquad (12)$$

where the sum $(t_a + t_d)$ is the total flight time, t_a being the time of ascent of the bed and t_d the time of descent; t_p is the period of the vibrations. The pressure drop under the incipient fluidization condition with vibration is interrelated to that without vibration as follows:

$$\frac{(-\Delta P_{mf})_v}{(-\Delta P_{mf})_s} = 1 - 0.935 \left(\frac{d_p}{H_f}\right)^{0.946} \left(\frac{\alpha\omega^2}{g}\right)^{0.606} \phi_s^{1.637} \qquad (13)$$

Gupta and Mujumda (1980) have proposed that for efficient operation in a vibrated fluidized bed, the air velocity must exceed a "minimum mixing velocity", U_{mm}, at which solids mixing could be observed visually. They have contented that this value is more practical from the design standpoint than the one determined from the pressure-drop-velocity curve. Based on their data for spherical and near-spherical particles, the following correlation has been proposed for this quantity

$$\frac{U_{mm}}{(U_{mf})_s} = 1.952 - 0.275 \left(\frac{a\omega^2}{g}\right) - 0.686 \left(\frac{a\omega^2}{g}\right)^2 \qquad (14)$$

where $(U_{mf})_s$ is the theoretically computed minimum fluidization velocity of the bed under the non-vibrating condition.

Bed Expansion

Beyond the point of incipient flnidization, further expansion of a fluidized bed is related in a complex manner to numerous parameters such as the physical properties of solids and fluids, the gas flow in excess of the minimum fluidization velocity, particle size and size distribution, and the bed-height to diameter ratio. Superimposed on this complicated relationship is the nonumiform voidage in the bed as identified by three distinct zones: (1) a distributor effect zone (2) a zone of constant bed density, followed

by (3) a zone of continuously decreasing solids density, which makes it difficult to estimate fluidized bed heights. Furthermnre, because of agitation of solids by the fluidizing medium, the top surface of the bed is usually uneven and oscillating. Thus the voidage, ϵ, and the bed height, H_f, can only be considered as time average values.

The published work on describing bed expansion on fluidization is generally based on (1) the two-phase theory of fluidization, which assumes that the gas in excess of that required for minimum fluidization velocity will pass through the bed in the form of bubbles (2) two-phase theory and hubble properties.

The relationship between voidage, ϵ, and fluidizing velocity, U_o, has been commonly used to determine particulate phase expansion. It has been known (see, e.g., Steinour, 1944; Lewis et al., 1949; Lewis and Bowerman, 1952; Richardson and Zaki, 1954) that for a particulate or ideal fluidized bed, a linear correlation on a logrithmic scale exists between bed voidage and fluidizing velocity. It takes the form

$$U_o = \epsilon^n U_t \tag{15}$$

where n is a function of d/D and Re_t (Richardson and Zaki, 1954; Richardson, 1971). This equation can also be expressed in terms of the linear fluid velocity, U_o/ϵ, as

$$\frac{U_o}{\epsilon} = \epsilon^{n-1} U_t \tag{16}$$

According to Kwauk (1963), the above relationship can be generalized in terms of the relative linear velocity between the fluid and particles as follows:

$$\frac{U_o}{\epsilon} - \frac{U_p}{1-\epsilon} = \epsilon^{n-1} U_t \qquad (17)$$

It is worth pointing out that eqn. (16) is also valid for nonideal or bubbling fluidized bed (Richardson, 1971). Accordingly, the same can be infered for eqn. (17).

If the so-called two-phase (bubble-emulsion) model of fluidization is adopted (see Fig. 9), ϵ can he related to the corresponding parameters in the model as

$$\epsilon = \delta_b + (1-\delta_b)\ \epsilon_{mf} \qquad (18)$$

and

$$1-\epsilon = (1-\delta_b)(1-\epsilon_{mf}) \qquad (19)$$

Equation (2-17) can then be rewritten for gas-solid system as

$$\frac{U_o}{\delta_b+(1-\delta_b)\epsilon_{mf}} - \frac{U_p}{(1-\delta_b)(1-\epsilon_{mf})} = [\delta_b+(1-\delta_b)\epsilon_{mf}]^{n-1} U_t \qquad (20)$$

Many empirical correlations have also been proposed for estimating fluidized bed expansion for a gas-solid fluidized system (see, e.g., Leva, 1957; Lewis, 1949; 8akker and Heertjes, 1960; Shen and Johnstone, 1955). A correlation based on the regression analysis of the available data has been proposed by Babu et al. (1978). It is

$$\frac{H_f}{H_{mf}} = 1 + \frac{14.311\ (U-U_{mf})^{0.738} d_p^{1.006} \rho_s^{0.376}}{U_{mf}^{0.937} \rho_g^{0.126}} \qquad (21)$$

This correlation is independent of the effect of column diameter for $D_c >$ 0.065 (m). It is, therefore, relatively reliahle for scale-up. Comparison of the calculated and measured expansion ratio hased on the correlation reveals that about 90% of the data is predicted within ± 12%.

Fluid Mechanistical Structure of the Bed

Formation of phases. It is now generally accepted that a one-phase representation of a fluidized bed (pseudo-homogeneous model) is inadequate for a bubbling fluidized bed, and that at least two hydrodynamically distinct phases should be visualized. One is the phase where gas percolates through, rather as in a packed bed, and the other the phase where much of the gas, existing in the form of bubbles, is out of contact with solids. In fluidization, the former is called the dense or emulsion phase and the latter the lean or bubble phase. Based on this visualization, a well-known, two-phase theory of fluidization has been developed (Twoomey and Jonestone, 1952). The theory further assumes that the flow of fluid in excess of minimum fluidization passes through the bed as bubbles and that the emulsion phase is similar to the bed at minimum fluidization. While various models have been proposed for fluidization, most of them are based on the two-phase theory. However, these models differ substantially regarding the assumptions of flow of gas through the two phase, the extent of mixing, and the mode of interphase exchange (see, e.g., Van Deemter, 1961; Orcutt et al., 1962; Davidson and Harrison, 1963; Partridge and Rowe, 1966; Kobayashi et al., 1967; Kato and Wen, 1969).

Another representation of the fluidized bed is the three-phase model (see, e.g., Kinni and Levenspiel, 1969; Frey and Potter, 1976; Mao and Potter, 1984) which considers the cloud and wake region as a separate phase (the cloud-wake phase) in addition to the emulsion and bubble phases.

Numerous experimental envidence exists to indicate that characteristics of a fluidized bed depend heavily on the behavior of bubbles. It affects the relative magnitudes of the bubble and emulsion phases, the mixing of solids and that of fluid, the interactions between the solids and fluid, and

those between the contents and the wall of the bed. It has been recognized that the coalescence of bubbles leads to an increase in the bubble size in the direction of flow. Various correlations have been published for predicting the axial distribution of bubble sizes; the most recent ones include those by Mori and Wen (1975), Rowe (1976), and Darton et al. (1977). Among them, the mechanistic model proposed by Darton et al. (1977) and the semi-empirical equation by Mori and Wen (1975) appear to be more accurate than the others in predicting the bubble size; therefore, they have been recommended for use by different researchers (see, e.g., Grace, 1981; Yates, 1983).

Almost all the available correlations suggest that the bubble size increases indefinitely in the direction of flow; however, it has been experimentally determined that the bubble size reaches a maximum in a fluidized bed containing fine particles (Geldart, 1973; Davidson et al., 1977). Furthermore, the growth of bubbles will be restricted in a bed equipped with internals. All of these indicate the difficulty of estimating the bubble size in a fluidized bed. Thus, various researchers have assumed the bubble size to be constant in modelling a fluidized bed; that is, no coalescence exists between the bubbles (see, e.g., Hoebink and Rietema, 1980(a) and 1980(b), Palancz, 1983). Another approach recognizes the growth of bubbles, but employs the effective bubble size throughout the bed or simply treats it as a parameter (see, e.g., Kunni and Levenspiel, 1969).

Although a substantial number of correlations have been proposed for the bubble size velocity, the semi-empirical equation proposed by Davidson and Harrison (1963) is overwhelmingly popular; it is

$$U_b = (U_o - U_{mf}) + 0.711(gd_b)^{0.5} \qquad (22)$$

This expression has been shown experimentally to give a good estimation of the bubble rise velocity (Rowe and Partridge, 1965, Kunni and Levenspiel, 1969).

Gas movement and gas mixing. The pioneering work by Davidson and Harrison (1963) on the characteristic features of a fluidized bed in the light of fluid mechanics has paved the way for the later systematic studies on the subject. The model suggested hy Davidson and Harrison includes some bold assumptions: (1) the original two-phase theory of Twoomey and Johnstone (1952) is valid and (2) the bubbles are circular in shape and behaves as if they were in inviscid liquid. Although the model is simple, it correctly predicts some significant flow characteristics, including the flow pattern of gas and movement of solids in the vicinity of bubbles, pressure distribution, and the fnrmation of cloud verified experimentally by Rowe (1964). The assumption of circular bubbles is obviously an over-simplified one. Experimental evidences show that a bubble normally has an indented base of solid particles, which is defined as the wake region. A theory based on this more realistic picture of buhbles has been proposed hy Murray (1965).

A variety of models have been proposed for the mixing of gas in the emulsion and hubble phases. These include, among others, the plug flow, perfect mixing and dispersive flow models. The flow of gas bubbles is usually assumed to be in the plug flow mode, that is, individual bubbles rise at a uniform velocity without coalescence. This is obviously an over-simplified assumption. Nevertheless, it is widely employed and yields surprisingly good predictions. No definitive experimental evidence is available to base the assumption ahout the flow pattern through the emulsion phase; thus, widely varied flow patterns are assumed in different models.

They include the perfect mixing, plug flow, tanks-in-series, dispersive flow, stagnant and down flow.

If the performance of a fluidized-bed dryer is controlled by diffusion of moisture through the solids, it will he relatively insensitive to the flow patterns of gas. Moreover, if most of the gas passes through the hed as bubbles, i.e., $U_o >> U_{mf}$, it is obvious that the contribution of the emulsion gas to the performance of the bed will be negligible, and the selection of the flow pattern of emulsion gas will not be critical. Except for these two special cases, the performance of the bed will be strongly influenced by the flow pattern of gas.

Solids Movement and Mixing

Experimental observations of the movement of solid particles in a fluidized bed have revealed that the solid particles move in a fairly random manner, and the movement and mixing are induced by the rising bubbles (Rowe and Partridge, 1965; Kunni and Levenspiel, 1969; Cranfield, 1978; Shi and Fan, 1982). Although the theory of Davidson and Harrison (1963) has heen successfully employed in explaining the local movement of particles around a bubhle, apparently it is incapable of explaining the glohal movement of solids and the resultant solids mixing in a fluidized bed. Three major mechanisms of the particle movement causing this mixing have heen reported (Rowe and Partridge, 1965; Cranfield, 1978). They include: (1) eddy diffusion, (2) bubhle-wake induced drift, and (3) bubble-induced drift. The mixing mechanism could he one, two or all three, depending mainly on particle size.

An equation, analogous to Fick's equation, has heen commonly used to describe the solids mixing. Its expression is

$$\frac{\partial C_s}{\partial t} = D_{sa} \frac{\partial^2 C_s}{\partial z^2} + \frac{1}{x^\alpha} \frac{\partial}{\partial x} \left(x^\alpha D_{sl} \frac{\partial C_s}{\partial x} \right) \qquad (23)$$

where $\alpha = 0, 1$, representing cylindrical and sperical geometry of the bed, respectively.

To facilitate the determination of the axial dispersion coefficient, D_{sa}, and the lateral (or radial) dispersion coefficient, D_{sl}, experiments are usually designed in such a way that these coefficients can be found separately from the experimentally determined solids concentration, C_s. Note that D_{sa} and D_{se} are sometimes named diffusion coefficients. Based on the experimental results, a substantial numher of correlating equations have been proposed to determine the influences of significant parameters, such as the minimum fluidization condition, fluid velocity, buhhle size, particle properties and bed geometry, on the magnitudes of the dispersion coefficients.

Solids motion in the vertical direction is mainly induced by the motion of bubbles; thus, it is somewhat inappropriate to consider a of diffusion process of the Fick's law type for vertical solids mixing. Arastoopour and Gidaspow (1979) have proposed a model for vertical countercurrent solids gas flow in fluidized bed reactors. According to their model, vertical countercurrent flow of gas and solids of a uniform size can be mathematically described by means of one-dimensional, isothermal steady-state mass and momentum balances. It is suggested that from hydrodynamics in the fluidized bed, the empirical transfer or diffusion coefficient approach be replaced with mixing predicted from the laws of motion of the gas and the solid particles.

The time constant for drying solids is usually much longer than that for the mixing of the solids. Thus an assumption that the solids in a free-bubbling bed is uniformly mixed is reasonable. Actually, this assumption has been confirmed by the experimental work by Vanecek et al. (1970), Brauer et al. (1970) and Hoebink (1977).

TRANSPORT PROCESS

Gas Interphase Exchange

Recognizing the existence of bubble and emulsion phases in the fluidized bed, questions arise as to the mode and rate of transfer of a fluid component between these two phases and as to the manner for expressing them in terms of measurable parameters. The first approach is to correlate the interphase exchange coefficient, defined empirically, similar to the mass transfer coefficient (see, e.g., May, 1959; Van Deemter, 1961). The second approach is to relate it to the characteristics of the fluid in general and bubbling mechanism in particular (see, e.g., Partridge and Rowe, 1966; Kunni and Levenspiel, 1969; Davidson et al., 1977). The latter is based on the fundamental mechanism, and therefore, it has the advantage that we can use it with confidence in scale-up; this is not usually the case for the former which is purely empirical.

Various expressions for the interphase exchange coefficient have been published. One of the common assumptions is that the gas enters from the bottom part of the bubble and leaves at the top (Partridge and Rowe, 1966 and Kunni and Levenspiel 1969); this generates a closed circulation of gas within the so-called cloud region. The interphase transfer of gas is usually considered to include two steps in series (see, e.g., Kunni and Levenspiel, 1969). One is expressed in terms of the exchange of gas between the bubble and cloud-wake phases, involving both convective and diffusive transfer, and the other between the cloud-wake and emulsion phases, involving mainly the diffusive transport. Accordingly, the overall interchange coefficient for mass transfer can be expressed as (Kunni and Levenspiel, 1969)

$$\frac{1}{K_{be}} = \frac{1}{K_{bc}} + \frac{1}{K_{ce}} \qquad (24)$$

The analogous form for heat transfer is

$$\frac{1}{H_{be}} = \frac{1}{H_{bc}} + \frac{1}{H_{ce}} \qquad (25)$$

The subscripts b, c, e represent bubble, cloud and emulsion phase respectively. It is worth pointing out that all the transfer coefficients in eqns. (24) and (25) should have the same volume base (which could be either bubble, emulsion or total bed). Thus $(K_{be})_b$, $(H_{be})_b$ etc. would denote the bubble volume on which transfer coefficients are defined. Partridge and Rowe (1966) have assumed that the bubble and cloud-wake phases are perfectly mixed; thus the limiting step of the mass transfer is between the cloud-wake and emulsion phases; in other words, $K_{bc} \rightarrow \infty$ and $H_{bc} \rightarrow \infty$ in eqns. (24) and (25), respectively.

Bokur *et al.* (1974) have reported that when $U_o > 2U_{mf}$ the cloud surrounding a rising bubble is very thin, and therefore, interchange can be considered to occur only between the bubble and emulsion phases. Davidson *et al.* (1977) has shown that the cloud is not closed in the region below the bubble and have chosen to ignore the recirculation of gas in the cloud region. In addition, several empirical correlations have been proposed. Among them, the equations proposed by Kobayashi *et al.* (1967) and Grace (1981), which incorporates the effect of bubble interaction, appear to represent the experimental data reasonably well.

Gas-to-Particle Heat Transfer

Mechanism. The flow of gas around particles in a fluidized bed is essentially streamline and the local Reynolds number is correspondingly small; thus, particle-to-fluid heat transfer coefficients are normally quite low. Typical values cited for these coefficients are 6-23 kW/m^2k (Botterill, 1975). On the other hand, the size of the bed particles is small and their number high, which leads to a large total surface area of solids per unit volume of the bed exposed to the flowing gas; values ranging between 5000 to 45000 m^2/m^3 are cited (see, e.g., Botterill, 1975). As a result, the overall heat transfer rate between the particles and the main stream of gas is very rapid.

There are a number of factors which will affect the heat transfer process between the particles and fluidizing gas. The presence of adjacent particles affects the thickness of the gas-film surrounding the individual particles while gas by-passing zones of the bed will adversely affect the rates of the heat transfer. The extent of by-passing is dependent on the bed material, degree of fluidization, design of the apparatus and consequent gross mixing patterns. A rigorous analysis of the heat transfer process will, therefore, require a large number of parameters, which is not feasible. Instead, empirical or semi-empirical correlations for overall coefficients are often sought for design purpose.

Correlations for Overall Transfer Coefficients. Because of its importance, an enormous amount of research has been carried out on this subject (Barker, 1965). Based on the available experimental data, numerous correlations have been proposed. Nevertheless, the most striking feature of the published expressions is the lack of agreement among observers with over a

thousand fold variation (Kunni and Levenspiel, 1969). It is, therefore,necessary that the experimental conditions are similar to those under our consideration and great caution should be taken when extrapolating the data. In particular, we must see what global flow pattern is assumed for the gas (e.g., plug flow or back mixing) since different flow patterns in terms of macromixing will yield substantially different heat transfer results.

Tbe analysis of the puhlished works, have indicated (Kunni and Levenspiel, 1969) that measurements based on a plug flow model present a more consistant pattern than those based on a perfect gas mixing model. The former can be correlated by the equations:

$$Nu_p = 0.03\ Re_p^{1.3} \tag{26}$$

This relationship, actually, is an overall correlation based on the works of several investigators (Richardson and Ayers, 1959; Kettering et al., 1950; Heertjes and McKibbens, 1956; Donnadieu, 1961; Walton et al., 1952). It is applicable approximately in the range

$$Re_p < 100 \tag{27}$$

For the same plug flow model, a different correlation has been proposed by Chang and Wen (1966). They measured the fluid-to-particle heat transfer coefficients in a baffled fluidized bed of large Raynolds number under transient conditions. The correlation based on their experimental results takes the form

$$j_h = 0.097\ \left(\frac{Re_p}{\epsilon}\right)^{-0.5}\ (Ar)^{0.2} \tag{28}$$

with

$$900 < \frac{Re_p}{\epsilon} < 40{,}000 \tag{29}$$

and

$$5.86 \times 10^{6} < Ar < 2.55 \times 10^{7} \tag{30}$$

Recently, microwave heating technique under unsteady-state conditions has been employed to collect fluid-to-particle heat transfer data. This has resulted in a relatively uniform temperature of the bed, consequently, reducing errors due to the temperature gradient within the bed and hence particle-to-particle heat transfer. The following correlation has heen proposed based on the experimental findings (Bhattacharyya and Pei, 1974)

$$j_h = 0.043\left[\frac{Ar}{(Re_p/\epsilon)^2}\right]^{0.25} \tag{31}$$

with

$$0.02 < \frac{Ar}{(Re_p/\epsilon)^2} < 10 \tag{32}$$

For additional information, readers are referred to Frantz, 1961; Ferron, 1962; Bradshaw, 1963; Barker, 1965; Gupta, 1974; Balakrishnan, 1975; McGaw, 1977; Selzer, 1977; and Botterill, 1981.

Bed-to-Surface Heat Transfer

Mechanism. In numerous fluidized bed processes, it is necessary to transfer heat hetween the hulk of the hed and a surface. The latter can be the surface of an immersed cooling or heating coil through which the heat transfer medium is circulated or it can be the wall of the column containing the bed. The variation with gas velocity of the bed-to-surface heat transfer coefficient can he characterized in three regions under the condition that radiation transfer may be neglected (see Fig. 10): (1) the region

below U_{mf} where the bed is in the packed state and the heat transfer coefficient is low, (ii) the region between U_{mf} and an optimum velocity where the coefficient increases sharply to a maximum value, (iii) the region above the optimum velocity where a gradual decrease sets in. It is generally believed that the sharp increase in the heat transfer coefficient above U_{mf} is caused by bubble-induced particle motion at the transfer surface while the decrease above the optimum velocity is the result of restricted particle surface contact under conditions of high bubble flow (Yate, 1981).

It is generally accepted that heat transfer to an immersed surface may be considered to comprise three additive components (Botterill, 1975; Yates, 1983)

(i) the particle convective component accounting for the conduction heat transfer across the gas layer separating the solid particles and surface. It depends on the contact time and thermal properties of both gas and solids.

(ii) the gas convective component which can be attributed to the interstitial flow in the case of emulsion phase contact and the bubble flow field in the case of bubble contact.

(iii) the radiative component that becomes important only at temperatures in excess of approximately 600°C.

By combining these three components, an overall prediction for heat transfer between the bed and an immersed surface can be achieved.

Correlations for overall coefficients. A correlation for the overall coefficients of the heat transfer between the wall and the bed has recently been developed (Bock, 1983), which incorporates the convective, conductive and radiative conponents of the wall-to-bed heat transfer.

The correlation for the gas convective contribution is (Baskakov et al., 1973)

$$h_{gc} = 0.009 \frac{k_g}{d_p} Pr^{1/3} \sqrt{Ar} \, (U/U_{max})^{0.3} \tag{33}$$

with U in the range

$$U_{mf} \leq U \leq U_{max} \tag{34}$$

The radiative component h_R is (Bock, 1983)

$$h_R = 0.04 \, \psi \, \sigma[(T_W - T_B)_{ln}/100]^3[1 + (\frac{T_W - T_B}{T_W + T_B})^2] \tag{35}$$

where

$$(T_W - T_B)_{ln} = \frac{T_W - T_B}{\ln \frac{T_W}{T_B}} \tag{36}$$

The particle convective heat transfer coefficient is evaluated as (Bock, 1983)

$$h_{pc} = \frac{1 - \delta_h}{[\frac{C}{h_{max}(1-\epsilon_{mf})} + \frac{\sqrt{\pi}}{2} \frac{t}{(k_p \rho_p c_p)}]} \tag{37}$$

where

$$h_{max} = \frac{4k_g}{d_p} [(1 + \frac{2B}{d_p}) \ln(1 + \frac{d_p}{2B}) - 1] \tag{38}$$

and

$$2B = 4\lambda(\frac{2}{\gamma} - 1) \tag{39}$$

The mean free path of gas molecules, λ, can be calculated from

$$\lambda = \frac{16}{5} \sqrt{\frac{RT}{2\pi M}} \frac{\mu}{P} \tag{40}$$

γ in eqn. (39) is the accommodation coefficient, accounting for the incomplete energy transfer during a molecule-wall collision. It is determined through the following relationship;

$$\log_{10}(\frac{1}{\gamma} - 1) = 0.6 - (\frac{1000}{T} + 1)\frac{1}{C_A} \tag{41}$$

The constant C_A has different values for different gases (see Boch, 1983). For air,

$$C_A = 2.8 \tag{42}$$

The contact time of the particle phase, t, in eqn. (37) is defined as

$$t = (1-\delta_b)/f_b \tag{43}$$

The constant C in eqn. (37) counts for the roughness of the particles and the heat transfer surface. C = 3 was reported for all the tested particles (Bock, 1983). The correlations from the three components of heat transfer are summed to yield the overall bed-to-surface heat transfer coefficient, h, as

$$h = h_{gc} + h_{pc} + h_R \tag{44}$$

The validity of the proposed correlation has been tested over a wide range of operating conditions. The predictions of the model show good agreement with many experimental observations.

Relatively simple correlations neglecting the radiant component, have also been developed. They are mainly based on the film or penetration theory. A review of the relevant correlations are available (Saxena and Gabor, 1981).

Most of the proposed correlations for the heat transfer coefficient in gas-solid fluidized beds are for relatively small particles. Attempts to extrapolate these correlations to large particles have been unsatisfactory

(see, e.g., Decker and Glicksman, 1983). For a small particle system, bubble dynamics and bubble-induced motinn of solid particles play a very significant role in the sense that the predominant mechanism of heat transfer is due to particle convection (Mathur and Saxena, 1985). Consequently, the heat transfer coefficient, h, decreases rapidly as the average diameter of the small particles increases. In a bed of large particles, the interstitial gas velocity is much greater than the hubble velocity, and as the fluidizing velncity increases this slow-moving bubble regime changes to the rapidly-growing bubble regime and finally to the turbulent regime (Catipovic et al., 1978). It has been shnwn (Borndulya et al., 1980) that in turbulent flow regime, the solids mixing is pnor. Under this circumstance, the heat transfer is induced mainly hy the convective flow of gas surrounding the particles and to a lesser extent by a steady-state heat conduction due tn contact between the particles and between the surface and particles. For such a system, the convective contrihution nf gas is far more important than the convection contrihution of the particles. As a result, the overall heat transfer is intensified with the increase in the particle diameter.

Various investigators (Butterill et al., 1981; Ganzha, et al., 1982; Decker and Glicksman, 1983; Mathur and Saxena, 1985) have recently developed correlations for bed-to-surface heat transfer in large particle fluidized beds. In defining "small" and "large" particles quantitatively, two powder classification schemes have been used. The classification scheme prnposed by Geldart (1973) is based on the hydrodynamic behavior of particles. For particles of small size or low density, bed expansinn occurs well befnre bubbling commences; in other words, minimum buhbling velocity U_{mb} is greater than minimum fluidization velocity, U_{mf}. For particles of large size or high density, the reverse is true. Since both minimum fludization and

minimum bubbling velocities can be related to the diameter and density of particles, the criteria for the classification of particles is set according to particles diameter and density. Geldart's groups B and D particles are usually referred to as small and large particles respectively. His group B particles are defined as particles with 40 $\mu m < \bar{d}_p < 500\ \mu m$, and 1400 $kg/m^3 < \rho_s < 4000\ kg/m^3$. His group D particles, on the other hand, satisfy the criterion that $(\rho_s - \rho_g)\bar{d}_p^2 > 10^{-3}$.

Saxena and Ganzha (1984) have shown that while Geldart's group D particles will exhibit the hydrodynamic bubbling behavior of a large particle bed, the heat transfer phenomenon of the bed may still reflect that of a small particle system. Consequently, a desirable particle classification can only be achieved if the fluid flow and heat transfer behavior are considered simultaneously. Note that Nusselt number representing heat transfer behavior and Reynolds number characterizing fluid flow conditions are related to each other through their common dependence on Archimedes number. Based on this fact, they obtained a powder characterization scheme by considering the Archimedes number together with the Reynolds number at minimum fluidization. It classifies powders into three different groups. Their so-called "large" particles are from groups II(B) and III, which are defined as

$$1.3 \times 10^5 \leq Ar \leq 1.6 \times 10^6 \qquad (45)$$

and

$$Ar \geq 1.6 \times 10^6 \qquad (46)$$

respectively.

Based on numerous published expressions for the bed-to-surface heat transfer coefficient, a general correlation based on Geldart's Powder groups has been proposed (Butterill et al., 1981), which gives

$$h_{max} = 35.8\ k_g^{0.6} d_p^{-0.36} \rho_p^{0.2} \tag{47}$$

for the group B particles, and

$$h_{pc,max} = \frac{k_g}{d_p} 0.843\ Ar^{0.15} \tag{48}$$

$$h_{gc} = \frac{k_g}{d_p} 0.86\ Ar^{0.39} \tag{49}$$

$$h_{max} = h_{gc} + h_{pc,max} \tag{50}$$

for the group D particles.

For a large particle fluidized bed, the convective contribution of gas to overall heat transfer coefficient is the most significant factor. Unlike the conductive heat transfer, the heat transfer by convective flow of gas is not much affected by the shape and roughness of the particles. This renders the modeling of the heat transfer between the particles and a surface relatively simple. A mechanistic model for heat transfer between a fluidized bed of group III particles and an immersed surface has been proposed (Ganzha et al., 1982); it involves parameters that can be easily determined. The model assumes that an orthorrombic configuration of particles are arranged around the heat transfer surface. It is further assumed that the particles can be replaced by equivalent cylinders whose volumes are the same as those of the particles and of a unit diameter-to-height ratio. All the resistance to heat transfer is considered to be confined to the first row of the particles near the heat transfer surface. The heat is transfered by conduction through the gas lens (with a diameter equal to that of the equivalent

cylinder), between the surface and the particle. Their proposed expression is

$$Nu = 8.95(1-\epsilon)^{0.667} + 0.12Re^{0.8}\,Pr^{0.43}\cdot\frac{(1-\epsilon)^{0.133}}{\epsilon^{0.8}} \qquad (51)$$

Mathur and Saxena (1985) have developed a new correlation which is based on a total of three hundred and thirty-six data points and the known mechanistic details of heat transfer by particle and gas convection. The proposed correlation takes the form

$$Nu = 5.95\,(1-\epsilon)^{2/3} + 0.055\,Ar^{0.3}Re^{0.2}Pr^{1/3} \qquad (52)$$

it is accurate within ± 35% for gas - fluidized bed systems characterized by Ar > 130,000.

Models with more involved mathematical treatment can be found in the work by Adams (1982), and Deck and Glicksman (1983).

Particle-to-Gas Mass Transfer

Mechanism. The overall Particle-to-Gas mass transfer generally is governed by (i) the density of the fluid; (ii) shape, size, and density of the solid particles; (iii) diffusion coefficient of the material being transferred; (iv) geometry of the system; and (v) operating conditions such as the flow rate of the fluid, bed height, voidage of the bed, the bubbling behavior and its accompanying features of gas by-passing and channelling.

In fluidized-bed drying, particle-to-gas mass transfer is caused by vaporization of moisture at the interface and its successive migration into the bulk phase of the drying gas. The vaporization of moisture at the interface depends on the interface temperature, gas moisture content, etc. The heat transfer across the interface resulting from a difference in temperature in two phases will raise the interphase temperature relative to the

bulk-phase temperature, and the equilibrium at the interface will then vary. Consequently, the particle-to-gas mass transfer in fluidized-bed drying is related to the corresponding heat transfer process. But in practical applications, in order to employ the fluidization characteristics to the maximum extent possible, drying operations in a fluidized bed is often conducted in such a way that, the mass transfer resistance at the interface between the gas stream and the solids is predominant or, in other words, drying operations mainly occur in so-called constant-rate drying period. Under this circumstance, the interface temperature, and the equilibrium at the interface remain unchanged if the same thing can be said for the state of the drying gas. As a result, the mass transfer coefficient together with concentration difference can appproximate the mass transfer rate with reasonable accuracy. This is especially true for the continuous operations since the emulsion gas is commonly assumed to he completely mixed with constant temperature and moisture content.

Correlation for overall mass transfer coefficients. Considerable attention has been paid to the gas-solid mass transfer and numerous attempts have been made to derive analytical expressions for the transfer process. Because of the large number of variahles involved and inadequate knowledge of the flow mechanism in the bed, purely mathematical or theoretical considerations are not much favored in expressing the relation between variables and more often than not, resort is taken to empirical correlations developed from the experimental findings.

The conventional method for relating the mass transfer coefficient, operating conditions, and the physical properties of the fluid is through the dimensionless groups. Attempts have been made to correlate the experimental results in terms of the mass transfer factor (J_D) or Sherwood

number (Sh) to the various forms of Reynolds number. To incorporate the effect of the bed expansion, the void fraction has also been used to improve the correlation.

Based on the available experimental data for the various systems reported in the literature, a generalized correlation has been developed (Dwivedi and Upadhyay, 1977), which can be used for the design of a fixed-bed or fluidized bed process unit. It is

$$\epsilon J_d = \frac{0.765}{Re^{0.82}} + \frac{0.365}{Re^{0.386}} \tag{53}$$

with

$$Re \geq 10 \tag{54}$$

and an average standard deviation of 17.95% with the experimental data. The proposed correlation resulted from iterative least - square analysis with minimization of residual errors, hence is purely empirical in nature. Starting from a theoretically derived relationship,

$$Sh \propto f(Re^{1/2}), \tag{55}$$

Paneey et al. (1981) have obtained, by regression analysis, the following correlation for large particle fluidized bed system

$$\epsilon Sh = 0.95 Re^{1/2} Sc^{1/2} \tag{56}$$

which has been shown to be an approximation of the Nelson-Galloway-Rowe asymptotic expression (Nelson and Galloway, 1975; Rowe, 1975).

A correlation based on the data obtained in both gas- and liquid-fluidized systems has been proposed (Beek, 1971) in the following form

$$St\, Sc^{2/3} \equiv \frac{K_{pg}}{U_o} \epsilon Sc^{2/3} = (0.6 \pm 0.1)\left(\frac{U_o d_p}{\nu}\right)^{-0.43} \tag{57}$$

for

$$50 < \frac{U_o d_p}{\nu} < 2000 \tag{58}$$

$$0.6 < Sc < 2000 \tag{59}$$

and

$$0.43 < \epsilon < 0.75 \tag{60}$$

According to Beek (1971), the expression seems to be the most accurate and reliable representation of available data within the applicable range of parameters.

Since the convective transfer coefficients for heat (h_p) and mass (K_{pg}) are both dependent on the flow of the air, attempts have been made to correlate these two coefficients. This is especially important in the sense that relatively few investigations have been made into the study of mass transfer process in different systems and under various operating conditions. An empirical relationship between heat and mass transfer coefficient has been developed (Holman, 1972), which takes the form

$$\frac{h_p}{K_{pg}} = \rho_p c_p \left(\frac{Sc}{Pr}\right)^{2/3} \tag{61}$$

Attempts have also been made (Kato et al, 1970) to adapt mass transfer correlations obtained from fixed beds for fluidized beds by employing bubble assemblage model. It has been shown that the following proposed mass transfer correlations in fixed beds (Kato et al, 1970)

$$Sh/Sc^{1/3} = 0.72[Re_p(d_p/H_f)^{0.6}]^{0.95} \tag{62}$$

for

$$0.1 < Re_p (d_p/H_f)^{0.6} < 5 \tag{63}$$

and

$$Sh/Sc^{1/3} = 1.25[Re_p(d_p/H_f)^{0.6}]^{0.63} \quad (64)$$

for

$$5 \leq Re_p\ (d_p/H_f)^{0.6} \leq 10^3 \quad (65)$$

can be applied to the bubble assemblage model to calculate the particle - gas mass transfer coefficient in fluidized beds by

(i) using the gas velocity equivalent to U_b, the bubble velocity, in calculating the mass transfer coefficient in the bubble phase

(ii) using the gas velocity equivalent to U_{mf} in calculating the mass transfer coefficient in the emulsion phase with U_b to be calculated as follows:

$$U_b = 1.1\ U_{mf}/\epsilon_{mf} \quad (66)$$

and

$$U_b = 0.711\ \sqrt{g d_b} \quad (67)$$

where

$$d_b = 1.4\ \rho_p d_p (\frac{U}{U_{mf}})(\Delta h_l) \quad (68)$$

and

$$\Delta h_l = \frac{(1.1U_{mf}/\epsilon_{mf})^2}{0.708\rho_p d_p (U/U_{mf})g} \quad (69)$$

Miscellaneous other correlations may be found in Upadhyay and Tripathi (1975), which contains some 365 references. All of the above mentioned research on mass transfer in fixed and fluidized bed was based on the assumption that heterogeneous system can be treated at least in principle as

quasi homogeneous systems. Also, the proposed mass transfer coefficients are obtained based nn steady state transpnrt processes. Some recent works, hnwever, do consider the transient cnmponent of fluid-particle mass transfer in fluidized-bed operatinns (see, e.g., Howebink and Rietema, 1980(a) and 1980(b)). Detailed discussion of their model is presented in section MODELING OF FLUIDIZED BED DRYING.

DRYING CHARACTERISTICS OF SOLIDS

The drying characteristics of a given species of solid under specified conditions of the drying medium are required to set up drying schedules and to determine the size of a dryer. These characteristics are often reflected in the drying rate curve. A typical drying rate curve is represented in Fig. 11. While different solids and different conditions of drying often give rise to curves of very different shapes, a drying rate curve usually exhibits two major parts, the so-called constant and the falling rate periods, as marked on the figure.

Constant Drying Rate Period

The mechanism of constant rate drying is that of evaporation from a liquid surface with little interference by the presence of the solid (Nonbehel & Moss, 1970). The resistance to mass transfer is usually assumed to be completely in the boundary layer of the drying gas. Though solid may affect the properties of the liquid surface so that the rate of evaporation is somewhat different from that obtained with a pure liquid, this solid effect is relatively small. It often corresponds to a reduction in the evaporation rate of not exceeding 20% (Nonbehel & Moss, 1970).

The rate of drying in the constant drying rate period is determined by the rate of vaporization of the liquid from the drying surface into the main body of the gas stream. The entire surface of a solid particle tends to stay at the wet-bulb temperature corresponding to the temperature, humidity and quantity of the drying gas. If the condition of the drying gas at the surface of solids remain constant, the surface or wet bulb temperature will also be constant. Consequently, the partial pressure and humidity at the

surface will be the saturation partial pressure and the saturation humidity at the wet-bulb temperature, respectively.

The velocity of the drying gas affects the mass transfer coefficient or equivalently; the resistance to the mass transfer. It should be noted that strictly speaking, a true equilibrium at the wet-bulb temperature is not always assured. However in practical drying situation, it can be assumed that the actual surface will approximate to the wet-bulb temperature for constant-rate drying with a sufficient quantity of the drying gas in the main stream and with heat supplied mainly through convection.

The moisture content at which the drying rate of a product changes from a constant rate to a falling rate, is called the critical moisture content. Generally, it increases with the increase in drying rate. It often depends on the physical properties of the solid, such as shape and size, and also on the drying conditions. It usually need he measured experimentally. Approximate values for many industrial solids are availahle (McCormick, 1973).

Falling-Rate Drying Period

During the falling-rate drying period the surface of a drying particle is not covered with a thin layer of water as is the case during the constant-rate period; the internal resistance to moisture transport becomes greater than the external resistance. As the moisture content of a product falls below the critical point, the drying force decreases along with the drying rate. Also, a moisture gradient appears within the drying product and the product temperature rises ahove the wet-bulh temperature.

The movement of moisture inside a drying specimen may occur by various mechanisms, including liquid diffusion, capillary flow and surface activated

diffusion, depending on the type of solids. For capillary porous products like cereal grains, for example, the following mechanisms are suggested (Brooker et al., 1981)

(1) liquid movement due to surface forces (capillary flow)

(2) liquid movement due to moisture concentration differences (liquid activated diffusion)

(3) liquid movement due to diffusion of moisture on the pore surface (surface diffusion);

(4) vapor movement due to moisture concentration differences (vapor diffusion)

(5) vapor movement due to temperature differences (thermal diffusion);

(6) water and vapor movement due to total pressure differences (hydrodynamic flow)

Luikov et al. (1966) have developed an mathematical model for describing the drying of capillary porous products based on the physical mechanisms listed above. The model equations are a system of partial differential equations of the following form:

$$\frac{\partial x_p}{\partial t} = \nabla^2 K_{11} x_p + \nabla^2 K_{12} T + \nabla^2 k_{13} P \qquad (70)$$

$$\frac{\partial T}{\partial t} = \nabla^2 K_{21} x_p + \nabla^2 K_{22} T + \nabla^2 k_{23} P \qquad (71)$$

$$\frac{\partial P}{\partial t} = \nabla^2 K_{31} x_p + \nabla^2 K_{32} T + \nabla^2 k_{33} P \qquad (72)$$

where K_{11}, K_{22} and K_{33} are the phenomenological coefficients, while the other K-values represent the coupling coefficients. The coupling results from the combined effects of moisture, temperature, and total pressure gradients on the moisture, energy and total mass transfer. At the present time, the phenomenological transfer coefficients are available only for a

very limited number of substances; therefore, Luikov's system of equation has not yet been widely employed.

In actual situations, many simplifying assumption have been made in translating Luikov's rigorous model into working equations. For example, in drying of cereal-grain, the pressure and temperature gradients usually do not have to be considered. Neglecting temperature and pressure gradients, the Luikov equation is reduced to the unsteady-state diffusion equation

$$\frac{\partial x_p}{\partial t} = \nabla^2(D x_p) \tag{73}$$

where

$$D = K_{11} \tag{74}$$

D is usually called the diffusion coefficient. With constant value of D equation (73) becomes the well-known Fukian diffusion equation

$$\frac{\partial x_p}{\partial t} = D\nabla^2 x_p \tag{75}$$

Assuming uniform initial moisture distribution and negligible external resistances, the solution to eqn. (75) for granular particles is (Crank, 1975)

$$\frac{x_p - x_{pe}}{x_{po} - x_{pe}} = \frac{6}{\pi^2} \sum_{h=1}^{\infty} \frac{1}{n^2} \exp\left(-\frac{n^2 \pi^2 X^2}{9}\right) \tag{76}$$

where

$$X = \left[\frac{6}{(d_p \phi_s)}\right] (Dt)^{1/2} \tag{77}$$

It is often feasible (see, e.g., Brooker et al., 1981) to further simplify eqn. (76) by employing only the first term of the infinite series. Thus we have

$$\frac{x_{p(t)}-x_{pe}}{x_{po}-x_{pe}} = \frac{6}{\pi^2} \exp(-Kt) \tag{78}$$

where

$$K = \frac{4\pi^2}{(d_p\phi_s)^2} D \tag{79}$$

The error is less than 5% if the dimensionless quantity Kt > 1.2. The values of the diffusion coefficient, D, in eqns. (76) and (78) are available for various foods (see, e.g., Chirife, 1983) and for cereal grains (see, e.g. Brooker et al. 1981) .

The temperature dependence of the diffusion coefficient is often expressed in an Arrhenius form, i.e.,

$$D=D_o\exp(-E_a/RT) \tag{80}$$

The values of D_o and E_a are available for various foods (Mujumdar, 1983), and for cereal grains (Brooker, 1981). Since the temperature of the material changes with time, the diffusion coefficient D in eqns. (76) and (78) should be replaced hy time-average value $\bar{D}$, which, by definition, is

$$\bar{D} = \frac{1}{t}\int_0^t D\, dt \tag{81}$$

Our discussion so far has implied the assumption of geometrically similar drying curves for the falling rate period of a given material, regardless of the initial moisture content of the material and the initial drying rate. When the diffusion coefficient varies strongly with moisture content, this approach can not be generalized to different initial moisture contents or initial drying rates by introducing a dimentionless moisture content since the diffusion coefficient depends on the ahsolute moisture content itself.

A method for calculating drying rates for the case of moisture-content dependent diffusion coefficient has heen developed (Schoeber, 1978). The method is applicable to a system in which the diffusivity decreases rapidly with declining moisture content below the critical value or to a case where the drying rate is governed hy the rate of mass transfer inside the material. For porous materials, however, the similarity approach has heen shown to be a valid approximation.

For design purposes, usually the data for the average drying rate rather than the average moisture content is preferred. Differentiation of eqn. (78) with respect to time and rearrangement of the resultant expression yields

$$\frac{dx_p}{dt} = -K(x_p - x_{pe}) \tag{82}$$

or

$$\frac{dx_p}{dt} = Ax_p + B \tag{83}$$

where

$$A = -K, \quad B = K \cdot x_{pe} \tag{84}$$

Equation (82) reveals a linear relationship between the average drying rate and moisture content. This is supported hy extensive experimental data and hence is widely used to approximate the drying-rate data.

Luikov (1968) and Lyaboshits *et al*. (1969) have proposed two other expressions for evaluating the average drying rate in terms of the excessive moisture content $x_p - x_{pe}$ as in eqn. (82). They are

$$\frac{dx_p}{dt} = \frac{(x_p - x_{pe})^n}{C + D(x_p - x_{pe})^n} \tag{85}$$

and

$$\frac{dx_p}{dt} = C'(x_p - x_{pe}) + D'(x_p - x_{pe})^2 \qquad (86)$$

where C,C',D,D' and n are experimentally determined constants. In drying of certain materials, like foods (see, Mujumdar, 1983), the drying rate in the falling rate period is characterized by two distinguishable stages. Results obtained by various authors (see, e.g., Jason, 1965; Vaccarezza et al., 1974 and Roman et al., 1979) indicate the existence of an initial straight-line portion, hitherto referred to as the "first falling-rate period," followed by a concave downward or another straight line of different slope, forming the second falling-rate period. The linear relationship between drying rate and moisture content in eqn. (82) or (83) suggests that the Fickian equation should be applicable to the first falling rate period. This has been verified by Vaccarezza et al. (1979). They measured internal moisture distribution during sugar-beet drying and compared the data with the theoretical moisture distributions predicted by Fick's law. A very good agreement was observed.

It has been found that in most cases, the moisture diffusivity is not constant with moisture content in the second falling-rate period (see, e.g., Mujumdar, 1983). Thus the more general diffusion equation, eqn. (73), is prefered for predicting the internal moisture distribution of this period. Crank (1956) has outlined methods for determining the functional dependence of the diffusion coefficient on the moisture content. Several empirical equations for drying cereal grain and foods in the falling rate period are also available (see, e.g., Brooker, 1981 and Mujumdar 1983).

MODELING OF FLUIDIZED BED DRYING

Drying characteristics of a single particle under given fluidization conditions do not adequately describe the drying process in a fluidized bed dryer as a whole, since particles are seldom dried individually. Hydrodynamics of the bed, such as bed expansion, generation and movement of bubbles and mixing of gas and solids, affect significantly the overall performance of the dryer. Thus, to describe its performance quantitatively and mechanistically will require a system of governing equations for the various processes and phenomena occuring in the dryer. A number of assumptions are often made to simplify the solution of such a system of governing equations; these include

(1) volume shrinkage is negligible during the drying process;

(2) temperature gradients within individual particles are negligible;

(3) particle-to-particle heat conduction is negligible;

(4) moisture equilibrium isotherm is known.

Modeling of drying operations in fluidized beds are also based on whether they are batch or continuous. Strictly speaking batch drying is a semi-batch process where the material to be dried is exposed to a continuously flowing stream of drying gas. In continuous operation, the substance to he dried and the gas both pass continuously through the bed.

Batch Operation

Batch fluidized beds are used often for small processing capacity. Capacities of 50 kg/hr or less have been categorized as being "small" (Viswanathan et al., 1982). References regarding the operating data are available (Viswanathan et al., 1982)

Design procedures for batch fluidized beds have been proposed by various investigators (see, e.g. Vanecek et al., 1966; Kunni and Levenspiel, 1969). Most of them, however, are simply based on the total heat and mass balances around the dryer. The interactions among some of the components and entities, for example, generation and motion of hubbles and their effects on transport processes are, generally, not considered. Thus, they are quite empirical in nature and heavily dependent on experimental data.

Recently, some comprehensive and mechanistic models have been developed (Hoebink and Rietema, 1980(a) and 1980(b); Viswanathan, 1982; Viswanathan and Rao, 1982; Viswanathan et al., 1983; Viswanathan and Rao, 1984) to describe the drying process in a gas-solid batch fluidized bed. These models have incorporated the effect of bubbling characteristics and various mechanisms of transport processes in the bed.

Model proposed by Viswanathan and Rao

As previously stated, Viswanathan and his co-workers have published a series of papers which eventually have culminated in a comprehensive model for a batch fluidized-bed dryer (Viswanathan and Rao, 1984). Their model is essentially based on the three phase theory of fluidization, which includes bubble, cloud-wake and emulsion phases (see Fig. 12 for schematic representation). The tanks-in-series model is assumed to be applicable to the emulsion phase; in other words, the emulsion phase is treated as being composed of a number of compartments, with emulsion gas being completely mixed in each compartment. Both the downflow and upflow modes (the latter is illustrated in Fig. 14) have been assumed separately for the overall flow of the emulsion gas. In the bubble and cloud-wake phases, the drying gas is considered to be in plug flow. The solids in the dryer are regarded as

being homogeneous with negligible internal resistance to mass and heat transfer. They are considered to be throughly mixed in the bed. Consequently, the temperature of the bed, the moisture content of the particles and hence the equilibrium surface moisture content of the drying gas are independent of the position in the bed. Furthermore, the drying gas is assumed to be at quasi-steady state with respect to the solids in the bed. This is due to the fact that the residence time of the drying gas is much shorter than the time needed to dry the solids. Thus, the moisture and energy transfer in the gas phase in conjunction with the solids is approximated by that under the steady state conditions. Based on these assumptions for the change of moisture and energy in various phases, a set of governing equations has been derived. The procedure of the derivation is described below

Bubble phase. A moisture balance around the controlled volume illustrated in Fig. 13 yields (see APPENDIX A)

$$u_b \frac{dx_b}{dz} = (K_{bc})_b (x_c - x_h) \tag{87}$$

Cloud-wake phase. Referring to Fig. 13, a similar governing equation for the cloud-wake phase can be derived as below (see APPENDIX B)

$$(\alpha+\beta)\epsilon_{mf} u_b \frac{dx_c}{dz} = (K_{ce})_b (x_{ei} - x_c) - (K_{bc})_h (x_c - x_b) + (\alpha+\beta)(1-\epsilon_{mf}) S_p K_{pg} (x_p^* - x_c) \tag{88}$$

Emulsion gas. For the case with drying gas flowing upward through the emulsion phase as depicted in Fig. 13, a moisture balance around compartment i results in (see APPENDIX C)

$$\frac{[1-\delta_b(1+\alpha+\beta)]}{\delta_b} u_e \epsilon_{mf} \frac{(x_{ei} - x_{in(i)})}{(z_i - z_{i-1})}$$

$$= \frac{[1-\delta_b(1+\alpha+\beta)]}{\delta_b} (1-\epsilon_{mf}) S_p K_{pg} (x_p^* - x_{ei}) + (K_{ce})_b (\bar{x}_c - x_{ei}) \quad (89)$$

$\bar{x}_c$ in eqn. (89) is the average moisture content of the gas in cloud in contact with the ith compartment. It is defined as

$$\bar{x}_c = \frac{1}{z_i - z_{i-1}} \int_{z_{i-1}}^{z_i} x_c dz \quad (90)$$

Equations (87), (88) and (89) can be rewritten in dimensionless form as

$$\frac{dx_b}{dZ} = a_o(x_c - x_b) \quad (91)$$

$$\frac{dx_c}{dZ} = a_1(x_{ei} - x_c) + a_2(x_b - x_c) + a_3(x_p^* - x_c) \quad (92)$$

$$\frac{(x_{ei} - x_{in(i)})}{(Z_i - Z_{i-1})} = a_4(x_p^* - x_{ei}) + a_5(x_c - x_{ei}) \quad (93)$$

where

$$a_0 = \frac{(K_{bc})_b H_f}{u_b}, \quad a_1 = \frac{(K_{ce})_b H_f}{(\alpha+\beta)\epsilon_{mf} u_b} \quad (94)$$

$$a_2 = \frac{(K_{bc})_b H_f}{(\alpha+\beta)\epsilon_{mf} u_b}, \quad a_3 = \frac{(\alpha+\beta)(1-\epsilon_{mf}) S_p K_{pg} H_f}{(\alpha+\beta)\epsilon_{mf} U_b} \quad (95)$$

$$a_4 = \frac{[1-\delta_b(1+\alpha+\beta)]}{\delta_b} (1-\epsilon_{mf}) S_p K_{pg} \delta_b H_f$$

$$a_5 = \frac{(K_{ce})_b \delta_b H_f}{[1-\delta_b(1+\alpha+\beta)] u_e \epsilon_{mf}} \quad (96)$$

$$Z = \frac{z}{H_f} \tag{97}$$

Eliminating x_c from eqn. (92) by resorting to eqn. (91) yields

$$b_2 \frac{d^2 x_b}{dZ^2} + b_1 \frac{d\, x_b}{dZ} + b_o x_b = x_{ei} + b x_p^* \tag{98}$$

where

$$b_0 = 1 + \frac{a_3}{a_1} \tag{99}$$

$$b_1 = \frac{a_o + a_1 + a_2 + a_3}{a_0 a_1} \tag{100}$$

$$b_2 = \frac{1}{a_0 a_1} \tag{101}$$

$$b = \frac{a_3}{a_1} \tag{102}$$

Tbe solution to eqn. (98) is

$$x_b = \frac{1}{b_0} (x_{ei} + b x_p^*) + d_1 \exp[m_1 (Z - Z_{i-1})] + d_2 \exp[m_2 (Z - Z_{i-1})],$$

$$Z_i \leq Z \leq Z_{i-1}, \qquad 1 \leq i \leq N \tag{103}$$

where

$$m_{1,2} = \frac{-b_1 \pm (b_1^2 - 4 b_0 b_2)^{0.5}}{2 b_2} \tag{104}$$

and

$$Z_o = 0 \tag{105}$$

d_1 and d_2 in eqn. (103) are constants to be determined from tbe boundary conditions for each compartment. Combining eqns. (91) and (103) we bave

$$x_c = \frac{1}{b_0}(x_{ei}+bx_p^*) + (1+\frac{m_1}{a_o})d_1\exp[(m_1(Z-Z_{i-1})]$$

$$+ (1+\frac{m_2}{a_o})d_2\exp[(m_2(Z-Z_{i-1})], \quad Z_{i-1}\leq Z\leq Z_i, \quad 1\leq i\leq N \qquad (106)$$

Substitution of eqn. (106) for x_c in eqn. (93) results in

$$x_{ei} - x_{in(i)} = -(\frac{b}{b_0}a_5 + a_4)(Z_1-Z_{i-1})x_{ei}$$

$$+ (a_4+a_5\frac{b}{b_0})(Z_i - Z_{i-1})x_p^*$$

$$+ a_5(1+\frac{m_1}{a_0})\frac{d_1}{m}[\exp(m_1Z_i) - \exp(m_1Z_{i-1})]$$

$$+ a_5(1+\frac{m_2}{a_0})\frac{d_2}{m_2}[\exp(m_2Z_i) - \exp(m_2Z_{i-1})] \qquad (107)$$

Rearrangement of this equation yields

$$x_{ei} = (x_{in(i)} + f_1d_1 + f_2d_2 + gx_p^*)/(1+g) \qquad (108)$$

where

$$f_1 = \frac{a_5}{m_2}(1+\frac{m_1}{a_0})[\exp(m_1Z_i) - \exp(m_1Z_{i-1})] \qquad (109)$$

$$f_2 = \frac{a_5}{m_2}(1+\frac{m_2}{a_0})[\exp(m_2Z_i) - \exp(m_2Z_{i-1})] \qquad (110)$$

$$g = (a_4+a_5\frac{b}{b_0})(Z_i - Z_{i-1}) \qquad (111)$$

From eqns. (103), (106) and (108), we obtain, respectively

$$x_c = x_b + a_0(m_1d_1\exp[m_1(Z-Z_{i-1})] + m_2d_2\exp[m_2(Z-Z_{i-1})]) \qquad (112)$$

and

$$x_b = \frac{x_{in(i)}}{b_0(1+g)} + \left[1 - \frac{1}{h_0(1+g)}\right]x_p^* + d_1\left\{\exp\left[m_1(Z-Z_{i-1})\right] + \frac{f_1}{b_0(1+g)}\right\} + d_2\left\{\exp\left[m_2(Z-Z_{i-1})\right] + \frac{f_2}{b_0(1+g)}\right\} \quad (113)$$

The continuity condition, stating that the mass flow of moisture in the emulsion gas at the entrance of each compartment is equal to that at the exit of the preceeding compartment, comprises the boundary condition for each compartment, except for the first one (see Fig. 14). In other words,

$$u_{e(i)}[1-\delta_h(1+\alpha+\beta_i)]x_{in(i)} = u_{e(i-1)}[1-\delta_b(1+\alpha+\beta_{i-1})]x_{ei-1} \quad \text{for } i > 1 \quad (114)$$

The boundary contion for the first compartment is

$$x_{in(1)} = x_b = x_c = x_o \quad \text{at } Z=0 \quad (115)$$

The compartment size Δh_i and other parameters in eqns. (108), (112) and (113) are determined from the relationships listed in tahle 3. The moisture content of the outlet gas is given hy

$$U_0 x_{out} = \delta_b u_b\left[x_b\right]_{Z=1} + (\alpha+\beta)\epsilon_{mf}x_c\left[_{Z=1}\right] + [1-\delta_b(1+\alpha+\beta)]u_e\epsilon_{mf}x_{eN} \quad (116)$$

Solid phase. A moisture balance around the entire solid phase results in (see APPENDIX D)

$$\frac{dx_p}{dt} = \frac{\rho U_0 A_t}{M_p}(x_{in} - x_{out}) \quad (117)$$

The appropriate initial condition is

$$x_p = x_{po} \quad \text{at } t = 0 \quad (118)$$

The corresponding energy balance is (see APPENDIX E)

$$\frac{dT}{dt} = \frac{\rho U_0 A_t}{M_p c_p} [(x_{in} - x_{out})\gamma_0 + (T_{in} - T)c_g] \tag{119}$$

The initial condition for this equation is

$$T = T_o \qquad \text{at } t = 0 \tag{120}$$

Equations (117) and (119) can also be rewritten respectively as

$$\frac{dx_p}{dt} = \frac{\rho U_0 A_t}{M_p} E(x_{in} - x_p^*) \tag{121}$$

$$\frac{dT}{dt} = \frac{\rho U_0 A_t}{M_p c_p} [(x_{in} - x_p^*)E\gamma_0 + (T_{in} - T)c_g] \tag{122}$$

where

$$E = \frac{(x_{in} - x_{out})}{(x_{in} - x_p^*)} \tag{123}$$

It has been assumed that the following relationship exists between the equilibrium surface moisture content of the gas and the moisture content of the particles

$$x_p^* = A\, x_p^n \tag{124}$$

where A is the equilibrium constant to be determined. To incorporate the effect of temperature on the equilibrium constant, it is further assumed that

$$A = BT^m \tag{125}$$

where B and m are constants. Now eqns. (121) and (122) become, respectively,

$$\frac{dx_p}{dt} = \frac{\rho U_0 A_t}{M_p} E(x_{in} - BT^m x_p^n) \tag{126}$$

$$\frac{dT}{dt} = \frac{\rho U_o A_t}{M_p c_p}[(x_{in} - BT^m x_p^n)E\gamma_o + (T_{in} - T)c_g] \qquad (127)$$

Equations (126) and (127) are coupled differential equations, which can only be solved numerically. If the variation in T^m is negligible compared to variation in x_p^n, eqns. (126) and (127) can be solved independently.

In the constant rate drying period, x_p^* is the saturated moisture content of gas at the surface of the particle, x_{po}^*, which is constant. It follows from eqn. (121), that

$$x_p = x_{po} - \frac{\rho U_o A_t}{M_p} E (x_{po}^* - x_{in})t \qquad (128)$$

Equations (108), (112), (113), (116), (126) and (127) with the appropriate initial and boundary conditions constitute the governing equations of the model. These governing equations need be solved simultaneously. Starting with t=0, $T=T_o$, $x_p=x_{po}$ and $x_p^*=x_{po}^*$, the use of eqns. (108), (112) and (113) for all the compartments, beginning at the one at the bottom gives the initial variation of moisture content of the gas in different phases along with the bed height. The moisture content of the exit gas x_{out} is evaluated from eqn. (116). Equation (126) and (127) can then be integrated to yield the temperature and moisture content of the particles within the time interval dt. These values are used for calculating the temperature and moisture content of the gas in the same time interval dt. Repeating the same procedure, the time-dependent profiles of temperature and moisture content of the particles and the gas can be obtained.

In the case where gas to particle mass transfer resistance is negligible, that is $x_p^*=x_e=x_c$, a simplified two-phase (emulsion-bubble phase) model can be employed. The governing equation for the bubble phase eqn. (91) becomes

$$\frac{dx_b}{dZ} = a_o(x_p^*-x_b) \tag{129}$$

The solution to this equation is

$$x_b(Z)=x_p^* + [x_b(Z_{i-1})-x_p^*]\exp[-\theta_i(Z-Z_{i-1})],$$

$$Z_{i-1} \leq Z \leq Z_i, \qquad i \geq 1 \tag{130}$$

where

$\theta_i=(K_{hc})_b H_f/u_b$, evaluated in ith compartment

and

$Z_o = 0$

From eqn. (130), the moisture content of the gas at the outlet of the ith and the i-1th compartments are, respectively, given by

$$x_b(Z_i) = x_p^*+[x_b(Z_{i-1})-x_p^*]\exp[-\theta_i(Z_i-Z_{i-1})] \tag{131}$$

and

$$x_b(Z_{i-1})=x_p^*+[x_b(Z_{i-2})-x_p^*]\exp[-\theta(Z_{i-1}-Z_{i-2})] \tag{132}$$

Combination of eqns. (131) and (132) yields

$$x_b(Z_i)=x_p^*+(x_b(Z_{i-2})-x_p^*)]\exp[-\theta_{i-1}(Z_{i-1}-Z_{i-2})-\theta_i(Z_i-Z_{i-1})] \tag{133}$$

Following this recurssive relationship, the moisture content of the outlet gas in the bubble phase from the top compartment (i=N) can be evaluated from

$$x_b(Z_N)=x_b(1)=x_p^*+(x_{in}-x_p^*)\exp[-\sum_{i=1}^{N}\theta_i\Delta Z_i] \tag{134}$$

Then the moisture content of the outlet gas at the exit of the bed is obtained by combining gas flow from the bubble phase and emulsion phase

$$U_o x_{out}=\delta_b u_b[x_b(1)+(\alpha+\beta)\epsilon_{mf}x_e]+[1-\delta_b(1+\alpha+\beta)]u_e\epsilon_{mf}x_e \tag{135}$$

where the parameters should be evaluated at the Nth compartment. From $x_c=x_e=x_p^*$, eqns. (92) and (93) can be combined into one governing equation for cloud-wake phase and emulsion gas. The resultant expression takes the form

$$x_{ei} = x_c = x_e, \qquad 1 < i < N \tag{136}$$

and for the first compartment

$$u_e[1-\delta_b(1+\alpha+\beta)]\epsilon_{mf}\frac{(x_e-x_o)}{Z_1} = (K_{bc})_b(\bar{x}_b^1-x_e) \tag{137}$$

where

$$\bar{x}_b^1 = \frac{1}{Z_1}\int_0^{Z_1} x_b dZ \tag{138}$$

The governing equations for the solid phase eqns. (126) and (127) remain invariant since no new assumptions are introduced in the derivation.

In summary, the governing equations for the simplified model consist of following five equations

$$x_b(Z)=x_{ei}+[x_h(Z_{i-1})-x_{ei}]\exp[-\theta_i(Z-Z_{i-1})] \tag{139}$$

$$U_o x_{out}=\delta_b u_b[x_b(1)+(\alpha+\beta)\epsilon_{mf}x_{eN}]+[1-\delta_h(1+\alpha+\beta)]u_e\epsilon_{mf}x_{eN} \tag{140}$$

$$u_e[1-\delta_b(1+\alpha+\beta)]\epsilon_{mf}\frac{x_e-x_o}{Z_1} = (K_{bc})_b(\bar{x}_b^1-x_e) \tag{141}$$

$$\frac{dx_p}{dt} = \frac{PU_o A_t}{M_p} (x_{in} - x_{out}) \tag{142}$$

$$\frac{dT}{dt} = \frac{PU_o A_t}{M_p C_p} [(x_{in} - x_{out})\gamma_o + (T_{in} - T)c_g] \tag{143}$$

The calculation procedure is similar to that described for the general model.

The criterion adopted to determine the validity of the simplified model is (Viswanthan et al., 1983)

$$N_r \geq 50 \tag{144}$$

where

$$N_r = S_p K_{pg} (1-\epsilon_{mf}) \frac{H_{mf}}{U_o} \tag{145}$$

The restrictions on the application of the model are the assumptions that the temperature and moisture content inside the particles, and the temperature of the bed are uniform. The former may be true only for small particles. Also, the gas-solid transfer mechanism in the emulsion phase may differ from that in wake region. The solids in the wake region are continuously washed out from the wake and replaced by the fresh emulsion solids. Thus, the moisture transfer between the solids and gas in the wake is determined by the exchange rate between solids in the wake and those in the emulsion phase; in other words, it is determined by the contact time between the solids and gas in the wake. In the proposed model, however, solids are treated simply as an entitiy and the mass transfer between the gas and solids in the emulsion phase and that in the wake region are considered to be the same.

Model proposed by Hoebink and Rietema

The gas-solids transfer mechanism in the emulsion phase and that in the cloud-wake have been investigated separately in the model proposed by Hoebink and Rietema (1980(a), 1980(b)). The former is considered to be affected by the profile of moisture content inside a particle, that is, the transfer mechanism is diffusion controlled. The latter is assumed to he governed only by the flow through a thin concentration boundary layer inside the particle because of the relatively short residence time of the gas in the cloud.

The model is based on the three phase theory of fluidization. For simplicity, a uniform bubble size is assumed throughout the bed. The conventional bubble-cloud model is modified through several additional assumptions: 1) the flow of both gas and solids through the cloud is constant and equal to the flow at the bubble equator; 2) the gas and solids pass the cloud in plug flow; 3) the zone of the cloud where exchange of moisture takes place between cloud and solids, and between cloud and emulsion gas is restricted to the hatched area, confined with $\pi/4 < \theta \quad 3\pi/4$ (see Figs. 15 and 16). The solids are assumed to be perfectly mixed. The emulsion gas is assumed to reach thermal and concentration equilibrium with the solids within a negligiblily short distance from the distributor. The solids are considered to be dried only in the falling rate drying period, during which moisture transfer is mainly controlled by diffusion process inside the particles. The Fickian diffusion model is assumed adequate in describing this diffusion process. The procedure in deriving the model is described below.

Cloud-wake phase. There are three different regions in the cloud-wake phase. The first region is confined hy $0 \leq \theta \leq \pi/4$, through which a through

flow of gas from the bubble phase passes. Since the moisture exchange does not occur in this region, the moisture content of the cloud in it equals that of the gas bubbles. The second region is represented by hatched area in Fig. 15, where moisture exchange takes place between cloud and emulsion gas, and between solids and gas in the cloud. Due to the moisture exchange, the moisture content of the cloud in this region increases with θ. The third region is bordered with $3\pi/4 \leq \theta \leq \pi$, where through-flow gas reenters the bubble at its base. Since there's no moisture transfer as in the first region, the moisture content of the cloud in this region remains constant.

For the second region, a moisture balance around the controlled volume depicted in Fig. 17 yields (see APPENDIX F)

$$\frac{Q_{gc}}{\sin\theta}\frac{\partial x_c}{\partial\theta} = 2\pi R_c^2 K_c(x_e-x_c)+\frac{2}{3}\pi(R_c^3-R_b^3)(1-\epsilon_{mf})S_p K_{pg}(x_p^*-x_c) \qquad (146)$$

The appropriate boundary condition is

$$x_c=x_b \qquad \text{at } \theta = \frac{\pi}{4} \qquad (147)$$

Assuming the mass transfer coefficient between cloud and solids K_{cp} to be constant, integration of eqn. (146), subject to eqn. (147), gives

$$\frac{\lambda_1 x_e+\lambda_2 x_p^*-(\lambda_1+\lambda_2)x_c}{\lambda_1 x_e+\lambda_2 x_p^*-(\lambda_1+\lambda_2)x_b} = \exp\left\{\frac{2\pi}{Q_{gc}}[R_c^2K_c+\frac{1}{3}(R_c^3-R_b^3)(1-\epsilon_{mf})K_{pg}S_p](\cos\theta-\frac{\sqrt{2}}{2})\right\} \qquad (148)$$

where

$$\lambda_1 = \frac{2\pi R_c^2 K_c}{Q_{gc}} \qquad (149)$$

and

$$\lambda_2 = \frac{\frac{2}{3}\pi(R_c^3-R_b^3)(1-\epsilon_{mf})K_{cp}S_p}{Q_{gc}} \qquad (150)$$

Since the moisture content of the emulsion gas is in equilibrium with the surface moisture content of the particles, it follows that $x_e = x_p^*$. Thus, eqn. (148) can be rewritten as

$$\frac{x_p^* - x_c}{x_p^* x_b} = \exp\left\{ \frac{2\pi}{Q_{gc}} [R_c^2 K_c + \frac{1}{3}(R_c^3 R_b^3)(1-\epsilon_{mf}) K_{pg} S_p](\cos\theta - \frac{\sqrt{2}}{2}) \right\} \quad (151)$$

The moisture content of the gas in the through flow reentering a huhhle at its base is denoted by, x_{en}. It is defined as

$$x_{en} = x_c \qquad \text{at } \theta = \frac{3}{4}\pi \quad (152)$$

Using the relationship between x_c and x_{en} and eqn. (52), we obtain

$$\frac{x_{en} - x_p^*}{x_b - x_p^*} = \exp\left\{ - \frac{2\sqrt{2}\pi}{Q_{gc}} [R_c^2 K_c + \frac{1}{3}(R_c^3 - R_b^3)(1-\epsilon_{mf}) K_{pg} S_p] \right\} \quad (153)$$

An energy balance around the controlled volume indicated in Fig. 17 leads tn (see APPENDIX G)

$$\frac{Q_{gc}\rho_g c_g}{\sin\theta} \frac{\partial T_c}{\partial \theta} = 2\pi R_p^2 H_{ce}(T_e - T_c) + \frac{2}{3}\pi(R_c^3 - R_b^3)(1-\epsilon_{mf}) h_p S_p (T_p - T_c) \quad (154)$$

The boundary condition is

$$T_c = T_b \qquad \text{at } \theta = \frac{\pi}{4} \quad (155)$$

Integration of eqn. (154), subject to eqn. (155), yields

$$\frac{\beta_1 T_e + \beta_2 T_p - (\beta_1 + \beta_2) T_c}{\beta_1 T_e + \beta_2 T_p - (\beta_1 + \beta_2) T_b} = \exp\left[\frac{2\pi}{Q_{gc}\rho_g c_g} (H_{ce} R_c^2 + \frac{R_c^3 - R_b^3}{3}(1-\epsilon_{mf}) h_p S_p)(\cos\theta - \frac{\sqrt{2}}{2}) \right] \quad (156)$$

where

$$\beta_1 = \frac{2\pi R_p^2 H_{ce}}{T_{in}} \quad , \qquad \beta_2 = \frac{\frac{2}{3}\pi(R_c^3 - R_b^3)(1-\epsilon_{mf})h_p S_p}{T_{in}}$$

and

$$\beta_3 = \frac{Q_{gc}\rho_g c_g}{T_{in}} \tag{157}$$

It is assumed that $T_p = T_e$, eqn. (156) then reduces to

$$\frac{T_c - T_p}{T_b - T_p} = \exp\{\frac{2\pi}{Q_{gc}\rho_g c_g}[H_{ce}R_c^2 + \frac{R_c^3 - R_b^3}{3}(1-\epsilon_{mf})h_p S_p](\cos\theta - \frac{\sqrt{2}}{2})\} \tag{158}$$

The temperature of the drying gas reentering the buhble at its base, T_{en}, is related to T_c through

$$T_{en} = T_c \qquad \text{at } \theta = 3/4\ \pi \tag{159}$$

Thus from eqn. (158),we obtain

$$\frac{T_{en} - T_p}{T_b - T_p} = \exp[\frac{-2\sqrt{2}\pi}{Q_{gc}\rho_g c_g}(H_{ce}R_c^2 + \frac{R_c^3 - R_b^3}{3}(1-\epsilon_{mf})h_p S_p)] \tag{160}$$

Buhble phase. A moisture balance around the controlled volume shown in Fig. 18 yields (see APPENDIX H)

$$\delta_b u_b \frac{dx_h}{dz} = n\, Q_{gc}(x_{en} - x_b) \tag{161}$$

where n is numher of bubbles per unit hed volume. The boundary condition for eqn. (161) is

$$x_b = x_{in} \qquad \text{at } z=0 \tag{162}$$

Substituting for x_{en} in eqn. (161) from eqn. (153) and integrating the resultant equation gives

$$\frac{x_b - x_p^*}{x_{in} - x_p^*} = \exp\left[-\frac{nQ_{gc}z}{u_b\delta_b}(1-\beta_m)\right] \tag{163}$$

where

$$\beta_m = \exp\left\{-\frac{2\pi\sqrt{2}}{Q_{gc}}\left[R_c^2K_c + \frac{1}{3}(R_c^3-R_b^3)(1-\epsilon_{mf})K_{pg}S_p\right]\right\} \tag{164}$$

In similar fashion, an energy balance yields (see APPENDIX I)

$$\delta_b u_b \frac{dT_b}{dz} = nQ_{gc}(T_{en}-T_b) \tag{165}$$

with the boundary condition

$$T_b = T_o \qquad \text{at } z = 0 \tag{166}$$

Equation (165), combined with eqn. (160), results in

$$\frac{T_b - T_p}{T_{in} - T_p} = \exp\left[-\frac{nQ_{gc}z}{\delta_b u_b}(1-\beta_h)\right] \tag{167}$$

where

$$\beta_h = \exp\left\{\frac{-2\pi\sqrt{2}}{Q_{gc}}\left(H_{ce}R_c^2 + \frac{R_c^3-R_b^3}{3}h_pS_p\right)\right\} \tag{168}$$

The temperature of the exit gas T_{out} can be determined from an energy balance over all the outlet streams. Neglecting the temperature difference between cloud and emulsion phases, it can be approximated as

$$T_{out} = (1-s)T_p + sT_b(H_f) \tag{169}$$

In the expression, s is the fraction of gas flowing through the bed as bubbles, and is evaluated through

$$s = \frac{u_b}{U_o}\delta_b \tag{170}$$

Since the bed temperature is assumed to be uniform, the moisture content of the exit gas, x_{out}, can be related to T_{out} via an energy balance over the entire dryer. It states

$$\gamma_o(x_{out}-x_{in}) = (c_g+x_{in}c_w)T_{in} - (c_g+x_{out}c_w)T_{out} \qquad (171)$$

Emulsion gas. From the assumptions at the outset of this section:

$$x_e=x_p^*$$

and

$$T_e=T_p$$

the state of the emulsion gas is determined by that of the particles.

Solid particles. Two mechanisms for the mass transfer between gas and solids are considered to exist. In the wake region, solid particles are exposed, for a very short period, to a gas concentration which is lower than that in the emulsion phase. The concentration profile inside the particle wouldn't be able to respond to such a sudden change in the gas concentration. Thus, it is reasonable to assume that the mass transfer is controlled by the resistance in the gas film surrounding the particle and the concentration difference across it. On the other hand, because of the relatively long contact time between particles and the emulsion gas, the mass transfer is likely to he affected also by the diffusion of moisture inside the particle. The combination of these two mechanisms gives an overall description of mass transfer between the solids and the drying gas.

a). Solids in the cloud-wake phase. The transport of moisture inside the particle follows Fick's law of diffusion. For constant diffusivity of moisture and a spherical particle, it can he rewritten as (see, e.g., Bird et al., 1960)

$$\frac{\partial x_p}{\partial t} = \frac{D}{r^2}\frac{\partial}{\partial r}\left(r^2\frac{\partial x_p}{\partial r}\right) \qquad (172)$$

The appropriate initial conditions are

$$t=0 \qquad x_p = x_{po} \qquad 0 < r \leq R_p \tag{173}$$

and the appropriate boundary conditions are

$$t>0 \begin{cases} \dfrac{\partial x_p}{\partial r} = 0 & r=0 \\ -D \dfrac{\partial x_p}{\partial r} 4\pi R_p^2 = V_p \dfrac{\partial x_p^*}{\partial t} & r=R_p \end{cases} \tag{174}$$

The second boundary condition states that the flow of moisture out of a particle through its surface is equal to the increase in the moisture content of the gas surrounding it. The solution of eqn. (172), subject to eqns. (173) and (174) is available (Crank, 1956; Carslaw and Jaeger, 1959). It takes the form

$$x_p = \frac{x_{po}}{E+1} - \frac{2ER_p x_{po}}{3r} \sum_{i=1}^{\infty} \exp(-q_i^2 F_{01}) \frac{E^2 q_i^4 + 3(2E+3)q_i^2 + 9}{E^2 q_i^4 + 9(E+1)q_i^2} \cdot \sin(q_i r/R_p) \sin q_i \tag{175}$$

where

$$F_{01} = Dt/R_p^2, \quad E = \frac{V_p}{\frac{4}{3}\pi R_p^3 m} \tag{176}$$

and q_i's are positive roots of the equation

$$(3+Eq_i^2)\tan q_i = 3q_i \tag{177}$$

m in eqn. (176) is equilibrium constant relating the moisture content of the drying gas and that of the particle. The moisture content of the particle in ultimate equilibrium with the drying gas, x_{pe} can be evaluated through eqn (175) by letting $t \to \infty$. It is

$$x_{pe} = \frac{x_{po}}{E+1} \tag{178}$$

The coefficient of mass transfer inside the particles, K_{p1}, is defined as

$$K_{p1}(x_{pR}-x_{pe}) = -D(\frac{\partial x_p}{\partial r})_{r=R_p} \tag{179}$$

Combining eqns, (175) and (179), we obtain

$$Sh_{p1} = \frac{K_{p1}R_p}{D} = \frac{1}{3} E \frac{\sum_{1}^{\infty} \exp(-q_i^2 F_{01}) \frac{q_i^2}{E^2 q_i^2 + 9(E+1)}}{\sum_{1}^{\infty} \exp(-q_i^2 F_{01}) \frac{1}{E^2 q_i^2 + 9(E+1)}} \tag{180}$$

So far, the resistance in the gas film has been neglected. If its effect is incorporated into the overall mass transfer coefficient, K_{cp}, we obtain

$$\frac{1}{K_{pg}} = \frac{1}{K_g} + \frac{1}{mK_{p1}} \tag{181}$$

K_{p1} is determined by eqn. (180) with $t=t_1$, the average residence time of solids in the cloud with volume V_θ. We consider the solids to pass through the cloud at the same velocity as that for the through-flow gas. t_1 is, therefore, determined by

$$t_1 = \frac{V_\theta}{Q_{gc}} = \frac{2}{3}\pi \frac{(R_c^3 - R_b^3)\epsilon_{mf}}{Q_g} (\frac{\sqrt{2}}{2} - \cos\theta) \tag{182}$$

and V_θ is enclosed between angles $\pi/4$ and θ. In case where

$$E \tilde{=} 1/m, \tag{183}$$

which implies $\epsilon \tilde{=} 0.5$, mK_{p1} can be approximated by (Hoebink and Rietema, 1980(b))

$$mK_{p1} = \frac{R_p}{3t_1} \tag{184}$$

Combining eqns. (181) and (182), we obtain

$$K_{pg} = \frac{K_g R_p}{R_p + 3K_g t_1} \tag{185}$$

Substituting for t_1 in eqn. (185) from eqn. (182) yields

$$K_{pg} = K_g \left[1+2\pi \frac{(R_c^3 - R_b^3)}{Q_g} (1-\epsilon_{mf}) \frac{K_g}{R_p} (\frac{\sqrt{2}}{2} - \cos\theta)\right]^{-1} \tag{186}$$

Recall that in deriving eqn. (151), we assume k_{pg} to be constant. It could now be replaced by its θ-average value, which can be obtained through integration of eqn. (186). A better way of doing it, however, is to go back to the original differential eqn. (146). Substituting for k_{pg} in eqn. (146) from eqn. (186) and following the same procedure as that in deriving eqn. (151), we obtain (see APPENDIX J)

$$\frac{x_c - x_{PR}/m}{x_b - x_{PR}/m} = \exp\left[\frac{2\pi R_c^2}{Q_{gc}} K_c (\frac{\sqrt{2}}{2} - \cos\theta)\right] \cdot \left[1+2\pi \frac{(R_c^3 - R_b^3)}{Q_{gc}} (1-\epsilon_{mf}) \frac{K_g}{R_p} (\frac{\sqrt{2}}{2} - \cos\theta)\right]^{-1} \tag{187}$$

x_{en} can be evaluated from the above equation by setting $\theta = \frac{3}{4}\pi$. Equation (163) can now be rewritten as

$$\frac{x_b - x_{PR/m}}{x_{in} - x_{PR/m}} = \exp\left[-\frac{nQ_g(1-\beta_m)z}{u_b \delta_b}\right] \tag{188}$$

in which

$$\beta_m = \exp(\frac{2\sqrt{2}\pi R_c^2}{Q_{gc}} K_c) \left[1 + 2\sqrt{2}\pi \frac{(R_c^3 - R_b^3)}{Q_{gc}} (1-\epsilon_{mf}) \frac{K_g}{R_p}\right]^{-1} \tag{189}$$

Taking an average of the moisture content of the gas from the emulsion phase and bubble phase at the exit, based on their flow rates, we ohtain the moisture content of the outlet gas as

$$x_{out} = (1-s)\frac{x_{pR}}{m} + sx_b(H_f) \tag{190}$$

Combination of eqns. (188) and (190) yields

$$\frac{x_{out}-x_{PR}/m}{x_{in}-x_{PR}/m} = s \exp\left[-\frac{Q_{gc}(1-\beta_m)H_f}{u_b\delta_b}\right] \tag{191}$$

b). Solids in the emulsion phase. The assumption of the complete mixing of solids and gas in the emulsion phase implies that the drying characteristics of particles can be represented by that of one single particle. Since all particles are assumed to be identical, the gas flow to which an individual particle is exposed equals the total gas volumetric flow divided by the total number of particles in the bed. The average moisture content of the particle tends to reach the ultimate equilibrium with the emulsion gas during its relatively long contact time with the emulsion gas. The profile of moisture concentration inside the particle can be obtained by solving the following Fickian diffusion equation;

$$\frac{\partial x_p}{\partial t} = \frac{D}{r^2}\frac{\partial}{\partial r}\left(r^2\frac{\partial x_p}{\partial r}\right) \tag{192}$$

with initial condition

$$x_p = x_{po} \qquad \text{for } t=0 \quad 0 < r \leq R_p \tag{193}$$

and the boundary conditions

$$\frac{\partial x_p}{\partial r} = 0 \qquad \text{for } t > 0 \quad r=0, \tag{194}$$

and

$$-D\frac{\partial x_p}{\partial r} = \bar{\phi}_p \quad \text{for } t > 0 \quad r=R_p \tag{195}$$

where $\bar{\phi}_p$ is the average moisture flux from the particles and is given by

$$4\pi R_p^2\bar{\phi}_p = Q_p(x_{out}-x_{in}) \tag{196}$$

Substituting for x_{out} from eqn. (190) yields

$$\bar{\phi}_p = \frac{(1-Y)Q_p}{4\pi R_p^2}\left(\frac{x_{PR}}{m} - x_{in}\right) \tag{197}$$

in which

$$Y = s \exp\left[- \frac{Q_{gc}(1-\beta_m)H_f}{u_b \delta_b} \right] \tag{198}$$

Q_p in eqn. (197) is the gas flow to which an individual particle is exposed. It is determined as

$$Q_p = \frac{Q_g}{N} = \frac{U_o A_t}{A_t H_f (1-\epsilon_{mf})(1-\delta_b)/(\frac{4}{3}\pi R_p^3)}$$

$$= \frac{4\pi R_p^3 U_o}{3H_f(1-\epsilon_{mf})(1-\delta_b)} \tag{199}$$

If we define the specific surface area of the particles based on unit volume of the bed, S_{pb}, as

$$S_{pb} = (1-\epsilon_{mf})(1-\delta_b)\frac{6}{d_p \phi_s} \tag{200}$$

Equation (197) can now be rewritten as

$$\bar{\phi}_p = \frac{(1-Y)U_o}{H_f S_{pb}}\left(x_{PR}/m - x_{in}\right) \tag{201}$$

$$= \bar{K}_g(x_{PR}/m - x_{in})$$

$\bar{K}_g$, which is defined in eqn. (201), is the average mass transfer coefficient. Substituting for $\bar{\phi}_p$ in eqn. (195) from eqn. (201), the boundary condition, eqn. (195), can be rewritten as

$$-D\frac{\partial x_p}{\partial r} = \bar{K}_g\left(\frac{x_{PR}}{m} - x_{in}\right) \qquad t > 0, \quad r = R_p \tag{202}$$

Equation (195), subject to eqns. (193) and (202) can be solved by means of Laplace transformation (Luikow, 1968), which takes the form

$$\frac{x_p(r)-mx_{in}}{x_{po}-mx_{in}} = 2\sum_{1}^{m}\left[\frac{\sin u_i-\mu_i\cos\mu_i}{\mu_i-\sin\mu_i\cos\mu_i}\right] x \left[\frac{\sin(\mu_i r)/R_p}{\mu_i r/R_p}\right] \exp(-\mu_i^2 Fo_2) \quad (203)$$

with

$$Fo_2 = Dt/R_p^2 \quad (204)$$

u_i in eqn. (203) are the non zero positive roots of

$$(1-B)\tan\mu_i=\mu_i \quad (205)$$

where

$$B = \frac{\bar{K}_g R_p}{mD} \quad (206)$$

which is the overall Biot number. The mass transfer coefficient for the particle in the emulsion phase, K_{p2}, is defined as

$$-D\left(\frac{\partial x_p}{\partial r}\right)_{r=R_p} = K_{p2}(\bar{x}_p - x_{PR}) \quad (207)$$

where x_p is the average moisture content of the particle. From eqn. (203), we obtain

$$Sh_{p2} = \frac{K_{p2}R_p}{D} = \frac{1}{3}\frac{\sum_{1}^{\infty}\frac{B}{\mu_i^2+B^2-B}\exp(-\mu_i^2 Fo_2)}{\sum_{1}^{\infty}\frac{B-\mu_i^2}{\mu_i^2+B^2-B}\exp(-\mu_i^2 Fo_2)} \quad (208)$$

From eqns. (202) and (207), the rate of drying of solid particles in the bed can be expressed by

$$-\frac{d\bar{x}_p}{dt} = \left(\frac{6}{d_p\phi_s}\right)\left(-D\left.\frac{\partial x_p}{\partial r}\right|_{r=R_p}\right)$$

$$= \left(\frac{6}{d_p\phi_s}\right)\left(\frac{x_{pR}}{m} - x_{in}\right)$$

$$= \left(\frac{6}{d_p\phi_s}\right)(\bar{x}_p - x_{PR}) \qquad (209)$$

Eliminating x_{PR} from the above equation, we obtain

$$-\frac{d\bar{x}_p}{dt} = \left(\frac{6}{d_p\phi_s}\right)\bar{K}_o(\bar{x}_p - mx_{in}) \qquad (210)$$

where $\bar{K}_o$ is the average overall mass transfer coefficient, defined by

$$\frac{1}{\bar{K}_o} = \frac{1}{K_{p2}} + \frac{m}{\bar{K}_g} \qquad (211)$$

If we define the drying efficiency as

$$\bar{X} = \frac{\bar{x}_p - mx_{in}}{x_{po} - mx_{in}} \qquad (212)$$

equation (210) can be rewritten as

$$-\frac{d\bar{X}}{dt} = \left(\frac{6}{d_p\phi_s}\right)\bar{K}_o\bar{X} \qquad (213)$$

The initial condition is

$$\bar{X}=1 \qquad \text{for } t=0 \qquad (214)$$

Integration of eqn. (213), subject to eqn. (214), yields

$$\bar{X} = \exp\left[-\left(\frac{6}{d_p\phi_s}\right)\int_o^t \bar{K}_o dt\right] \qquad (215)$$

The governing equations of the model are eqns. (167), (169), (171), (187), (188), (191), (203), and (215). To obtain the profiles of temperature and moisture contents of the gas and solids, first x_{PR} is determined from eqn. (203). Then $x_b(z)$ can be evaluated through eqn. (188). With $x_b(z)$, and x_{PR} known, $x_c(\Theta)$ can he calculated from eqn. (187). Subsequently, the outlet gas concentration is obtained with the aid of eqn. (191). It follows that the outlet gas temperature can be determined by eqn. (171). Solving simultaneously eqns. (154), (167), and (169) results in T_b, T_c, and T_p, therehy yielding the overall performance of the hatch fluidized hed dryer.

Continuous Operation

In contrast to a batch fluidized-bed dryer whose content of solid particles is fixed, the solids in a continuous fluidized-bed dryer are constantly added to and removed from the bed. Though a single particle can be viewed as a batch dryer, the performance of a continuous fluidized-bed dryer contining a multitude of particles can not be evaluated by merely considering the behavior of an individual particle. This is due to the fact that the state of the drying gas by which drying characteristics of solids are affected depends also on the flow of solids. Consequently, the modeling of a continuous fluidized-bed dryer is even more complicated than that of a batch fluidized-bed dryer.

Relatively little has been published on the modeling of continuous fluidized-bed drying. In the few existing models (see, e.g., Vanecek et al., 1966; Kunni and Levenspiel, 1969; Palancz and Part., 1973), it is often assumed that the bed temperature is constant and the outlet streams are in thermal or concentration equilibrium. The fluid mechanical behavior of the drying gas is considered homogeneous; in other words, the drying gas is not partitioned into different phases of the fluidized-bed, such as the emulsion and bubble phases. Instead, these models are based on the overall heat and mass balances over the dryer. They do not take into account the intricate transport processes of moisture and energy among various phases, and thus these models are often restricted to specific applications.

Model proposed by Palancz

Recently, a mechanistic model has been developed for continuous fluidized bed drying (Palancz, 1983). In essenced, the proposed model is based on the two phase theory of fluidization. The bubbling behavior and

its effect on the performance of the dryer are characterized by the visualization that a solid-free buhhle phase exists in the bed and that this phase constantly interacts with the emulsion phase. The moisture in the bubble phase is enriched by the emulsinn gas circulating through it. As a result, the moisture content of the gas bubbles increases along the bed height. The energy transfer accompanied by the moisture influx to the bubble phase tends to increase its enthalpy. Nevertheless, the temperature difference between the buhhles and emulsion gas generates a net heat flux from the former to the latter. This temperature difference is due to a decrease in the temperature of the emulsion gas caused by supplying heat tn the solids for vaporizatinn of moisture. Consequently, the temperature of the bubbles also decreases during their passage through the bed.

The bubbles are considered to he of the same size and their movement tn he in plug flow. This implies that the hubble breakage and coalescence are neglected. The emulsion gas and solids are assumed to be completely mixed. The solids are also assumed to he homogeneous with negligible internal resistance to the heat and mass transfer. The moisture evaporated is assumed to pass through a thin stagnet gas film surrounding the solids before it reaches the main stream of the emulsion gas. The resistance in this gas film and the concentration difference across it govern the moisture migration from the solids to the emulsion gas.

By superimposing the mechanisms of moisture and energy transport in various phases presented in the proceeding paragraphs, the following governing equations have been derived (Palancz, 1983)

$$x_b = x_e - (x_e - x_{in}) \exp\left[-\frac{(K_{he})_b \delta_b}{U_b} z\right] \qquad (216)$$

$$\frac{\rho_g U_{mf}}{H_f \delta_b}(x_e - x_{in})$$

$$= \rho_g (K_{be})_b (\bar{x}_b - x_e) + \left(\frac{6}{d_p}\right) \frac{(1-\epsilon_{mf})(1-\delta_b)}{\delta_h} K_{pg}(\bar{x}_p^* - x_e)$$

$$- \frac{\rho_s}{1 + \frac{\rho_s}{\rho_w} x_{po}} \frac{dx_p}{dt_s} = \left(\frac{6}{d_p}\right) K_{pg}(x_p^* - x_e) \qquad (217)$$

$$T_b = T_e + (T_o - T_e) \exp\left[-\frac{(H_{be})_b}{\rho_g u_b c_{wg}} \delta_b\right] \qquad (218)$$

$$\frac{C_{wg} \rho_g U_{mf}}{\delta_b H_f}(T_0 - T_e)$$

$$= (H_{be})_b (T_e - \bar{T}_b) + \left(\frac{6}{d_p}\right) \frac{(1-\epsilon_{mf})(1-\delta_b)}{\delta_b} [h_p(T_e - \bar{T}_p) - K_{pg}(\bar{x}_p^* - x_e) c_{mg} T_e]$$

$$- h_w (T_w - T_e) \frac{a_w}{\delta_b} \qquad (219)$$

$$\rho_s (c_p + c_w x_p) \frac{dT_p}{dt_s}$$

$$= \frac{6}{d_p} \frac{1 + \frac{\rho_s}{\rho_w} x_{po}}{\rho_s} [h_p(T_e - T_p) - K_{pg}(x_p^* - x_e)(\gamma_o + c_{wg} T_e - c_w T_p)] \qquad (220)$$

The solution of the above system of equations determines the temperature and moisture content of solids and gas in the different phases. These values can be used to evaluate the outlet gas temperature and moisture content as well as the average temperature and moisture content of the solids leaving the dryer.

The Palantz's model assumes a constant specific heat of the drying gas throughout the drying process. This implies that the change of moisture

content in the gas, or to be more precise, the change in the moisture content of the bubbles is negligible; this contradicts the plug flow postulate for the bubble phase or, in other words, the governing equation of the model, eqn. (216).

NOTATION

A_h cross-sectional area of the bubble phase, m^2

A_c cross-sectional area of the cloud-wake phase, m^2

A_e cross-sectional area of the emulsion phase, m^2

A_t cross-sectional area of the bed, m^2

Ar Archimedies number, dimensionless

a_w specific heat transfer surface of the dryer wall, m-1

c_g specific heat of dry gas, kJ kg^{-1} $°C^{-1}$

c_p specific heat of particles, kJ kg^{-1} $°C^{-1}$

c_w specific heat of water (liquid state) kJ kg^{-1} $°C^{-1}$

c_{wg} specific heat of wet gas, kJ kg^{-1} $°C^{-1}$

D diffusion coefficient, $m^2 s^{-1}$

D_c diameter of bed column, m

d_b bubble diameter, m

d_p particle diameter, m

E_a activation energy, KJ $kmol^{-1}$

g gravitational acceleration, m s^{-2}

H_f fluidized-bed height, m

H_{mf} bed height at minimum fluidization, m

H_T overall height of the tapered section in a tapered fluizied bed, m

H_{bc} volumetric heat transfer coefficient between the bubble and cloud-wake regions, $J\ s^{-1}m^{-3}\ °C^{-1}$

H_{be} volumetric heat transfer coefficient between the bubble and emulsion phases

H_{ce} volumetric heat transfer coefficient between the cloud-wake region and the emulsion phase, $Js^{-1}m^{-3}\ °C^{-1}$

H_T overall height of the tapered bed section, m

j_h heat transfer factor, dimensionless

j_o mass transfer factor, dimensionless

K_{bc} coefficient of gas interchange between the bubble and cloud-wake regions, s^{-1}

K_{be} coefficient of gas interchange between the bubble and emulsion phases, s^{-1}

K_{ce} coefficient of gas interchange between the cloud-wake region and the emulsion phase, s^{-1}

K_c mass transfer coefficient between the cloud-wake region and the emulsion phase based on the area of the interface $m^{-2}s^{-1}$

K_g mass transfer coefficient in the gas film

k_g thermal conductivity of the gas, $Jm^{-1}\ °C^{-1}$

K_{pg} gas-particle mass transfer coefficient, $m^{-2}s^{-1}$

ℓ length of tapered bed, m

ℓ_o length of bottom of the tapered fluidized bed, m

L top length of the tapered bed, m

M molecular weight, kg $kmol^{-1}$

ΔP pressure differential, $N\ m^{-2}$

ΔP_{mf}	pressure differential at minimum fluidization condition, Nm^{-2}
Q_{gc}	volumetric flow rate of tbrougb-flow gas per bubble, m^3s^{-1}
Nu	Nusselt number, dimensionless
Nu_p	particle Nusselt number, dimensionless
R_p	radius of the particle, m
R_e	Reynolds number, dimensionless
Re_{mf}	Reynold's number at minimum fluidization, dimensionless
Re_p	Particle Reynold's number, dimensionless
r_i	inside radius of the fluidized bed, m
r_o	outside radius of the bed, m
Sc	Schmidt number, dimensionless
Sb	Sherwood number, dimensionless
St	Stanton number, dimensionless
S_p	specific surface of solids, m^{-1}
t	time, s
T	temperature, °C or °K
T_b	temperature of bubble c phase, °C or °K
T_B	temperature of bed, °C or °K
Tc	temperature of gas cloud, °C or °K
Te	temperature of the emulsion gas, °C or °K
T_{in}	temperature of gas at tbe inlet, °C or °K
T_p	particle temperature, °C or °K
T_w	wall temperature, °C or °K

u_c critical fluidizing velocity in terms of the superficial velocity at the bottom of the tapered fluidized bed, ms^{-1}

u_b linear velocity of bubbles, ms^{-1}

u_e linear velocity of emulsion gas, ms^{-1}

u_{oc} critical fluidilzing velocity based on outside radius, ms^{-1}

U_b superficial gas velocity in the bubble phase, based on total cross-sectional area of the bed, ms^{-1}

U_{mf} superficial gas velocity at minimum fluidilzing conditions, ms^{-1}

U_t terminal velocity of a falling particle, ms^{-1}

U_p particle velocity, ms^{-1}

W width of tbe tapered bed

x spacee coordinate, m

x_b moisture content of gas bubbles (dry basis), dimensionless

x_c moisture content of gas cloud (dry basis), dimensionless

x_e moisture cnntent of emulsion gas (dry basis), dimensionless

x_{in} moisture content of gas at the inlet (dry basis), dimensionless

x_{out} moisture content of gas at tbe outlet (dry basis), dimensionless

x_p moisture content of a particle (dry basis), dimensionless

x_p^* moisture content of the drying gas on tbe surface of a particle (dry basis), dimensionless

x_{pe} equilibrium moisture cnntent of particle (dry basis), dimensionless

y mnle fraction of non-diffusivc component, dimensionless

z space coordinate, m

GREEK LETTERS

γ_o heat of vaporization, KJ kg^{1}

δ_b fraction of the fluidized bed consisting of bubbles, dimensionless

ϵ void fraction of the bed, dimensionless

ϵ_e void fraction in the emulsion phase, dimensionless

ϵ_{mf} void fraction at minimum fluidizing conditions, dimensionless

μ viscosity, kg $m^{-1}s^{-1}$

ν kinematic viscosity, $m^{2}r^{-1}$

ρ_g density of gas, kg m^{-3}

ρ_f density of fluid, kg m^{-3}

ρ_p density of particle, kg m^{-3}

σ Stefan-Boltzmann constant

ω angular velocity, s^{-1}

ψ effective emissivity, dimensionless

LITERATURE CITED

Adams, R. L., Coupled Gas Convection and Unsteady Conduction Effects in Fluid Bed Heat Transfer Based on a Single Particle Model, Int. J. Heat Mass Transfer, 25, 1819-1828 (1982).

Arastoopour, H. and D. Gidaspow, Vertical Countercurrent Solids Gas Flow, Chem. Eng. Sci., 34, 1063-1066 (1979).

Hakker, P. J. and P. M. Heertjes, Porosity Distributions in a Fluidized Bed, Chem. Eng. Sci., 12, 260-271 (1960).

Balakrishnan, A. R. and D. C. T. Pei, Fluid-Particle Heat Transfer in Gas Fluidized Beds, Can. J. of Chem. Eng., 53 231-233 (1975).

Barker, J. J., Heat Transfer in Fluidized Beds, Ind. Eng. Chem., 57, 33-39 (1985).

Baskakov, A. P., B. V. Berg, O. K. Vitt, N. F. Filippoviski, V. A. Kirakosyan, J. M. Goldobin and V. K. Maskaev, Powder Technol., 8, 273-282 (1973).

Beek, W. J., Mass Transfer in Fluidized Beds, in Fluidization ed. by J. F. Davison and D. Harrison, pp 431-470, Academic Press, London, (1971).

Bhattacharyya, D. and D. C. T. Pei, Fluid-to-Partide Heat Transfer in Fluidized Beds, Ind. Eng. Chem. Fundam., 13, 199-203 (1974).

Bock, H. J., Heat Transfer in Fluidized Beds, Proceedings of the Fourth International Conference on Fluidization, Kashikojima, Japan (May 29 - June 3, June 3, 1983).

Hokur, D. B., C. V. Wittmann and N. R. Amundson, Analysis of a Model for a Nonisothermal Continuous Fluidized Bed Catalytic Reactor, Chem. Eng. Sci., 29, 1173-1192 (1974).

Horodulya, V. A., V. L. Ganzha, S. N. Upadhyay and S. C. Saxena, Heat Transfer from In-Line and Staggered Horizontal Smooth Tube Bundles Immersed in a Fluidized Bed of Large Particles, Int. J. Heat Mass Transfer 23, 1602-1604 (1980).

Botterill, J. S. M., Fluid-Hed Heat Transfer, Academic Press, N.Y. (1975).

Botterill, J. S. M., Y. Teoman and K. R. Yuregir, Temperature Effects on the Heat Transfer Behavior of Gas Fluidized Heds, AICHE Sym. Ser. 77 (208), 330-339 (1981).

Bradshaw, R. D. and V. E. Myers, Heat and Mass Transfer in Fixed and Fluidized Beds of large Particles, AICHE, 9 (5), 590-595 (1963).

Brauer, H., J. Mühle and M. Schmidt, Untersuchungen an einer mehrstufigen Rieselboden-Wirbelschicht, Chem. Ing. Technik, 42, 494-502 (1970).

Brit. Chem. Eng., Drier for Sticky, Granular Materials, p. 514 (1961).

Hrnnker, D. B., F. W. Bakker-Arkema and C. W. Hall, Drying Cereal Grains, The Avi Publishing Company, Westport, Connecticut, (1981).

Carslaw, H. S. and J. C. Jaeger, Conduction of Heat in Solids, p. 240, Oxford University Press, London, (1959).

Catipovic, N. M., G. N. Jovannvic and T. J. Fitzgerald, Regimes of Fluidization for Large Particles, AIChE J. 24, 543-547 (1978).

Chang, T. M. and C. Y. Wen, Fluid-To-Particle Heat Transfer in Air-Fluidized Beds, Chem. Eng. Prog. Symp. Series, 62 (67), 111-117 (1966).

Cherrett, N., A Fluidized Bed Dryer/Cooler for Polymer Chip, Brit. Chem. Eng. (Dec. 1964).

Chirife, J., Advanies in Drying, vol. 2, ed. by A. S. Mujumdar, Chapter 3, McGraw-Hill, Washington, (1983).

Cranfield, R. R. and B. J. Gliddon, Adsorption in Shallnw Fluidized Beds of Large Particles, AlChE Symp. Ser., 74 (176), 55-64 (1978).

Crank, J., The Mathematics of Diffusion, 2nd Ed., Oxford University Press, Lnndon, 1975.

Darton, R. C., R. D. LaNauze, J. F. Davidson and D. Harrison, Bubble Growth Due to Coalescence in Fluidized Beds, Trans. I. Chem. E., 55, 274-280 (1977).

Davidson, J. F. and D. Harrison, Fluidized Particles, Camhridge University Press, 1963.

Davidson, J. F., D. Harrisnn, R. C. Darton and R. D. Darton and R. D. LaNauze, The Two-Phase Theory of Fluidization and Its Application tn Chemical Reactnrs, Chapter 10 nf "Chemical Reactnr Theory", ed. by Lapidus L. and N. R. Amundson, Prentice-Hall, Englewood Cliffs, N. J., 583 (1977).

Decker, N. and L. R. Glicksman, Heat Transfer in Large Particle Fluidized Beds, Int. J. Heat Mass Transfer, 26, 1307-1320 (1983).

Donnadieu, G., Heat Transfer in Granular Media - Fixed Beds and Fluidized Beds, Rev. Inst. Franc. Petrole Ann. Combust. Liquids, 16, 1330-1356 (1961).

Dwivedi, P. N. and S. N. Upadhyay, Particle-Fluid Mass Transfer in Fixed and Fluidized Beds, Ind. Engr. Chem. Proc. Des. Dev., 16, 157-165 (1977).

Ergun, S., Fluid Flow Through Packed Columns, Chem. Eng. Prog., 48, 89-94 (1952).

Fan, L. T., C. C. Chang, Y. S. Yu, T. Takahashi and Z. Tanaka, Incipient Fluidization Condition for a Centrifugal Fluidized Bed, AIChE J., 31, 999-1009 (1985).

Ferron, J. R. and L. L. Watson, Studies of Gas-Solid Heat Transfer in Fluidized Beds," Chem. Eng. Prog. Symp. Series, 58 (38), 79-86 (1962).

Frantz, J. F., Fluid-to-Particle Heat Transfer in Fluidized Beds, Chem. Eng. Progr., 57 (7), 35-42 (1961).

Fryer, C. and D. E. Potter, Experimental Investigation of Models for Fluidized-Bed Catalytic Reactors, AIChE J., 22, 38-47 (1976).

Ganzka, V. L., A Mechanistic Theory for Heat Transfer between Fluidized Beds of Large Particles and Immersed Surfaces, J. Heat Mass Transfer, 25, 1531-1540 (1982).

Geldart, D., Types of Gas Fluidization, Powder Tech., 7, 285-292 (1973).

Grace, J. R., An Evaluation of Models for Fluidized-Bed Reactors, AIChE Symp. Ser. 67 (116), 159-167 (1971).

Grace, J. R., Fluidized Bed Reactor Modelling: An Dverview, ACS Symp. Ser., 168, 3-12 (1981).

Gupta, R. and Majumdar, A. S., Aerodynamics of a Vibrated Fluid Bed, Can. J. Chem. Eng., 58, 332-338 (1980).

Hanni, P. F., D. F. Farkas and G. E. Brown, Design and Operating Parameters for a Continuous Centrifugal Fluidized Bed Drier, J. Food Sci., 41, 1172-1179 (1976).

Heertjes, P. M. and S. W. McKibbins, The Partial Coefficient of Heat Transfer in a Drying Fluidized Bed, Chem. Engr. Sci., 5, 161-167 (1956).

Heywood, B., Continuos Vibrating Fluid Bed Drying, Food Processing Ind., April, pp. 21-25, 1978.

Hoebink, J., Thesis, Technical University Eindhoven, Holland, 1977.

Information Bulletin on Foreign Chemical Industry, U.S.S.R., No. 24/79/52853 (1960).

Jason, A. C., Effects of Fat Content on Diffusion of Water in Fish Muscle, J. Sci. Food Agric., 16, 281-288 (1965).

Jinesiu, G. I., Equation of the Minimum Fluidization Rate in Condition of Vibration, Rev. Roum. Chim., 16, 1255-1268 (1971).

Kato, K. and C. Y. Wen, Gas-Particle Heat Transfer in Fixed and Fluidized Beds, Chem. Eng. Progr. Symp. Ser., 66(1D5), 1D0-1D8 (197D).

Kato, K., H. Kubota and C. Y. Wen, Mass Transfer in Fixed Fluidized Beds, Inst. Chem. Engr. Symp. Ser., 66(1D5), 86-99 (1970).

Kettenring, K. N., E. L. Manderfield and J. M. Smith, Heat and Mass Transfer in Fluidized System, Chem. Engr. Progr. 46(3) 139-145 (1950).

Kobayashi, H., F. Arai and T. Sunawaka, Determination of Gas Cross-Flow Coefficient Between the Buble and Emulsion Phase by Measuring the Residence Time Distribution of Fluid in a Fluidized Bed, Kagaku Kogaku, 31, 239-246 (1967).

Kroger, D. G., E. K. Levy and J. C. Chen, Flow Characteristics in Packed and Fluidized Rotating Beds, Powder Technol., 24, 9-18 (1979).

Kunii, D. and O. Levenspiel, Fluidization Engineering, Wiley, N.Y. (1969).

Kwauk, M., Generalized Fluidization I. Steady-State Motion, Scientia Sinica, 12 (4), 587-612 (1963).

Leva, M., Correlations in Fluidized Systems, Chem. Eng., Nov., pp. 266-270, 1957.

Levy, E., N. Martin and J. Chen, Minimum Fluidization and Startup of a Centrifugal Fluidized Bed, in Fluidization, pp. 71-75,, ed. by D. L. Kearins, Cambridge University Press, Cambridge (1978).

Lewis, E. W. and E. W. Bowerman, Fluidization of Solid Particles in Liquid, Chem. Engr. Prog., 48, 603-610 (1952).

Lewis, W. K., E. R. Gilliland and W. C. Bauer, Characteristics of Fluidized Particles, Ind. Engr. Chem., 41, 1104-1117 (1949).

Luikov, A. V., Heat and Mass Transfer in Capillary-Porous Bodies, Pergamon Press, London, 1966.

Luikov, A. V., Theory of Drying, Energiya, Moscow, 1968.

Luikov, A. V., Analytical Heat Diffusion Theory, Academic Press, New York, 1968.

Lyuboshits, I. L., L. S. Slobodkin, and I. J. Pikus, Drying of Dispersed Thermolabile Materials, Naukai Tekhnika, Minsk, 1969.

Mathur, A., S. C. Saxena, A. Correlation for Heat Transfer Between Immersed Surface and Gas-Fluidized Beds of Large Particles, to be presented at the VIII National Heat and Mass Transfer Conference, Visadhapatman, India, December, 1985.

Mao, Q. M. and O. E. Potter, Modelling Fluidized Bed Reactors, in 'Frontiers in Chemical Reaction Engineering', Vol. I, ed. by L. K. Doraiswamy and R. A. Mashelkar, Wiley, Eastern Limited, New Delhi, India, 1984.

May, W. G., Fluidized-Bed Reactor Studies, Chem. Eng. Prog., 55 (12), 49-56 (1959).

McGaw, R. R., The Development of a Mechanism for Gas-Particle Heat Transfer in Shallow Fluidized Beds of Large Particles, Chem. Engr. Sci., 32, 11-18 (1977).

McCormick, P. Y., in R. H. Perry and C. H. Chilton (eds.), "Chemical Engineers' Handoobk," 5th ed., sec. 20, McGraw-Hill Book Company, New York, 1973.

Mori, S. and C. Y. Wen, Estimation of Bubble Diameter in Gaseous Fluidized Beds, AIChE J., 21, 109-115 (1975).

Mrowiec, M. and W. Ciesielczyk, Fluidized-bed Dryers for Paste Materials, International Chem. Eng., 17, 273-379 (1977).

Murray, J. D., On the Mathematics of Fluidization. Part 1. Fundamental Equations and Waste Propogation, J. Fluid. Mech., 21, 465-472 (1965).

NASA, Rotating Fluidized Bed Reactor for Space Nuclear Propulsion - Annual Report, NASA Agreement No. 13254, Washington (September, 1972).

Nelson, P. A. and T. R. Galloway, Particle-to-Fluid Heat and Mass Transfer in Dense Systems of Fine Particles, Chem. Eng. Sci., 30, 1-6 (1975).

Nonhebel, G. and A. A. H. Moss, Drying of Solids in the Chemical Industry, Chapter 2, Butterworth, London, 1971.

Niro Atomizer Inc., Fluid Bed Dryers, Catalog number B-Na-171, Columbia, Maryland (19B0).

Orcutt, J. C., J. F. Davidson and R. L. Pigford, Residence Time Distributions in Fluidized Catalytic Reactors, Chem. Eng. Prog. Sym. Ser., 5B (38) 1-15 (1962).

Osinskii, V. P., B. S. Sazhin and E. A. Chuvpilo, Chem. Pet. Eng. (English Translation) 11, B66-B69 (1969).

Pandey, D. K. and S. N. Upadhyay, Mass Transfer between the Particles and the Fluid in Fluidized Beds of Large Particles, Int. J. Heat Mass Transfer, 24, 1221-1228 (19B1).

Partridge, B. A. and P. N. Rowe, Chemical Reacton in a Bubbling Gas-Fluidized Bed, Trans. Inst. Chem. Engrs., 44, T335-T34B (1966).

Priestley, R. J., Where Fluidized Solids Stand Today, Chem. Eng., 69(14) 125-132 (1962).

Richardson, J. F. and W. N. Zaki, Sedimentation and Fluidization: Part I, Trans. Inst. Chem. Engrs., 32, 35-53 (1954).

Richardson, J. F. and P. Ayers, Heat Transfer Between Particles and a Gas in a Fluidized Bed, Trans. Inst. Chem. Engrs., 37, 314-322 (1959).

Richardson, J. F., Incipient Fluidization and Particulate Systems, in Fluidization, ed. by J. F. Davidson and D. Harrison, Academic Press, New York (1971).

Roman, G. N., E. Rotestein and M. J. Urbicain, Kinetics of Water Vapor Desorption from Apples, J. Food Sci., 44, 193-197 (1979).

Rowe, P. N., A Note on the Motion of a Bubble Rising Through a Fluidized Bed, Chem. Eng. Sci., 19, 75-77 (1964).

Rowe, P. N. and B. A. Partridge, An X-Ray Study of Bubbles in Fluidized Beds, Trans. Inst. Chem. Engr., 43, 1157-1175 (1965).

Rowe, P. N., Particle-to-Liquid Mass Transfer in Fluidized Beds, Chem. Eng. Sci., 30, 7-9 (1975).

Rowe, P. N., Prediction of Bubble Size in a Gas Fluidized Bed, Chem. Eng. Sci., 31, 285-288 (1976).

Saxena, S. C. and J. D. Gabor, Mechanism of Heat Transfer Between a Surface and a Gas-Fluidized Bed for Combustor Application, Prog. Energy Combust. Sci., 7, 73-102 (1981).

Saxena, S. C. and V. L. Ganzha, Heat Transfer to Immersed Surfaces in Gas-Fluidized Beds of Large Particles and Powder Characterization, Powder Tech. 39, 199-208 (1984).

Schoeber, W. J. A. H., A Short-cut Method for the Calculation of Drying Rates in Case of a Concentration Dependence Diffusion Coefficient, Proceedings of the First International Symposium on Drying, Science Press, Princeton (1978).

Selzer, V. W. and W. J. Thomson, Fluidized-Bed Heat Transfer--The Packet Theory Devisited, AIChE Symp. Ser., 73 (161) 29-37 (1977).

Sen Gupta, A., R. B. Chanbe, and S. N. Upadhyay, Fluid-Particle Heat Transfer in Fixed and Fluidized Beds, Chem. Engr. Sci., 29, 839-843 (1974).

Shen, C. Y. and L. T. Jonestone, Gas-solid Contact in Fluidized Beds, AIChE J. 1, 349-354 (1955).

Shi, Y., Y. S. Yu, and L. T. Fan, Incipient Fluidization Condition for a Tapered Fluidized Bed, Ind. Eng. Chem. Fundam., 23, 484-489 (1984).

Shi, Y. and L. T. Fan, Lateral Mixing of Solids in Batch Gas-Solids Fluidized Beds, Ind. Eng. Chem. Process Des. Dev., 23, 337-341 (1984).

Shi, Y. and L. T. Fan, Lateral Mixing of Solids in Gas-Solids Fluidized Beds with Continuous Flow of Solids, Powder Technol., 41, 23-28 (1985).

Slenov, V. A., and N. V. Mikhailov, Vibrofluidized Bed, (in Russian) Nauka, Moscow (1972).

Steinour, H., Rate of Sedimentation -- Nonflocculated Suspensions of Uniform Spheres, Ind. Eng. Chem., 36, 618-624 (1944).

Trebal, R. E., Mass Transfer Operations, Third Edition, Chapter 12, McGraw-Hill, New York, 1980.

Twomey, R. D. and H. F. Johnstone, Gaseous Fluidization of Solids Particles, Chem. Eng. Prog., 48, 220-226 (1952).

Upadhyay, S. N. and G. Tripathi, Mass Transfer in Fixed and Fluidized Bed, J. Scient. Ind. Res., 34, 10-35 (January, 1975).

Vaccarezza, L. M., Thesis, Facultad de Ciencias Exactasy Naturales, Universidad de Buenos Aires, Argentina, 1975.

Van Deemter, J. J., Mixing and Contacting in Gas-Solid Fluidized Beds, Chem. Eng. Sci., 13, 143-154 (1961).

Vanecek, V., M. Markvart, R. Drbohlav and R. L. Hummel, Experimental Evidence on Operation of Continuous Fluidized-Bed Dryers, Chem. Engr. Prog. Symp. Ser., 66 (105) 243-252 (1970).

Viswanathan, K., D. Subba Rao and B. C. Raychaudhury, Coherent Representation of the Drying of Gas and Solids in Fluidized Beds, Indian Chem. Engr., 14, 12-23 (1982).

Viswanathan, K., Semicompartmental Approach to Fluidized Bed Reactor Modeling -- Application to Catalytic Reactions, Ind. Eng. Chem. Fundam., 21, 352-360 (1982).

Viswanathan, K., D. Khakar and D. Subba Rao, Fluidized Bed Absorber, Chem. Eng. Commun., 20, 235-251 (1983).

Viswanathan, K. and D. Subba Rao, Drying of Gas and Solids in Fluidized Beds, in Drying '82, ed. by A. S. Mujumda, McGraw-Hill, Washington, 1984.

Walton, J. S., R. L. Olson and O. Levenspiele, Gas-Solid Film Coefficients of Heat Transfer in Fluiidzed Coal Beds, Ind. Engr. Chem., 44, 1474-1480 (1952).

Wen, C. Y. and Y. H. Yu, A Generalized Method for predicting the Minimum Fluidization Velocity, AIChE J., 12, 610-612 (1966).

Yates, J. G., Fundamentals of Fluidized-Bed Chemical Processes, Butterworths, London, 1983.

APPENDIX A. DERIVATION OF EQN. (87)

For the controlled volume element in the bubble phase with a size of $A_b \Delta z$ shown in Fig. 13, a quasi-steady state moisture balance around this volume element yields

$$0 = \left\{ \begin{array}{c} \text{rate of moisture in} \\ \text{by convection} \end{array} \right\} - \left\{ \begin{array}{c} \text{rate of moisture} \\ \text{out by convection} \end{array} \right\}$$

$$+ \left\{ \begin{array}{c} \text{rate of moisture in through} \\ \text{gas exchange with the cloud} \\ \text{phase} \end{array} \right\} \qquad \text{(A-1)}$$

The individual terms in eqn. (A-1) are

$$\left\{ \begin{array}{c} \text{rate of moisture in} \\ \text{by convection at } z \end{array} \right\} = (U_b A_b)\rho_g x_b\big|_z$$

$$\left\{ \begin{array}{c} \text{rate of moisture out} \\ \text{by convection at } z+\Delta z \end{array} \right\} = (U_b A_b)\rho_g x_b\big|_{z+\Delta z}$$

$$\left\{ \begin{array}{c} \text{rate of moisture in through} \\ \text{gas exchange with the} \\ \text{cloud-wake phase} \end{array} \right\} = (A_b \Delta_z)\rho_g (K_{be})_b (x_c - x_b)$$

Substituting these individual terms into eqn. (A-1), dividing the resultant expression by $A_b \Delta z \rho_g$ and letting $\Delta z \to 0$, we obtain

$$U_b \frac{dx_b}{dz} = (K_{bc})_b (x_c - x_b) \qquad \text{(A-2)}$$

This is eqn. (87) in the text.

APPENDIX B. DERIVATION OF EQN. (88)

Consider the controlled volume element in cloud-wake phase with a size of $A_c \Delta z$ represented in Fig. 13, a quasi-steady state moisture balance around this volume element gives

$$0 = \left\{ \begin{array}{c} \text{rate of moisture in} \\ \text{by convection} \end{array} \right\} - \left\{ \begin{array}{c} \text{rate of moisture out} \\ \text{by convection} \end{array} \right\}$$

$$+ \left\{ \begin{array}{c} \text{rate of moisture in} \\ \text{through gas exchange} \\ \text{with the bubble phase} \end{array} \right\} - \left\{ \begin{array}{c} \text{rate of moisture out} \\ \text{through gas exchange} \\ \text{with the emulsion phase} \end{array} \right\}$$

$$+ \left\{ \begin{array}{c} \text{rate of moisture in} \\ \text{through interphase exchange} \\ \text{between gas and solids} \end{array} \right\} \qquad \text{(B-1)}$$

The individual terms in (B-1) are

$$\left\{ \begin{array}{c} \text{rate of moisture in} \\ \text{by convection atz} \end{array} \right\} = (u_b A_c \epsilon_{mf}) \rho_g x_c \big|_z$$

$$\left\{ \begin{array}{c} \text{rate of moisture out} \\ \text{by convection at } z+\Delta z \end{array} \right\} = (u_b A_c \epsilon_{mf}) \rho_g x_c \big|_{z+\Delta z}$$

$$\left\{ \begin{array}{c} \text{rate of moisture in through} \\ \text{gas exchange with the} \\ \text{bubble phase} \end{array} \right\} = (A_b \Delta_z) \rho_g (K_{bc})_h (x_b - x_c)$$

$$\left\{ \begin{array}{c} \text{rate of moisture in through} \\ \text{gas exchange with the} \\ \text{emulsion phase} \end{array} \right\} = (A_h \Delta_z) \rho_g (K_{bc})_b (x_{ei} - x_c)$$

$$\left\{\begin{array}{c}\text{rate of moisture in through}\\ \text{interphase exchange between}\\ \text{gas and solids}\end{array}\right\}$$

$$= (A_c \Delta_z) \quad (1-\epsilon_{mf}) \quad \rho_g \cdot S_p \quad K_{pg}(x_p^*-x_c)$$

volume of cloud	*volume fraction of solids*	*specific surface of solids*	*transfer rate of moisture per unit surface area of solids*

Substituting these individual terms into eqn. (B-1), dividing the resultant expression by $A_b \Delta z$ and letting $\Delta z \to 0$, we obtain

$$u_b \frac{A_c}{A_b} \epsilon_{mf} \frac{dx_c}{dz} = (Kce)_b (x_{ei}-x_c) + (K_{ce})_b (x_b-x_c)$$

$$+ \frac{A_c}{A_b} (1 - \epsilon_{mf}) S_p K_{pg}(x_p^*-x_c) \qquad \text{(B-2)}$$

Realizing that

$$\frac{A_c}{A_b} = \frac{V_c}{V_b}$$

$$= \frac{V_t \delta_b (\alpha+\beta)}{V_t \delta_b}$$

$$= (\alpha + \beta) \qquad \text{(B-3)}$$

Equation (B-2) now becomes

$$(\alpha + \beta) \epsilon_{mf} u_b \frac{dx_c}{dz} = (K_{ce})_b (x_{ei} - x_c) + (K_{bc})(x_b-x_c)$$

$$+ (\alpha + \beta)(1-\epsilon_{mf}) S_p K_{pg}(x_p^*-x_c) \qquad \text{(B-4)}$$

This is eqn. (88) in the text.

APPENDIX C. DERIVATION OF EQN. (89)

Referring to Fig. 13, under quasi-steady state assumption a moisture balance around the emulsion gas in ith compartment yields

$$0 = \left\{\begin{array}{c}\text{rate of moisture in}\\ \text{by convection}\end{array}\right\} - \left\{\begin{array}{c}\text{rate of moisture out}\\ \text{by convection}\end{array}\right\} + \left\{\begin{array}{c}\text{rate of moisture in}\\ \text{through gas exchange}\\ \text{with the cloud-wake phase}\end{array}\right\} + \left\{\begin{array}{c}\text{rate of moisture in}\\ \text{through interphase exchange}\\ \text{between gas and solids}\end{array}\right\}$$

The individual terms in eqn. (C-1) are

$$\left\{\begin{array}{c}\text{rate of moisture in}\\ \text{by convection at the}\\ \text{inlet of ith compartment}\end{array}\right\} = (u_e A_e \epsilon_{mf})\rho_g x_{in}(i)$$

$$\left\{\begin{array}{c}\text{rate of moisture out}\\ \text{by convection at the}\\ \text{outlet of ith compartment}\end{array}\right\} = (u_e A_e \epsilon_{mf})\rho_g x_{ei}$$

$$\left\{\begin{array}{c}\text{rate of moisture in through}\\ \text{gas exchange with the}\\ \text{cloud-wake phase}\end{array}\right\} = A_b(z_i - z_{i-1})\rho_g (K_{ce})_b (\bar{x}_c - x_{ei})$$

$$\left\{\begin{array}{c}\text{rate of moisture in through}\\ \text{interphase exchange between}\\ \text{gas and solids}\end{array}\right\} = A_e(z - z_{i-1})\rho_g (1-\epsilon_{mf})\, S_p\, K_{pg}(x_p^* - x_{ei})$$

Substituting the individual terms into eqn. (C-1) and dividing the resultant expression by $A_b(z-z_{i-1})\rho_g$ yields

$$u_e \frac{A_e}{A_b} \frac{(x_{ei} - x_{in(i)})}{z - z_{i-1}} \epsilon_{mf}$$

$$= \frac{A_e}{A_b} (1 - \epsilon_{mf}) S_p K_{pg}(x_p^* - x_{ei})$$

$$+ (K_{ce})_b(\bar{x}_c - x_{ei}) \qquad \text{(C-2)}$$

but

$$\frac{A_e}{A_b} = \frac{A_t[1-\delta_b(1+\alpha+\beta)]}{A_t\delta_b}$$

$$= \frac{[1-\delta_b(1+\alpha+\beta)]}{\delta_b} \qquad \text{(C-3)}$$

Thus, we have

$$\frac{[1-\delta_b(1+\alpha+\beta)]u_e\epsilon_{mf}(x_{ei}-x_{in}(i))}{\delta_b}$$

$$= \frac{[1-\delta_b(1+\alpha+\beta)]}{\delta_b} (1-\epsilon_{mf}) S_p K_{pg}(x_p^* - x_{ei})$$

$$+ (K_{ce})_b (\bar{x}_c - x_{ei}) \qquad \text{(C-4)}$$

This is eqn. (89) in the text.

APPENDIX D. DERIVATION OF EQN. (117)

The moisture content of particles in the dryer decreases with time due to evaporation. Applying moisture balance around the entire solid phase in the bed yields

$$\left\{\begin{array}{c}\text{rate of accumula-}\\ \text{tion of moisture}\end{array}\right\} = \left\{\begin{array}{c}\text{rate of}\\ \text{moisture in}\end{array}\right\} - \left\{\begin{array}{c}\text{rate of moisture out}\\ \text{by evaporation}\end{array}\right\} \quad \text{(D-1)}$$

The three terms in eqn. (D-1) are

$$\left\{\begin{array}{c}\text{rate of accumulation}\\ \text{of moisture}\end{array}\right\} = M_p \frac{dx_p}{dt}$$

$$\left\{\begin{array}{c}\text{rate of}\\ \text{moisture in}\end{array}\right\} = 0$$

$$\left\{\begin{array}{c}\text{rate of moisture out}\\ \text{by evaporation}\end{array}\right\} = \left[\begin{array}{c}\text{rate of moisture}\\ \text{adsorbed by the}\\ \text{surrounding drying gas}\end{array}\right]$$

$$= (U_o A_t)\rho_g (x_{in} - x_{out})$$

Substituting the individual terms into eqn. (D-1) and dividing each term by M_p, we obtain

$$\frac{dx_p}{dt} = \frac{\rho_g U_o A_t}{M_p} (x_{in} \quad x_{out}) \qquad \text{(D-2)}$$

This is eqn. (87) in the text.

APPENDIX E. DERIVATION OF EQN. (119)

Recall the bed temperature is assumed to be homogeneous. Applying energy balance around the entire bed, we obtain

$$\left[\begin{array}{c}\text{rate of accumulation}\\ \text{of thermal energy}\end{array}\right] = \left[\begin{array}{c}\text{rate of thermal energy}\\ \text{in accompanied by}\\ \text{inflow drying gas}\end{array}\right] - \left[\begin{array}{c}\text{rate of thermal energy}\\ \text{out carried by}\\ \text{exit drying gas}\end{array}\right] \qquad \text{(E-1)}$$

Choosing T = °C as the reference temperature, we can write the individual terms in eqn. (E-1) as below

$$\left[\begin{array}{c}\text{rate of accumulation}\\ \text{of thermal energy}\end{array}\right] = c_p M_p \frac{dT}{dt}$$

$$\left[\begin{array}{c}\text{rate of thermal energy}\\ \text{in accompanied by}\\ \text{inflow drying gas}\end{array}\right] = (U_o A_t)\rho_g [x_{in}(r_o + c_{wg}T_{in}) + c_g T_{in}]$$

$$\left[\begin{array}{c}\text{rate of thermal energy}\\ \text{out carried by exit}\\ \text{drying gas}\end{array}\right] = (U_o A_t)\rho_g [x_{out}(r_o + c_{wg}T) + c_g T]$$

Substituting the individual terms into eqn. (E-1) and rearrangement of the resultant expression give

$$\frac{dT}{dt} = \frac{\rho_g U_o A_t}{M_p C_p}\left[(x_{in} - x_{out})\gamma_o + c_g(T_{in} - T) + c_{wg}(T_{in}x_{in} - Tx_{out})\right] \qquad \text{(E-2)}$$

In most practical cases,

$$|c_g(T_{in} - T)| >> |c_{wg}(T_{in}x_{in} - Tx_{out})| \qquad \text{(E-3)}$$

Accordingly, eqn. (E-2) is simplified as

$$\frac{dT}{dt} = \frac{\rho_g U_o A_t}{M_p c_g} [(x_{in} - x_{ouA}) \gamma_o + c_g (T_{in} - T)] \qquad \text{(E-4)}$$

This is eqn. (119) in the text.

APPENDIX F. DERIVATION OF EQN. (146)

Referring to Fig. 17, the portion of the cloud confined between θ and $\theta+\Delta\theta$ has volume

$$V_\theta = \int_{R_b}^{R_c} \int_0^{2\pi} \int_\theta^{\theta+\Delta\theta} \rho^2 \sin\theta' d\theta' d\psi d\rho$$

$$= \frac{2}{3}\pi (R_c^3 - R_b^3) \int_\theta^{\theta+\Delta\theta} \sin\theta' d\theta' \qquad \text{(F-1)}$$

Under quasi-steady state assumption, a moisture balance around the gas cloud in this controlled volume leads to

$$0 = \left\{ \begin{array}{c} \text{rate of moisture in by} \\ \text{through-flow gas} \end{array} \right\} - \left\{ \begin{array}{c} \text{rate of moisture out} \\ \text{by through-flow gas} \end{array} \right\}$$

$$+ \left\{ \begin{array}{c} \text{rate of moisture in through} \\ \text{interphase exchange between} \\ \text{gas and solids} \end{array} \right\}$$

$$+ \left\{ \begin{array}{c} \text{rate of moisture in through} \\ \text{exchange between cloud and} \\ \text{emulsion phase} \end{array} \right\} \qquad \text{(F-2)}$$

The individual terms in eqn. (F-2) are

$$\left\{ \begin{array}{c} \text{rate of moisture in} \\ \text{by through-flow gas} \\ \text{at } \theta \end{array} \right\} = Q_{gc} \rho_g x_c \big|_\theta$$

$$\left\{ \begin{array}{c} \text{rate of moisture out} \\ \text{by through-flow gas} \\ \text{at } \theta+\Delta\theta \end{array} \right\} = Q_{gc} \rho_g x_c \big|_{\theta+\Delta}$$

$$\left\{\begin{array}{c}\text{rate of moisture in}\\ \text{through exchange between}\\ \text{gas and solids}\end{array}\right\} = V_\theta \quad (1-\epsilon_{mf}) \quad S_p \quad \rho_g K_{pg}(x_p^*-x_c)$$

volume of cloud — *volume fraction of solids* — *specific surface of solids* — *moisture transfer rate per unit surface area of solids*

$$\left\{\begin{array}{c}\text{rate of moisture in}\\ \text{through exchange between}\\ \text{cloud and emulsion phase}\end{array}\right\} = (2\pi R_c)(R_c d\theta)\cdot\rho_g K_c(x_e-x_c)\sin\theta$$

interface area — *transfer rate of moisture per unit area in the direction normal to the interface*

Insertion of individual terms into eqn. (F-2) and substituting V_θ from eqn. (F-1) yield

$$0 = Q_{gc}(x_c|_\theta - x_c|_{\theta+\Delta\theta}) + \frac{2}{3}\pi(R_c^3 - R_b^3)\left(\int_\theta^{\theta+\Delta\theta} \sin\theta' d\theta'\right)(1-\epsilon_{mf})S_p \cdot K_{pg}(x_p^*-x_c) + (2\pi R_c)R_c\sin\theta d\theta \cdot K_c(x_e-x_c) \qquad \text{(F-3)}$$

Dividing by $\Delta\theta \sin\theta$ and letting $\Delta\theta \to 0$, we obtain

$$\frac{Q_{gc}}{\sin\theta}\frac{\partial x_c}{\partial\theta} = \frac{2}{3}\pi(R_c^3-R_b^3)(1-\epsilon_{mf})S_p\cdot K_{pg}(x_p^*-x_c) + (2\pi R_c)R_c\cdot K_c(x_e-x_c) \qquad \text{(F-4)}$$

This is eqn. (146) in the text.

APPENDIX G. DERIVATION OF EQN. (154)

Under pseudo-steady state assumption, an energy balance around the controlled volume depicted in Fig. 17 gives

$$0 = \left\{\begin{array}{c}\text{thermal energy in}\\ \text{accompanied by through}\\ \text{flow gas}\end{array}\right\} - \left\{\begin{array}{c}\text{thermal energy out}\\ \text{accompanied by through}\\ \text{flow gas}\end{array}\right\}$$

$$+ \left\{\begin{array}{c}\text{thermal energy in}\\ \text{through exchange between}\\ \text{gas and solids}\end{array}\right\}$$

$$+ \left\{\begin{array}{c}\text{thermal energy in}\\ \text{through exchange between}\\ \text{cloud and emulsion gas}\end{array}\right\} \qquad \text{(G-1)}$$

Choosing $T = 0°C$ as reference temperature, we can express three individual terms in eqn. (G-1) as

$$\left\{\begin{array}{c}\text{thermal energy in}\\ \text{accompanied by through-}\\ \text{flow gas at } \theta\end{array}\right\} = Q_{gc}\rho_g c_g \, T\big|_{\theta}$$

$$\left\{\begin{array}{c}\text{thermal energy out}\\ \text{accompanied by through-}\\ \text{flow gas at } \theta+\Delta\theta\end{array}\right\} = Q_{gc}\rho_g c_g \, T\big|_{\theta+\Delta\theta}$$

$$\left\{\begin{array}{c}\text{thermal energy through}\\ \text{exchange between}\\ \text{gas and solids}\end{array}\right\}$$

$$= \underset{\substack{\text{volume}\\ \text{of}\\ \text{cloud}}}{V_\theta} \cdot \underset{\substack{\text{volume}\\ \text{fraction}\\ \text{of solids}}}{(1-\epsilon_{mf})} \cdot \underset{\substack{\text{specific}\\ \text{surface}\\ \text{of solids}}}{S_p} \cdot \underset{\substack{\text{transfer rate of}\\ \text{thermal energy per unit}\\ \text{surface area of solids}}}{h_p(T_s - T_c)}$$

$$\left[\begin{array}{c}\text{thermal energy in through}\\ \text{exchange between cloud}\\ \text{and emulsion gas}\end{array}\right]$$

$$= \underbrace{(2\pi R_c)\ (R_c d\theta)}_{\text{interface area}}\ \underbrace{H_{ce}\ (T_e - T_c)}_{\substack{\text{transfer rate of thermal}\\ \text{energy per unit area in}\\ \text{the direction normal to}\\ \text{the interface}}}\ \sin\theta$$

Substituting these individual terms and the expression for $V\theta$ into eqn. (H-1), dividing each term by $\sin\theta d\theta$ and taking $\Delta\theta \rightarrow 0$ give

$$\frac{Q_g \rho_g c_g}{\sin\theta}\frac{dT}{d\theta} = 2\pi R_p^2 H_{ce}\ (T_e - T_c) + \frac{2}{3}\pi\ (R_c^3 - R_b^3)(1-\epsilon_{mf})\ S_p h_p (T_p - T_c) \qquad \text{(G-2)}$$

This is eqn. (154) in the text.

APPENDIX H DERIVATION OF EQN. (161)

For the controlled volume with a size of $A_b \Delta_z$ depicted in Fig. 18, a quasi-steady state moisture balance leads to

$$0 = \left[\begin{array}{c}\text{rate of moisture in by}\\ \text{in by convection}\end{array}\right] - \left[\begin{array}{c}\text{rate of moisture out}\\ \text{by convection}\end{array}\right] + \left[\begin{array}{c}\text{rate of moisture in through}\\ \text{exchange with cloud-}\\ \text{wake phase}\end{array}\right] \qquad \text{(H-1)}$$

The various contributions to eqn. (H-1) are

$$\left[\begin{array}{c}\text{rate of moisture}\\ \text{in by convection}\\ \text{at z}\end{array}\right] = (u_b A_b)\rho_g x_b\big|_z$$

$$\left[\begin{array}{c}\text{rate of moisture}\\ \text{out by convection}\\ \text{at } z+\Delta z\end{array}\right] = (u_b A_b)\rho_g x_b\big|_{z+\Delta z}$$

$$\left[\begin{array}{c}\text{rate of moisture in through}\\ \text{exchange with cloud-}\\ \text{wake phase}\end{array}\right] = \frac{(A_b \Delta z)}{S_b} \; nQ_{gc}\rho_g \cdot (x_{en} - x_b)$$

volume of bed with height Δz — *flow rate of through-flow gas per unit volume of bed* — *concentration difference between through-flow gas entering and leaving bu*

Substituting these individual terms into eqn. (H-1), dividing each term by $\rho_g \Delta z \dfrac{A_b}{\delta_b}$ and letting $\Delta z \to 0$, we obtain

$$\delta_b u_b \frac{dx_b}{dz} = n\, Q_{gc}\, (x_{en} - x_b) \qquad \text{(H-2)}$$

This is eqn. (161) in the text.

APPENDIX I. DERIVATION OF EQN. (165)

Referring to Fig. 16, a quasi-steady state energy balance around the controlled volume with size of Ab oz is

$$0 = \left\{\begin{array}{c}\text{rate of thermal}\\ \text{energy in by}\\ \text{convection}\end{array}\right\} - \left\{\begin{array}{c}\text{rate of thermal}\\ \text{energy out by}\\ \text{convection}\end{array}\right\}$$

$$+ \left\{\begin{array}{c}\text{rate of thermal energy}\\ \text{in by exchange with}\\ \text{cloud-wake phase}\end{array}\right\} \qquad (I\text{-}1)$$

The individual terms in eqn. (I-1) are

$$\left\{\begin{array}{c}\text{rate of thermal}\\ \text{energy in by}\\ \text{convection at z}\end{array}\right\} = (A_b u_b)\rho_g c_g T|_z$$

$$\left\{\begin{array}{c}\text{rate of thermal}\\ \text{energy in by}\\ \text{convection at z+}\Delta z\end{array}\right\} = (A_b u_b)\rho_g c_g T|_{z+\Delta z}$$

$$\left\{\begin{array}{c}\text{rate of thermal energy}\\ \text{in through exchange}\\ \text{with cloud-wake phase}\end{array}\right\}$$

$$= \frac{(A_b \Delta z)}{\delta_b} \cdot nQ_{gc}\rho_g \cdot (T_{en} - T_b)$$

volume of bed associated with the c — *flow rate of through-flow gas per unit volume of bed* — *temperature difference between the through-flow gas entering and leav bu*

Inserting these individual terms into eqn. (J-1), dividing each term by $(\frac{A_b}{\delta_b}$ $\Delta z\ c_g\rho_g)$ and letting $\Delta z \rightarrow 0$ yields

$$u_b\delta_b \frac{dT_b}{dz} = n\,Q_{gc}\,(T_{en} - T_b) \qquad (I\text{-}2)$$

This is eqn. (165) in the text.

APPENDIX J. DERIVATION OF EQN. (187)

Equation (146) can be rewritten as below

$$\frac{\partial x_c}{\partial y} - \{\alpha_1[1+\alpha_2(\frac{\sqrt{2}}{2} - y)]^{-1} + \alpha_3\}x_c = -\alpha_4[1+\alpha_2(\frac{\sqrt{2}}{2} - y)]^{-1} - \alpha_5 \qquad (J-1)$$

where

$$\alpha_1 = \frac{2}{3}\pi \frac{R_c^3-R_b^3}{Q_{gc}}(1-\epsilon_{mf})S_p K_g,\ \alpha_2 = 2\pi \frac{R_c^3-R_b^3}{Q_{gc}}(1-\epsilon_{mf})\frac{K_g}{R_p},$$

$$\alpha_3 = \frac{2\pi R_c^2-K_c}{Q_{gc}},\ \alpha_4 = \frac{2}{3}\pi \frac{R_c^3-R_b^3}{Q_{gc}}(1-\epsilon_{mf})s_p k_g x_p,$$

$$\alpha_5 = \frac{2\pi R_c^2 K_c}{Q_{gc}} x_e,\ y = \cos\theta \qquad (J-2)$$

To solve eqn. J-1, first evaluate integration factor, which is determined by

$$\exp\{-\int_0^y \{\alpha_1[1+\alpha_2(\frac{\sqrt{2}}{2} - y)]^{-1} + \alpha_3\}dy\}$$

$$= [\frac{1}{1 + \alpha_2(\frac{\sqrt{2}}{2} - y)}]^{-\frac{\alpha_1}{\alpha_2}} \cdot \exp(-\alpha_3 y) \qquad (J-3)$$

Multiplying both sides of eqn. (J-1) by the integration factor and rearranging the resultant expression yields

$$\frac{d}{dy}\{x_c [\frac{1}{1 + \alpha_2(\frac{\sqrt{2}}{2} - y)}]^{-\frac{\alpha_1}{\alpha_2}} \cdot \exp(-\alpha_3 y))$$

$$= -\alpha_4 [\frac{1}{1 + \alpha_2(\frac{\sqrt{2}}{2} - y)}]^{1-\frac{\alpha_1}{\alpha_2}} \cdot \exp(-\alpha_3 y)$$

$$- \alpha_5 \left[\frac{1}{1 + \alpha_2(\frac{\sqrt{2}}{2} - y)}\right]^{-\frac{\alpha_1}{\alpha_2}} \cdot \exp(-\alpha_3 y) \qquad \text{(J-3)}$$

From eqn. (J-2), we obtain

$$\frac{\alpha_1}{\alpha_2} = \frac{R_p}{3} S_p \qquad \text{(J-4)}$$

For spherical particles, $\phi_s = 1$ and

$$S_p = \frac{6}{d_p \phi_s} = \frac{6}{d_p} \qquad \text{(J-5)}$$

Thus

$$\frac{\alpha_1}{\alpha_2} = \frac{R_p}{3} S_p = 1 \qquad \text{(J-6)}$$

Now eqn. (J-3) becomes

$$\frac{d}{dy}\left(x_c[1+\alpha_2(\frac{\sqrt{2}}{2} - y)] \cdot \exp(-\alpha_3 y)\right)$$

$$= - \alpha_5[1+\alpha_2(\frac{\sqrt{2}}{2} - y)] \cdot \exp(-\alpha_3 y) \qquad \text{(J-7)}$$

Integration of eqn. (J-7) gives

$$x_c[1+\alpha_2(\frac{\sqrt{2}}{2} - y)] \cdot \exp(-\alpha_3 y)$$

$$= \{\frac{\alpha_4}{\alpha_3} + \frac{\alpha_5}{\alpha_3}[1+\alpha_2(\frac{\sqrt{2}}{2} - y)] - \frac{\alpha_2\alpha_5}{\alpha_3^2}\} \exp(-\alpha_3 y)$$

$$+ \text{constant} \qquad \text{(J-8)}$$

Using boundary condition, eqn. (147), we obtain

$$x_b \exp(-\alpha_3 \frac{\sqrt{2}}{2}) = (\frac{\alpha_4}{\alpha_3} + \frac{\alpha_5}{\alpha_3} - \frac{\alpha_2\alpha_5}{\alpha_3^2}) \exp(-\alpha_3 \frac{\sqrt{2}}{2}) + \text{constant}$$

or

$$\text{constant} = \exp(-\alpha_3\frac{\sqrt{2}}{2}) \left(x_b - \frac{\alpha_4}{\alpha_3} - \frac{\alpha_5}{\alpha_3} + \frac{\alpha_2\alpha_5}{\alpha_3^2}\right) \tag{J-9}$$

Substituting into eqn. (J-8) results in

$$x_c = [1+\alpha_2(\frac{\sqrt{2}}{2} - y)^{-1}\{\{\frac{\alpha_4}{\alpha_3} + \frac{\alpha_5}{\alpha_3}[1 - \alpha_2(\frac{\sqrt{2}}{2} - y)] - \frac{\alpha_2\alpha_5}{\alpha_3^2}\}$$

$$+ \exp[\alpha_3(y - \frac{\sqrt{2}}{2})] \left(x_b - \frac{\alpha_4}{\alpha_3} + \frac{\alpha_5}{\alpha_3} + \frac{\alpha_2\alpha_5}{\alpha_3^2}\right)\} \tag{J-10}$$

From eqn. (J-2), we can determine

$$\frac{\alpha_4}{\alpha_3} = \frac{(R_c^3-R_b^3)}{3R_c^2K_c}(1 - \epsilon_{mf})S_p x_p^* k_g, \qquad \frac{\alpha_5}{\alpha_3} = x_e,$$

$$\frac{\alpha_2\alpha_5}{\alpha_3^2} = x_e \frac{(R_c^3-R_b^3)k_g}{R_c^2K_c R_p} \tag{J-11}$$

Substituting expressions in (J-11), together with $y=\cos\theta$, into eqn. (J-10), and rearrangement of the resultant equation gives

$$x_c = [1+2\pi \frac{(R_c^3-R_b^3)}{Q_{gc}}(1 - \epsilon_{mf})\frac{k_g}{R_p}(\frac{\sqrt{2}}{2} - \cos\theta)]^{-1}$$

$$\cdot \{[1 + \frac{(R_c^3-R_b^3)}{R_c^2K_c}(1 - \epsilon_{mf})k_g + 2\pi \frac{(R_c^3-R_b^3)}{Q_{gc}}\frac{k_g}{R_p}(1 - \epsilon_{mf})(\frac{\sqrt{2}}{2} - \cos\theta)]x_e$$

$$- \frac{(R_c^3-R_b^3)S_p k_g}{3R_c^2 K_c}(1 - \epsilon_{mf})x_p^* + \exp[-\frac{2\pi R_c^2 K_c}{Q_{gc}}(\frac{\sqrt{2}}{2} - \cos\theta)]$$

$$\cdot \{x_b + [1 + \frac{(R_c^3-R_b^3)k_g}{R_c^2K_c R_p}(1 - \epsilon_{mf})]x_e\}$$

$$- \frac{(R_c^3-R_b^3)S_p}{3R_c^2K_c}(1-\epsilon_{mf})K_g x_p^*\}) \quad \text{(J-12)}$$

Substituting $S_p = \frac{3}{R_p}$ into eqn. (J-12) and rearrangement yield

$$\frac{\beta(\theta)x_c-[\beta^*+\beta(\theta)]x_e+\beta^* x_p^*}{x_b-(1+\beta^*)x_e+\beta^* x_p^*}$$

$$= \exp\left[-\frac{2\pi P_c^2}{Q_{ge}} k_c \left(\frac{\sqrt{2}}{2}-\cos\theta\right)\right] \quad \text{(J-13)}$$

where

$$\beta(\theta) = 1 + 2\pi \frac{R_c^3-R_b^3}{Q_{gc}}(1-\epsilon_{mf})\frac{k_g}{R_p}\left(\frac{\sqrt{2}}{2}-\cos\theta\right)$$

and

$$\beta^* = \frac{R_c^3-R_b^3}{R_c^2K_cR_p}(1-\epsilon_{mf}) \quad \text{(J-14)}$$

Under the assumption $x_c = x_p^*$, eqn. (J-13) reduces to

$$\frac{x_c-x_e}{x_b-x_e} = \frac{1}{\beta(\theta)} \exp\left[-\frac{2\pi R_c^2}{Q_{gc}} K_c \left(\frac{\sqrt{2}}{2}-\cos\theta\right)\right]$$

$$= \left[1 + 2\pi \frac{(R_c^3-R_b^3)}{Q_{gc}} \frac{k_g}{R_p}\left(\frac{\sqrt{2}}{2}-\cos\theta\right)\right]^{-1}$$

$$\cdot \exp\left[-\frac{2\pi R_c^2 K_c}{Q_{gc}}\left(\frac{\sqrt{2}}{2}-\cos\theta\right)\right] \quad \text{(J-15)}$$

This is eqn. (187) in the text.

Table 1. Classification of fluidized-bed dryers based on operating modes.

Mode	number of stages	equipment type	References
a. Batch	single	stationary vibrating rotating	information Bull., 1960; Cherret, 1964
b. Continuous	single	stationary vibrating rotating	Priestley, 1962; Toei, 1966 Osinskii, 1969; Niro Atomizer, 1980 Hanni, 1976
	multiple	stationary vibrating rotating	Brit. Chem. Eng., 1961; Toei, 1966; Mrowiec, 1977

Table 2. Classification of the dryer types based on structural and mechanical features.

				References
a. Geometry	Bed with constant cross-section	cylindrical	stationary vibrating rotating	Toei, 1966 Niro Atomizer, 1980 Hanni, 1976
		rectangular	stationary vibrating	Toei, 1976 Osinskii, 1969
	Bed with varying cross-section	tapered	stationary vibrating	Brit. Chem. Eng., 1961
		cyclic	stationary vibrating	
b. Bed Depth	Deep		stationary vibrating rotating	Mrowies, 1977; Niro Atomizer, 1980
	Shallow		stationary vibrating rotating	Toei, 1966; Niro Atomizer, 1980 Niro Atomizer, 1980

Table 3. Evaluation of the parameters used in the semicompartment model.

Parameter	Evaluating Equation	Reference
Bubble size	$d_b = d_{bm} - (d_{bm} - d_{bo}) \exp(\frac{-0.3}{D_c} z)$	Mori and Wen, 1975
	$d_{bm} = 0.65 [A_t(U_o - U_{mf})]^{0.4}$	
	$d_{bo} = 0.00376(U_o - U_{mf})^2$	
Compartment size	$\Delta z_i = \bar{d}_{bi} = 3.33 D_c \ln[F + (1-F)\exp(\frac{0.3}{D_c} d_{bm})]$	
	where $F = (1-d_{bo}/d_{bm})\exp(\frac{-0.3}{D_c} z_{i-1})$	Viswanathan, 1982
	$\bar{d}_{bN} = d_{bm}/[1-\ln(d_{bN-1}/d_{bN})/(\frac{0.3}{D_c} \Delta z_n)]$	
Bubble rise velocity	$u_b = U_o - u_e \epsilon_{mf} + 0.71 (g \bar{d}_{bi})^{1/2}$	Viswanathan and Rao, 1980
Emulsion gas velocity	$u_e \epsilon_{mf} = u_{mf} - \alpha \delta u_b \epsilon_{mf}/(1-\delta_b-\alpha\delta_b)$	ibid
Cloud size	$\beta = 3u_f/(u_b - u_f)$	ibid
Wake size	$\frac{\alpha}{1+\alpha} = 0.3$	Rowe and Partridge, 1965
Bubble fraction	$\delta_b = \frac{U_o - u_e \epsilon_{mf}}{[1 + (\alpha + \beta)\epsilon_{mf}] u_h - [1 + \alpha + \beta] u_c \epsilon_{mf}}$	Viswanathan and Rao, 1984
Gas exchange coefficients	$(K_{bc})_b = 4.5 \frac{u_{mf}}{d_b} + 5.85 \frac{D^{0.5} g^{0.25}}{d_b^{1.25}}$	Davidson and Harrison, 1963
	$(K_{ce})_b = 6.78 (\frac{D\epsilon_{mf} u_b}{d_b^3})^{0.5} + 3 \frac{(1-\delta_b)u_{mf}}{d_b(1-\delta_b-\alpha\delta_b)(1-u_f/u_b)}$	Kunni and Levenspiel, 1969; Viswanathan, 1982
Particle to gas mass transfer coefficient	$K_{pg} = \frac{D}{\phi_s d_p y} [2 + 1.8 Re_{mf}^{0.5} Sc^{0.33}]$	Kunni and Levenspiel, 1969

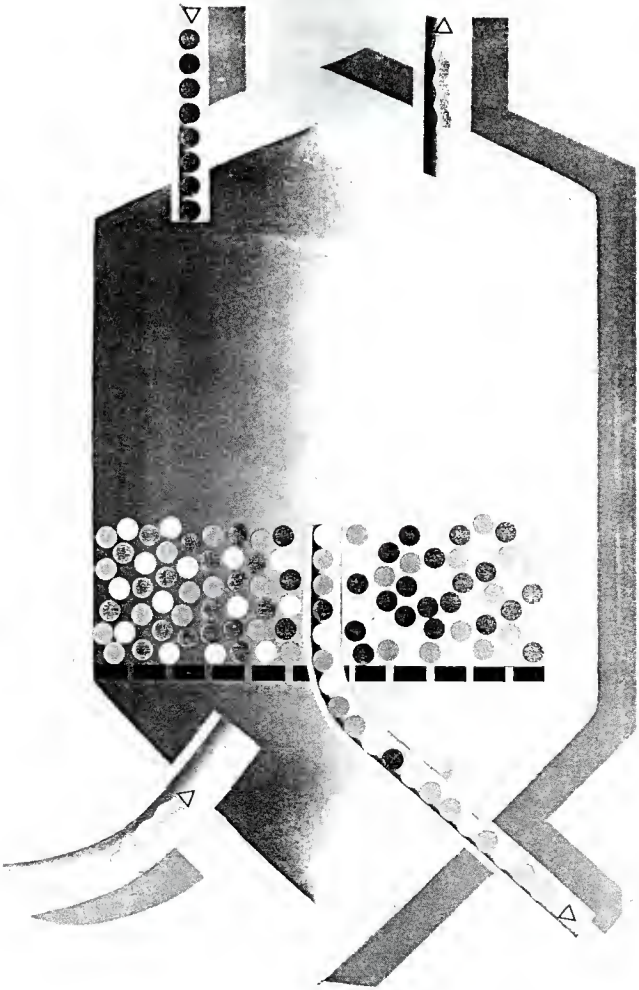

Fig. 1. Single-stage cylindrical fluidized-bed dryer
(Niro Atomizer, 1980)

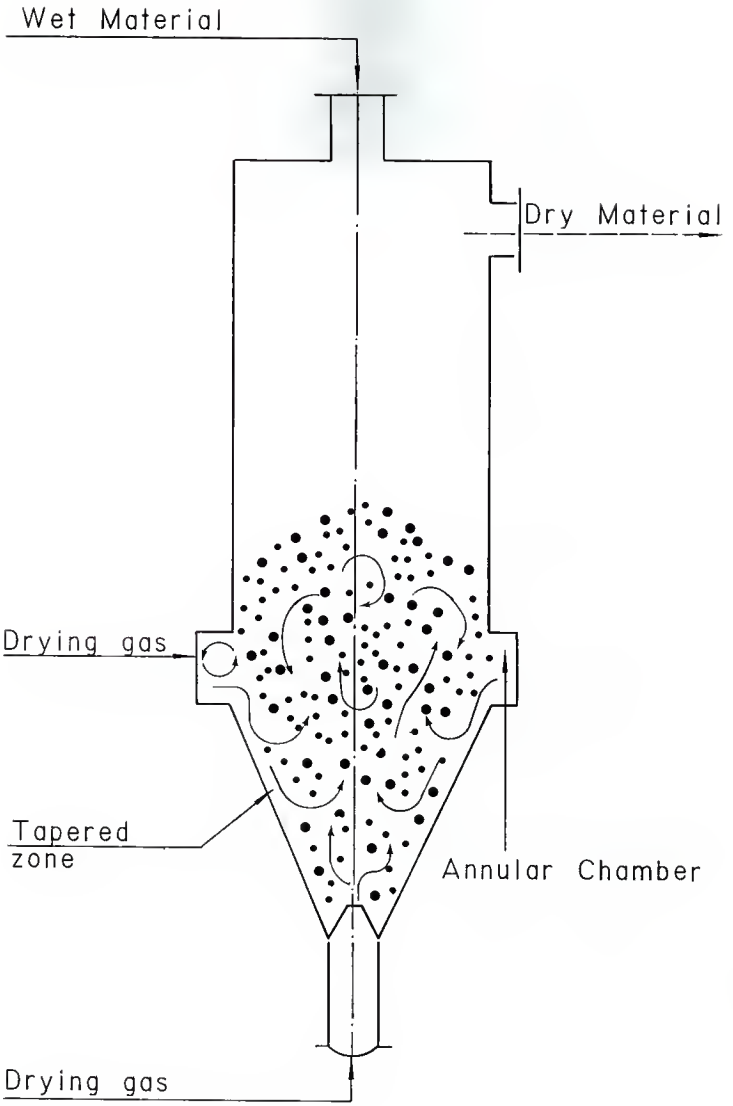

Fig. 2. Schematic of a tapered fluidized-bed dryer

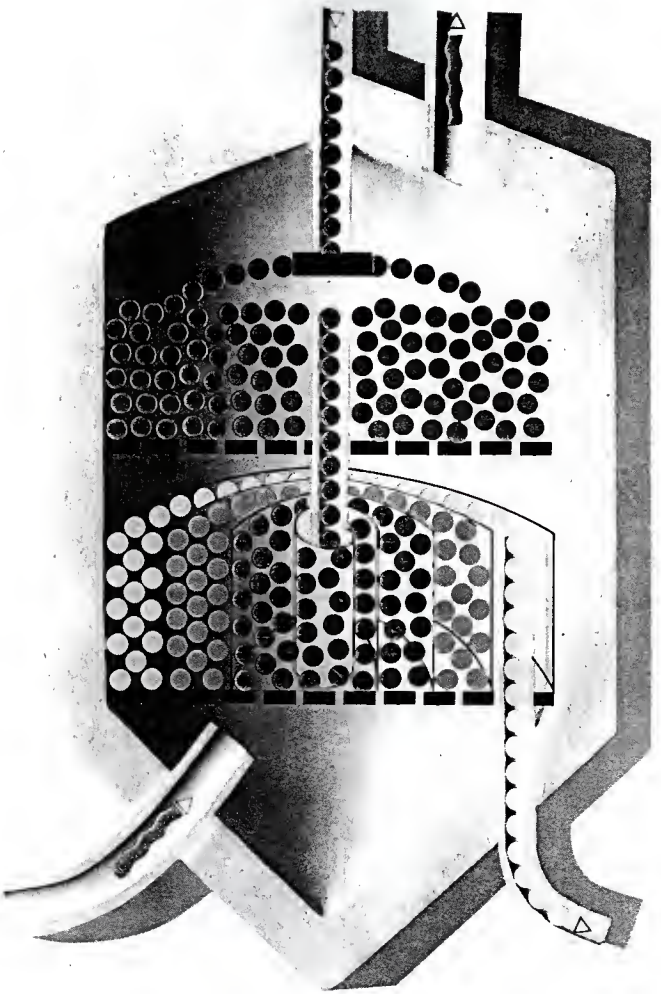

Fig. 3. Two-stage fluidized-bed drying system (Niro Atomizer, 1980)

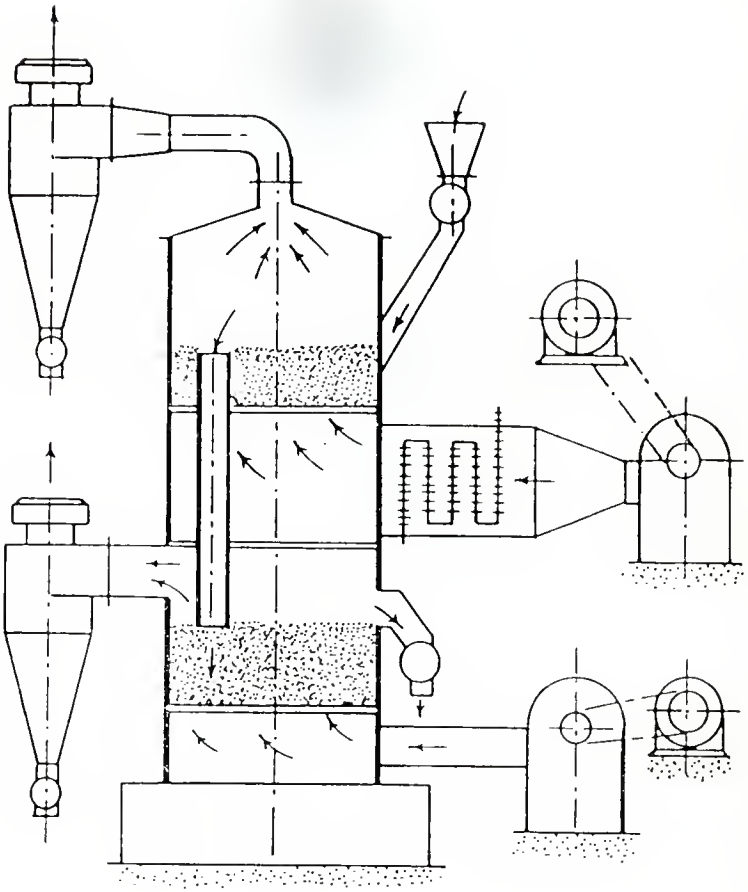

Fig. 4. Continous multi-stage fluidized-bed dryer (Toei, 1966)

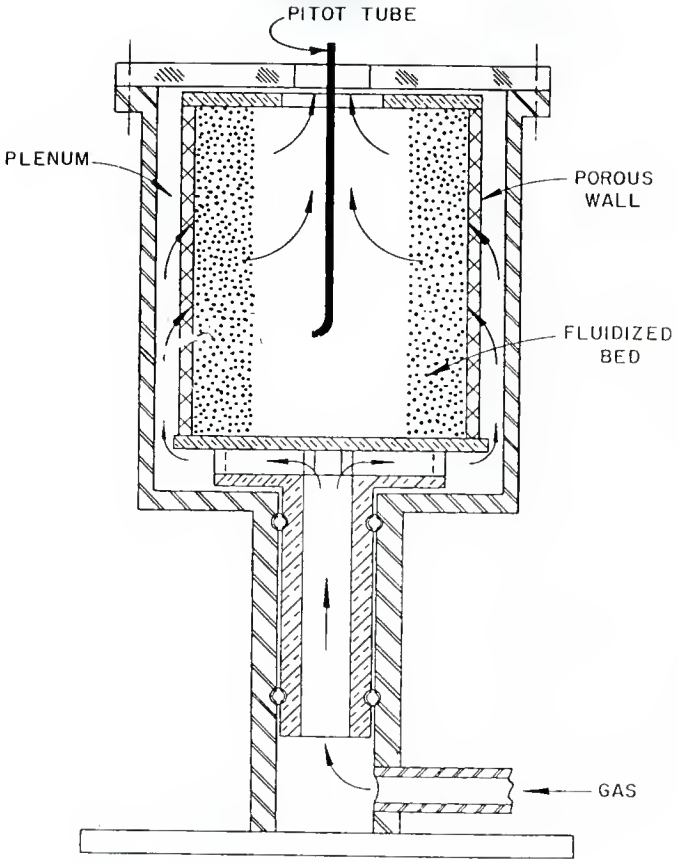

Fig. 5. Schematic of centrifugal fluidized-bed apparatus .
(NASA, 1972)

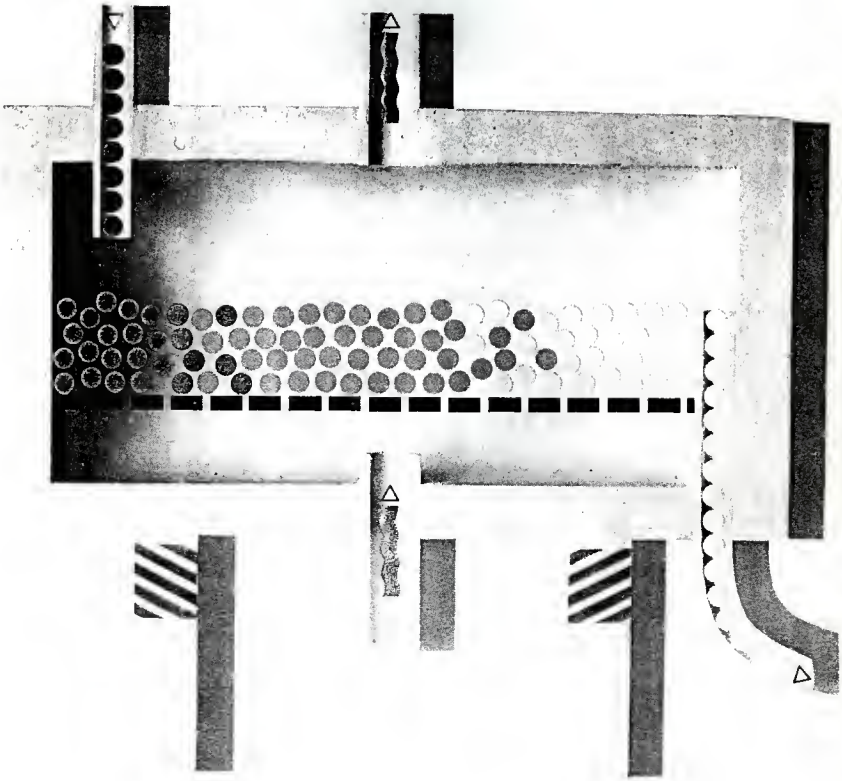

Fig. 6. Vibro-fluidized bed dryer (Niro Atomizer, 1980)

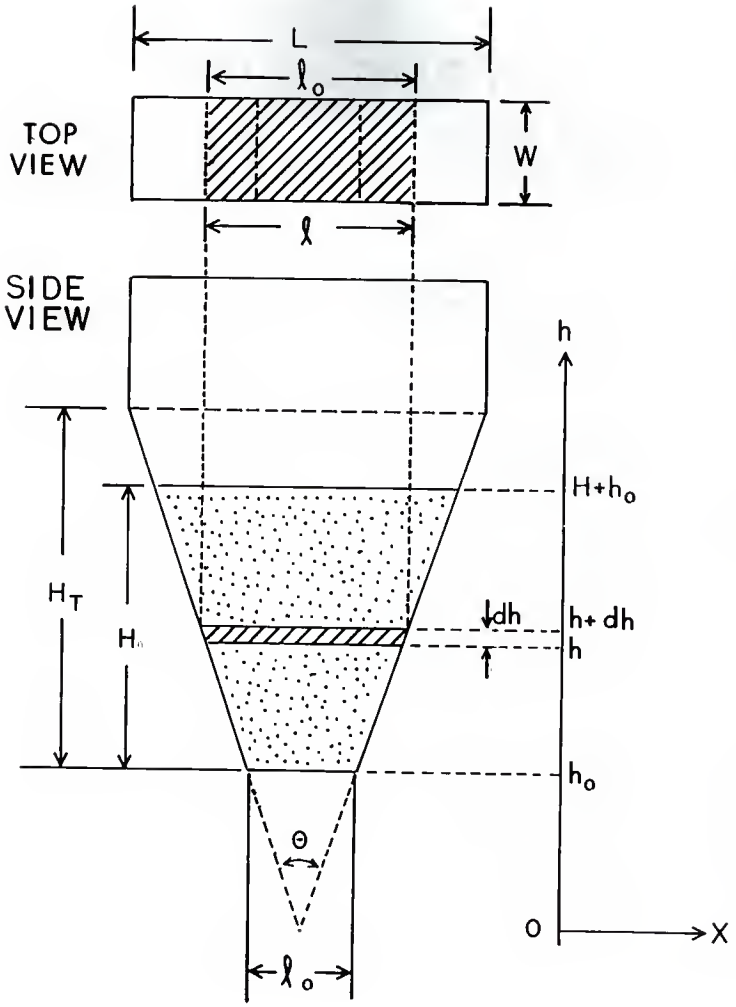

Fig. 7. Structural representation of a tapered fluidzed-bed dryer

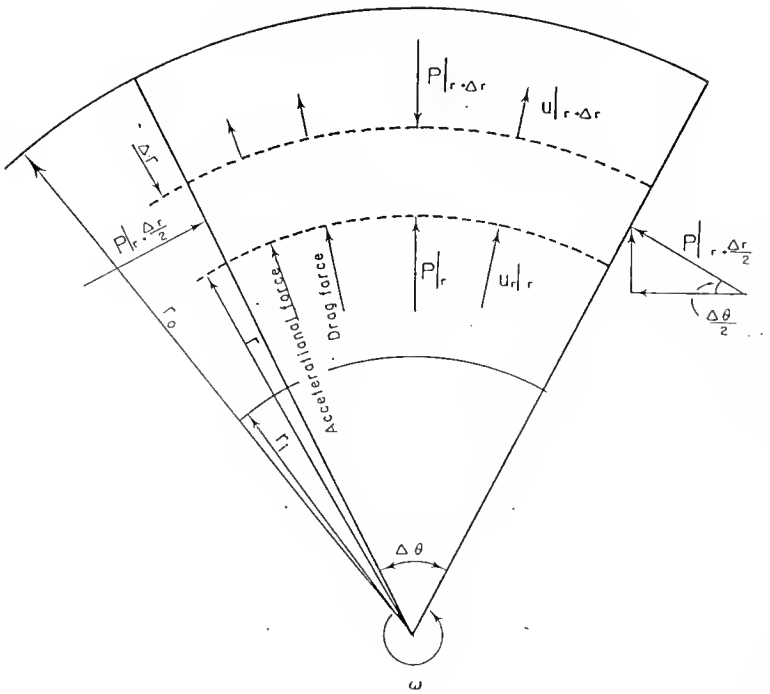

Fig. 8. Schematic of a section of a centrifugal fluidized-bed

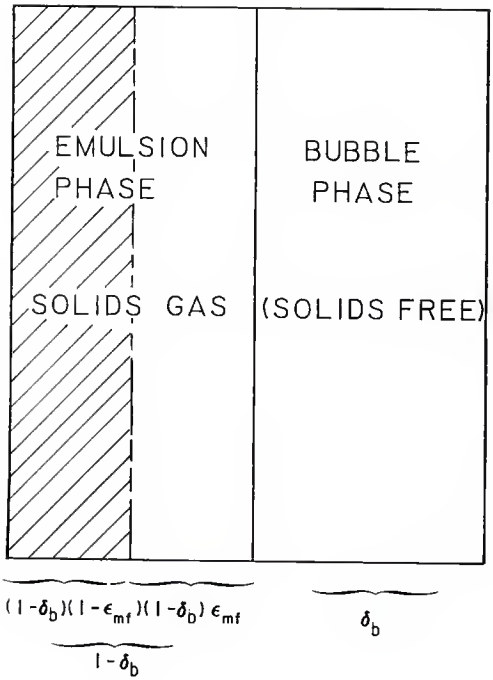

Fig. 9. Schematic representation of two-phase theory of fluidization

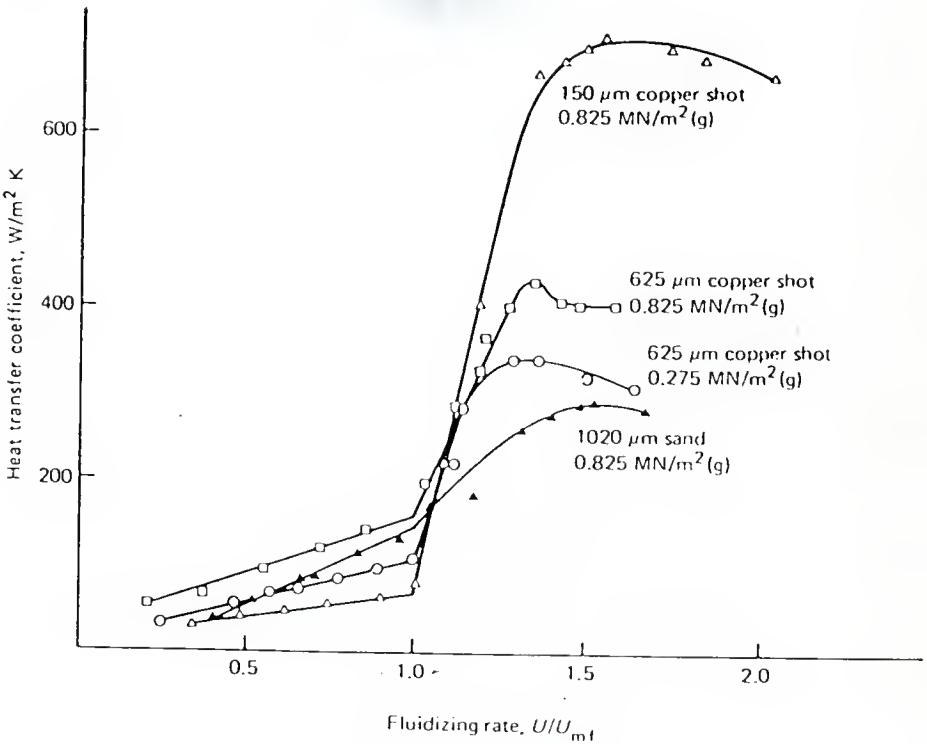

Fig. 10. The variation with gas velocity of the bed-to-surface heat transfer coefficient without radiation transfer (Botterill, 1975)

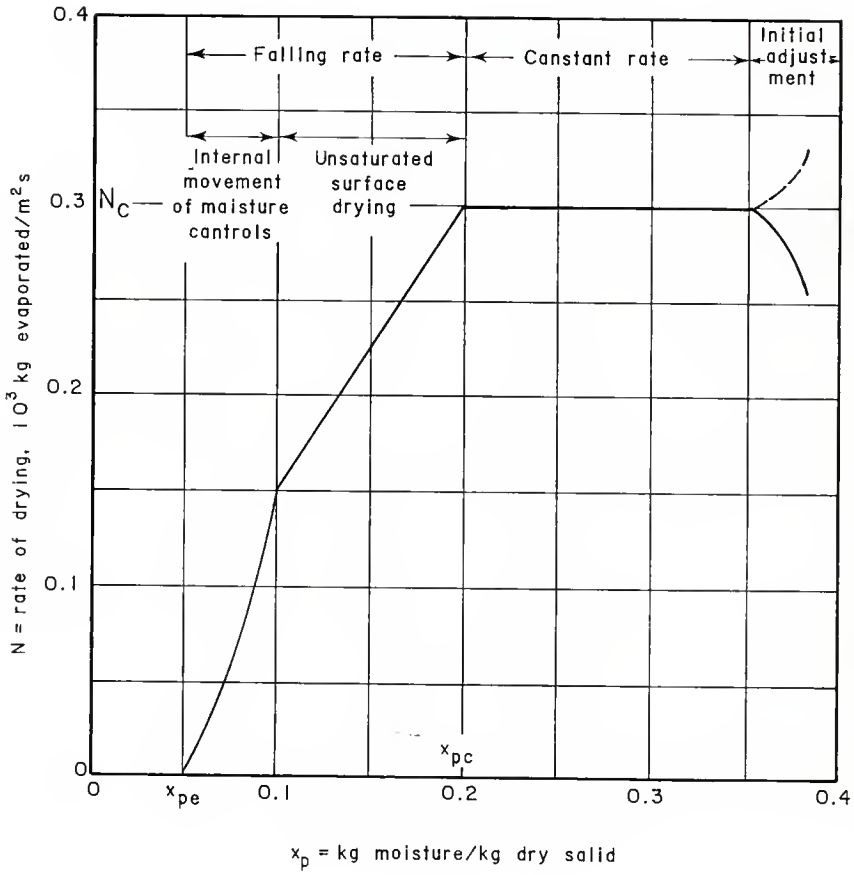

Fig. 11. Typical rate-of-drying curve (Trebal, 1980)

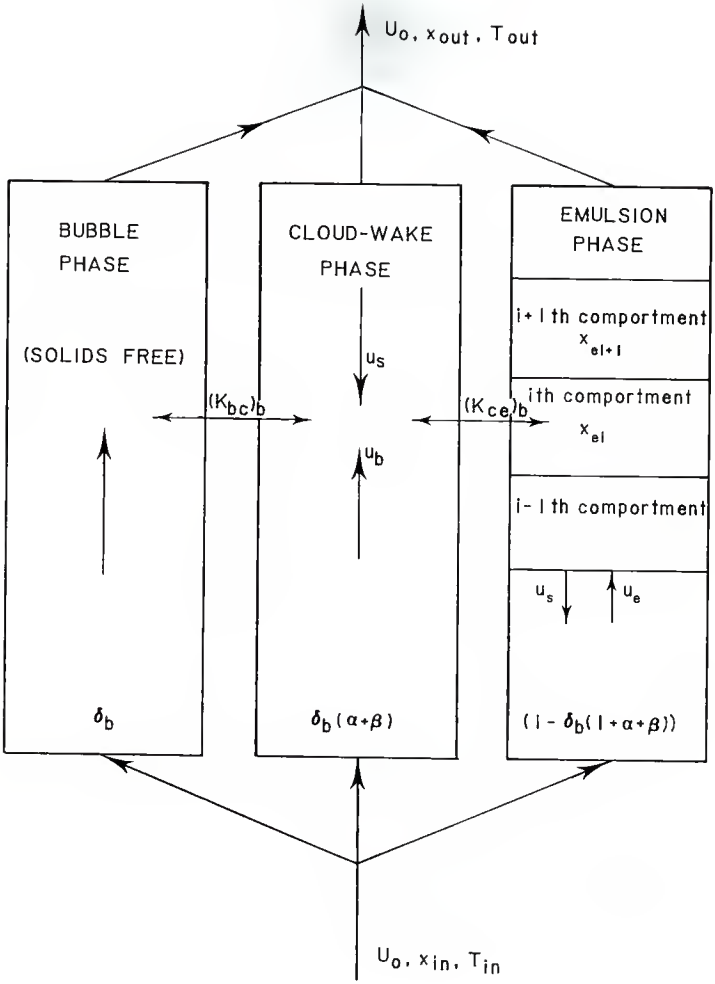

Fig. 12. Schematic representation of three-phase and semi-compartment model for a batch fluidized bed dryer

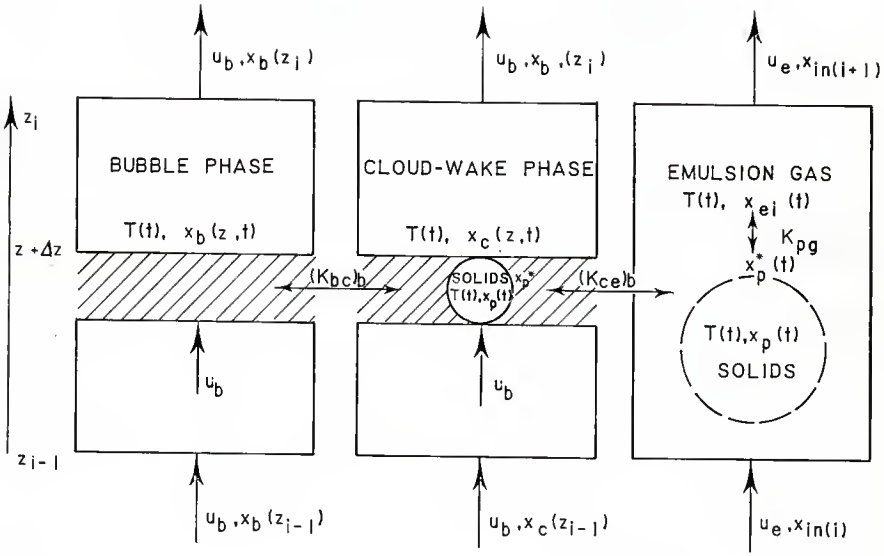

Fig. 13 Moisture transfer between phases with respect to ith compartment

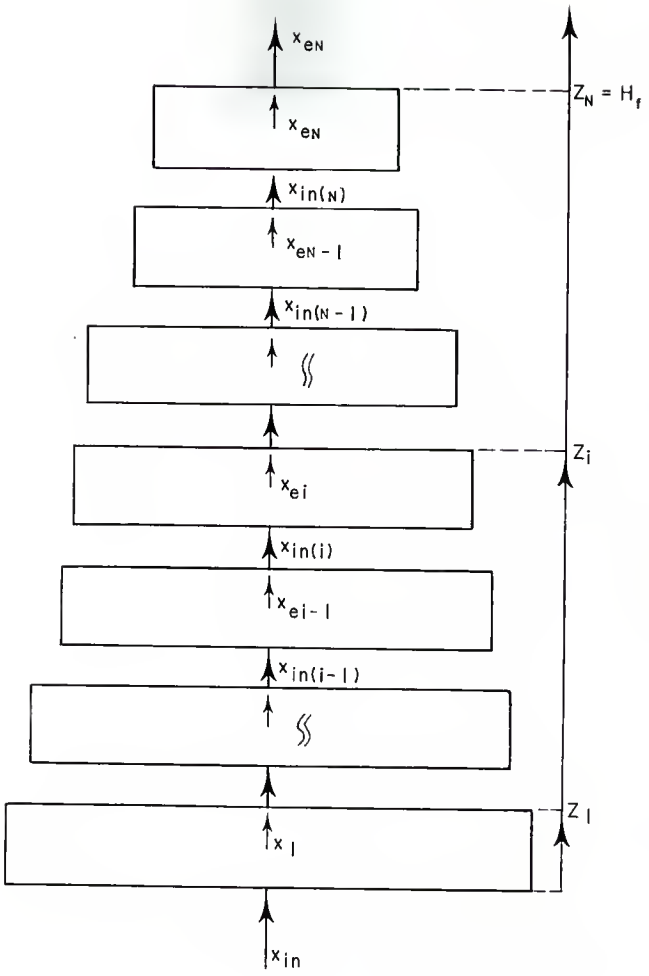

Fig. 14. Representation of compartments of upflow emulsion gas

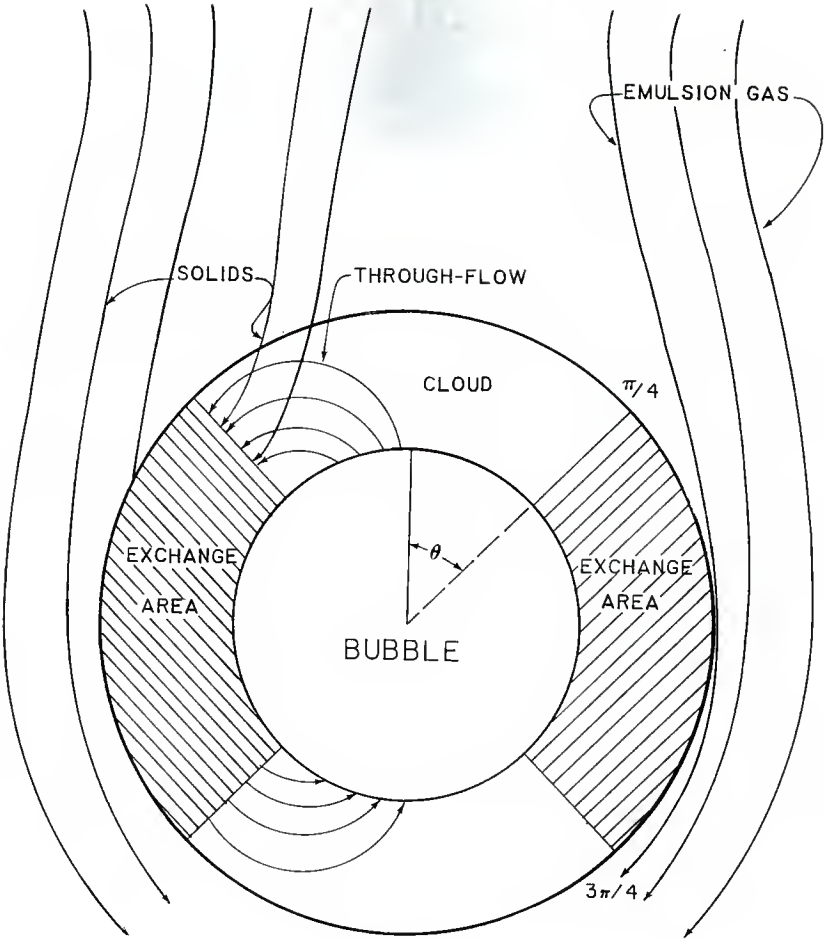

Fig. 15. Schematic representation of bubble-cloud model

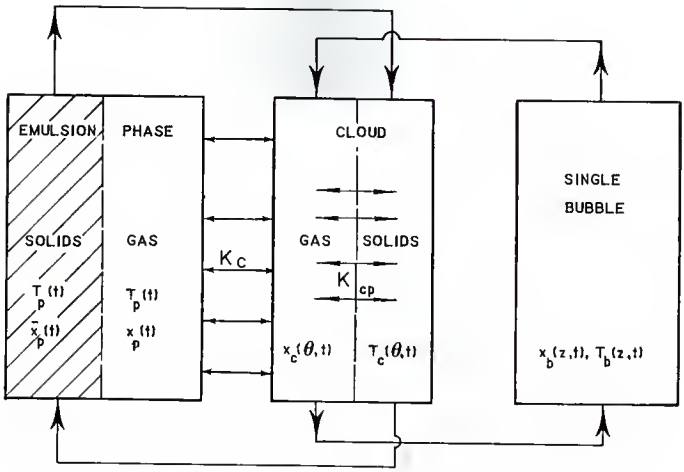

Fig. 16. Moisture transport in a single bubble, its surrounding cloud and in emulsion phase

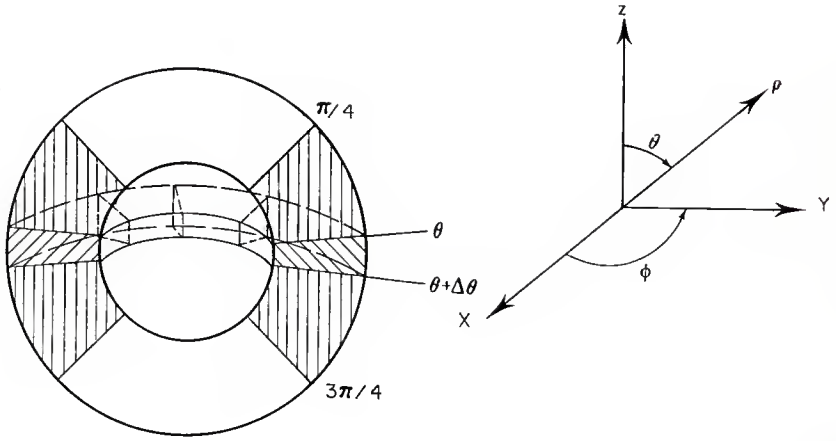

Fig. 17. Representation of the exchange zone in cloud

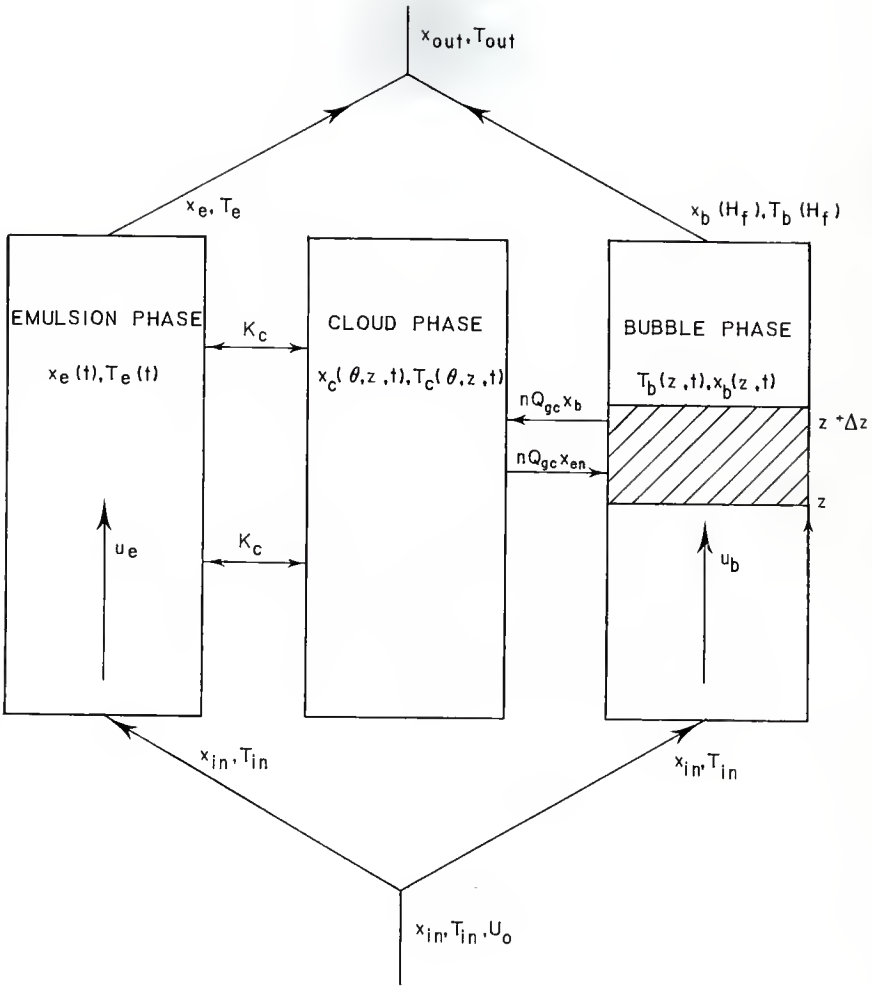

Fig. 18. Moisture transfer between phases

CHAPTER III

MODELING AND SIMULATION OF A CONTINUOUS FLUIDIZED-BED DRYER

MATHEMATICAL MODELING

A schematic diagram of the model is shown in Fig. 1. The present model is based on the two-phase theory of fluidization (see, e.g., Davison and Harrison, 1963). The underlying assumptions of this theory are that the bed is divided into two phases, a bubble phase and an emulsion phase (which remains in minimum fluidization conditions), and that the excess flow of the fluidizing fluid above minimum fluidization passes through the bed as bubbles. The fluid in the bubble and emulsion phases and the solid particles are considered to be continua. Additional simplifying assumptions imposed in deriving the present model are as follows:

1. The bubble phase is solid-free and the size of bubbles is uniform and fixed at the so-called effective bubble size.
2. The movement of bubbles through the bed is of plug flow.
3. The clouds surrounding the rising bubbles are very thin, and therefore, the bubble phase exchanges mass and energy only with the emulsion gas.
4. The emulsion gas and solid particles are perfectly mixed.
5. Solid particles are added and removed at a constant rate.
6. The inlet temperature and moisture content of solids are assumed to be uniform.
7. The internal resistance of solids to mass and heat transfer is negligible.
8. Particles are considered to be uniform in size, shape and physical properties.
9. The temperature and moisture content of each particle depend on its age, t_s, that is, the length of its stay in the dryer.

As a consequence of assumptions 4 and 5, the residence time distribution function for solids under a steady-state condition is

$$f(t_s) = \frac{1}{\bar{t}_s} \exp(-\frac{t_s}{\bar{t}_s}) \tag{1}$$

10. Viscous dissipation is negligible.

11. The changes in the physical properties of both solids and drying gas due to the change of temperature are negligible.

These assumptions give rise to the mass and energy conservation equations for each phase of the fluidized-bed dryer.

Mass Conservation Equations

A. Bubble phase. A steady-state moisture balance around the controlled volume depicted in Fig. 2 gives (see APPENDIX A)

$$\frac{U_b}{\delta_b} \frac{dx_b}{dz} = (K_{be})_b (x_e - x_b) \tag{2-a}$$

with the boundary condition

$$x_b = x_0 \quad \text{at} \quad z = 0 \tag{2-b}$$

Integration of eqn. (2-a), subject to eqn. (2-b), gives

$$x_b = x_e - (x_e - x_0) \exp[\frac{-(K_{be})_b \delta_b}{U_b} z] \tag{3}$$

The parameters in this expression are evaluated from the following relationships.

1. The bed fraction of the bubble phase, δ_b:

$$\delta_b = 1 - \frac{H_{mf}}{H_f} \tag{4}$$

where H_f/H_{mf} is given by (Babu et al. 1978)

$$\frac{H_f}{H_{mf}} = 1 + \frac{14.311(U_0-U_{mf})^{0.738} d_p^{1.006} \rho_p^{0.736}}{U_{mf}^{0.937} \rho_g^{0.126}} \tag{5}$$

Alternatively,

$$\delta_b = \frac{(U_0 - U_{mf})}{(U_0 - U_{mf}) + U_{br}} \tag{6}$$

where U_{br} is given by (Davison and Harrison, 1963)

$$U_{br} = 0.711(gd_b)^{0.5} \tag{7}$$

2. The superficial gas velocity through the bubble phase, U_b:

$$U_b = U_0 - U_{mf} \tag{8}$$

3. The minimum fluidization velocity, U_{mf} (Wen and Yu, 1966):

$$\frac{d_p U_{mf} \rho_g}{\mu_g} = \left((33.7)^2 + 0.0408 \frac{d_p^3 \rho_g (\rho_{ws} - \rho_g) g}{\mu_g^2} \right)^{0.5} - 33.7 \tag{9}$$

4. The gas interchange coefficient based on volume of bubbles, $(K_{be})_b$ (Kunii and Levenspiel, 1969):

$$(K_{be})_b = \frac{1}{1/(K_{ce})_b + 1/(K_{bc})_b} \tag{10}$$

where

$$(K_{bc})_b = 4.5 \frac{U_{mf}}{d_b} + 5.85 \frac{D_g^{1/2} g^{1/4}}{d_b^{5/4}} \tag{11}$$

$$(K_{ce})_b = 6.78 \left(\frac{\varepsilon_{mf} D_{eff} U_b}{d_b^3 \delta_b} \right)^{1/2} \tag{12}$$

with

$$D_{eff} = \varepsilon_{mf} D_g \tag{13}$$

ε_{mf} in the above expression can be approximated by (Broadhurst and Becker, 1975),

$$\varepsilon_{mf} = 0.586\phi_s^{-0.72}\left[\frac{\mu_g^2}{\rho_g(\rho_{ws}-\rho_g)gd_p^3}\right]^{0.029}\left(\frac{\rho_g}{\rho_{ws}}\right)^{0.021} \tag{14}$$

B. Emulsion gas. From a moisture balance around the entire emulsion gas, illustrated in Fig. 3, we obtain (see APPENDIX B)

$$0 = (U_{mf}A_t)\rho_g(x_0-x_e) + \int_0^{H_f} A_b\rho_g(K_{be})_b(x_b-x_e)dz$$

$$+ (H_fA_t)(1-\delta_b)(1-\varepsilon_{mf})\left(\frac{6}{d_p}\right)\sigma(\bar{x}_p^* - x_e) \tag{15}$$

If we define the average moisture content of gas bubbles, $\bar{x}_b$, as

$$\bar{x}_b = \frac{1}{H_f}\int_0^{H_f} x_b dz \tag{16}$$

eqn. (14) can be rewritten as

$$\rho_g \frac{U_{mf}}{H_f\delta_b}(x_e-x_0)$$

$$= \rho_g(K_{be})_b(\bar{x}_b-x_e) + \frac{(1-\varepsilon_{mf})(1-\delta_b)}{\delta_b}\frac{6}{d_p}\sigma(\bar{x}_p^*-x_e) \tag{17}$$

The parameters in the above equation can be evaluated from the following relationships

1. Evaporation coefficient, σ, (Palancz, 1983):

$$\sigma = \frac{h_p \rho_g D}{k_g} \tag{18}$$

where

$$h_p = c_g U_0 \rho_g j_h Pr_g^{-2/3} \tag{19}$$

$$j_h = \frac{Nu_p}{Re_p Pr_g^{1/3}} = \begin{cases} 1.77\ Re_p^{-0.44} & \text{if } Re_p \geq 30 \\ 5.70\ Re_p^{-0.78} & \text{if } Re_p < 30 \end{cases} \tag{20}$$

with

$$Nu_p = \frac{h_p d_p}{k_g}, \quad Pr_g = \frac{c_g \mu_g}{k_g}, \quad Re_p = \frac{d_p U_0 \rho_g}{(1-\varepsilon_{mf})\mu_g} \tag{21}$$

2. Average moisture content of the drying gas on the surface of a particle, $\bar{x}_p^*$:

$$\bar{x}_p^* = \int_0^\infty \frac{1}{\bar{t}_s} \exp\left(-\frac{t_s}{\bar{t}_s}\right) x_p^* \, dt_s \tag{22}$$

where x_p^* may be expressed as (Palancz, 1983)

$$x_p^* = \phi_1(T_p)\ \phi_2(x_p) \tag{23}$$

with

$$\phi_1(T_p) = 0.622 \frac{P_w}{760 - P_w} \tag{24}$$

and

$$\phi_2(x_p) = \begin{cases} 1 & \text{if } x_p > x_{pc} \\ \dfrac{x_p^n (x_{pc}^n + K)}{x_{pc}^n (x_p^n + K)} & \text{if } x_p \leq x_{pc} \end{cases} \qquad (25)$$

In eqn. (24)

$$P_w = 10^{\left(0.622 + \frac{7.5T_p}{238 + T_p}\right)} \qquad (26)$$

and n and k are constants.

C. Single solid particle. A moisture balance around a particle depicted in Fig. 3, results in (See APPENDIX C)

$$\rho_s \frac{dx_p}{dt_s} = -\left(1 + \frac{\rho_s}{\rho_w} x_{pc}\right) \frac{6}{d_p} \sigma (x_p^* - x_e) \qquad (27\text{-a})$$

with the boundary condition

$$x_p = x_{p0} \qquad \text{at } t_s = 0 \qquad (27\text{-b})$$

Equation (27-a) is coupled with T_p since x_p^* is a function of both x_p and t_p. The average moisture content of particles, $\bar{x}_p$, is obtained as

$$\bar{x}_p = \int_0^\infty \frac{1}{\bar{t}_s} \exp\left(-\frac{t_s}{\bar{t}_s}\right) \cdot x_p \, dt_s \qquad (28)$$

Energy Conservation Equations

A. Bubble Phase. From Fig. 2, a steady-state energy balance around the controlled volume gives (see APPENDIX D)

$$\rho_g \frac{U_b}{\delta_b} \frac{di_b}{dz} = (H_{be})_b (T_e - T_b) + \rho_g (K_{be})_b (x_e - x_b) i_{we} \tag{29}$$

where

$$i_b = c_g (T_b - T_{ref}) + x_b [c_{wv} (T_b - T_{ref}) + \gamma_0] \tag{30}$$

$$i_{we} = c_{wv} (T_e - T_{ref}) + \gamma_0 \tag{31}$$

From eqn. (3),

$$(K_{be})_b (x_e - x_b) = (K_{be})_b (x_e - x_0) \exp\left(\frac{-(K_{be})_b \delta_b}{U_b} z\right) \tag{32}$$

Using the above three expressions along with eqn. (2-a), we can rewrite eqn. (29) as

$$\frac{dT_b}{dz} = \frac{T_e - T_b}{(c_g + c_{wv} x_b)} \left[\frac{(H_{be})_b \delta_b}{U_b \rho_g} + \frac{\delta_b (K_{be})_b (x_e - x_0) c_{wv}}{U_b} \exp\left(- \frac{K_{be}}{U_b} \delta_b z\right) \right] \tag{33-a}$$

The appropriate boundary condition is

$$T_b = T_0 \qquad \text{at } z=0 \tag{33-b}$$

$(H_{be})_b$ in eqn (33-a) can be determined by (Kunni and Levarspiel, 1969)

$$(H_{be})_b = \frac{1}{1/(H_{bc})_b + 1/(H_{ce})_b} \tag{34}$$

where

$$(H_{bc})_b = 4.5 \frac{U_{mf}\rho_g c_g}{d_b} + 5.85 \frac{(k_g \rho_g c_g)^{1/2} g^{1/4}}{d_b^{5/4}} \tag{35}$$

$$(H_{ce})_b = 6.78(\rho_g c_g k_g)^{1/2} \left(\frac{\epsilon_{mf} U_b}{d_b \delta_b}\right)^{1/2} \tag{36}$$

B. Emulsion gas. Referring to Fig. 3, a steady-state energy balance around the entire emulsion gas gives (See APPENDIX E)

$$\begin{aligned} 0 = {} & (U_{mf}A_t)\rho_g(i_0 - i_e) + (H_f A_t)(1-\delta_b)(1-\epsilon_{mf})\frac{6}{d_p}\sigma(\bar{x}_p^* - x_e)\bar{i}_{ws} \\ & + \int_0^{H_f} A_b (H_{be})_b (T_b - T_e)dz + S_w h_w (T_w - T_e) \\ & - \int_0^{H_f} \rho_g A_b (K_{be})_b (x_e - x_b) i_{we} dz \\ & - (H_f A_t)(1-\delta_b)(1-\epsilon_{mf})\frac{6}{d_p} h_p (T_e - \bar{T}_p) \end{aligned} \tag{37}$$

where

$$\bar{i}_{ws} = c_{wv}(\bar{T}_p - T_{ref}) + \gamma_0 \tag{38}$$

$$i_0 = c_g(T_0 - T_{ref}) + x_0[c_{wv}(T_0 - T_{ref}) + \gamma_0] \tag{39}$$

$$i_e = c_g(T_e - T_{ref}) + x_e[c_{wv}(T_e - T_{ref}) + \gamma_0] \tag{40}$$

$$\bar{T}_p = \int_0^\infty \frac{1}{\bar{t}_s} \exp\left(-\frac{t_s}{\bar{t}_s}\right) T_p \, dt_s \tag{41}$$

We define the average temperature of gas bubbles, $\bar{T}_b$, as

$$\bar{T}_b = \frac{1}{H_f} \int_0^{H_f} T_b \, dz \tag{42}$$

and the specific heat transfer surface of the dryer wall

$$a_w = \frac{S_w}{V_{tot}} \tag{43}$$

Insertion of eqns. (38) through (43) into eqn. (37) yields

$$\begin{aligned} 0 = \frac{\rho_g U_{mf}}{H_f} \{ & c_g(T_0 - T_{ref}) + x_0[c_{wv}(T_0 - T_{ref}) + \gamma_0] - c_g(T_e - T_{ref}) \\ & - x_e[c_{wv}(T_e - T_{ref}) + \gamma_0]\} + \delta_b (H_{be})_b (\bar{T}_b - T_e) \\ & + (1-\delta_b)(1-\varepsilon_{mf}) \frac{6\sigma}{d_p} (\bar{x}_p^* - x_e)[c_{wv}(\bar{T}_p - T_{ref}) + \gamma_0] \\ & + a_w h_w (T_w - T_e) - (1-\delta_b)(1-\varepsilon_{mf}) \frac{6}{d_p} h_p (T_e - \bar{T}_p) \\ & - \rho_g \delta_b (K_{be})_b (x_e - x_b)[c_{wv}(T_e - T_{ref}) + \gamma_0] \end{aligned} \tag{44}$$

or

$$\frac{\rho_g U_{mf}}{H_f} \{ c_g(T_e - T_0) + (x_e - x_0)\gamma_0 + c_{wv}[(T_e - T_{ref})x_e - (T_0 - T_{ref})x_0]\}$$

$$= \delta_b (H_{be})_b (\bar{T}_b - T_e) + (1-\delta_b)(1-\varepsilon_{mf})\frac{6}{d_p} \{ \sigma(x_p^* - x)_e [c_{wv}(\bar{T}_p - T_{ref}) + \gamma_0]$$

$$- h_p(T_e - \bar{T}_p) \} + \rho_g \delta_b (K_{be})_b (\bar{x}_b - x_e)[c_{wv}(T_e - T_{ref}) - \gamma_0]$$

$$+ a_w h_w (T_w - T_e) \qquad (45)$$

Eliminating the term, $(K_{be})_b(\bar{x}_b - x_e)$, from the above expression by resorting to eqn. (17), eqn. (45) can be rewritten as

$$\frac{\rho_g U_{mf}}{H_f}(c_g + c_{wv}x_0)(T_e - T_0)$$

$$= \delta_b (H_{be})_b (\bar{T}_b - T_e) + (1-\delta_b)(1-\varepsilon_{mf})\frac{6}{d_p}(\bar{T}_p - T_e)[c_{wv}\sigma(\bar{x}_p^* - x_e) + h_p]$$

$$+ a_w h_w (T_w - T_e) \qquad (46)$$

The heat transfer coefficient between air and dryer wall, h_w, is correlated as (Li and Finlayson, 1977)

$$\frac{h_w d_p}{k_g} = 0.16\ Re^{0.93} \qquad (47)$$

C. Single particle. Referring to Fig. 4, an unsteady-state energy balance around a particle yields (see APPENDIX F)

$$\rho_s \frac{di_p}{dt_s} = (1 + \frac{\rho_s}{\rho_w} x_{pc})\frac{6}{d_p}[q_s - \sigma(x_p^* - x_e) i_{ws}] \qquad (48)$$

where

$$i_p = c_p(T_p - T_{ref}) + x_p c_w(T_p - T_{ref}) \tag{49}$$

$$i_{ws} = \gamma_0 + c_{wv}(T_p - T_{ref}) \tag{50}$$

The energy balance around the stagnant film surrounding the particle yields (see Fig. 4)

$$q_s + \sigma(x_p^* - x_e) i_{we} = h_p(T_e - T_p) + \sigma(x_p^* - x_e) i_{ws} \tag{51}$$

or

$$q_s - \sigma(x_p^* - x_e) i_{ws} = h_p(T_e - T_p) - \sigma(x_p^* - x_e) i_{we} \tag{52}$$

Insertion of eqns. (49), (52) and (31) into Eq. (48) and rearrangement of the resultant equation yield

$$\rho_s[(c_p + x_p c_w)\frac{dt_p}{dt_s} + c_w(T_p - T_{ref})\frac{dx_p}{dt_s}]$$

$$= (1 + \frac{\rho_s}{\rho_w} x_{pc})\frac{6}{d_p}\{h_p(T_e - T_p) - \sigma(x_p^* - x_e)[c_{wv}(T_e - T_{ref}) + \gamma_0]\} \tag{53}$$

or

$$\rho_s(c_p + x_p c_w)\frac{dt_p}{dt_s} = (1 + \frac{\rho_s}{\rho_w} x_{pc})\frac{6}{d_p}\{h_p(T_e - T_p) - \sigma(x_p^* - x_e)$$

$$\cdot[c_{wv}(T_e-T_{ref}) + \gamma_0]] - \rho_s c_w (T_p-T_{ref}) \frac{dx_p}{dt_s} \tag{54}$$

Eliminating dx_p/dt_s from eqn. (54) by resorting to eqn. (27-a), we obtain

$$\rho_s(c_p+x_p c_w) \frac{dt_p}{dt_s} = (1+\frac{\rho_s}{\rho_w} x_{pc}) \frac{6}{d_p} \{ h_p(T_e-T_p) - \sigma(x_p^*-x_e) \cdot[c_{wv}(T_e-T_{ref}) - c_w(T_p-T_{ref}) + \gamma_0] \} \tag{55}$$

γ_0 in eqn. (54) is to be evaluated at T_{ref}. It can be related to the heat of vaporization at any arbitary temperature , T, as follows:

$$c_w T_{ref} - c_{wv} T_{ref} + \gamma_0\Big|_{T_{ref}} = c_w T - c_{wv} T + \gamma_0\Big|_{T} \tag{56}$$

For convenience, we choose T = 0°C, then we have

$$c_w T_{ref} - C_{wv} T_{ref} + \gamma_0\Big|_{T_{ref}} = \gamma_0\Big|_{T=0°C} \tag{57}$$

Thus, eqn. (55) becomes

$$\rho_s(c_p+x_p c_w) \frac{dt_p}{dt_s} = (1+\frac{\rho_s}{\rho_w} x_{pc}) \frac{6}{d_p} [h_p(T_e-T_p) - \sigma(x_p^*-x_e)(c_w T_e - c_w T_p + \gamma_0)] \tag{58-a}$$

with the boundary condition

$$T_p = T_{p0} \quad \text{at } t_s=0 \tag{58-b}$$

and γ_0 to be evaluated at T=0°C. The average temperature of particles, $\bar{T}_p$, can be evaluated from

$$\bar{T}_p = \int_0^\infty \frac{1}{\bar{t}_s} \exp\left(-\frac{t_s}{\bar{t}_s}\right) T_p dt_s \tag{59}$$

The moisture content and temperature of the outlet gas, x_{out} and T_{out}, can be evaluated from moisture and energy balances, respectively:

$$U_0 x_{out} = U_{mf} x_e + U_b x_b(H_f) \tag{60}$$

and

$$\begin{aligned} & U_0 \left[c_g T_{out} + x_{out}(c_{wv} T_{out} + \gamma_0)\right] \\ &= U_{mf} \left[c_g T_e + x_e(c_{wv} T_e + \gamma_0)\right] \\ &+ U_b \left[c_g T_b(H_f) + x_b(H_f)(c_{wv} T_b(H_f) + \gamma_0)\right] \end{aligned} \tag{61}$$

Rearrangement gives

$$x_{out} = \frac{1}{U_0} \left[U_{mf} x_e + U_b x_b(H_f)\right] \tag{62}$$

and

$$\begin{aligned} T_{out} = \frac{1}{U_0(c_g + x_{out} c_{wv})} & \{U_{mf}[c_g T_e + x_e(c_{wv} T_e + \gamma_0)] \\ & + U_b[c_g T_b(H_f) + x_b(H_f)(c_{wv} T_b(H_f) + \gamma_0)] \\ & - U_0 x_{out} \gamma_0\} \end{aligned} \tag{63}$$

Equations (3), (17), (33-a), (46), (27-a) and (58-a) with the appropriate initial and boundary conditions constitute the governing equations of the present model. To determine the drying characteristics, these equations need be solved simultaneously. Because of the coupling and non-linearity amoung them, it is necessary to employ numerical solutions.

NUMERICAL SIMULATION

The soultion of the model equations is obtained through a two dimensional trial-and-error procedure. To determine $\bar{x}_p$ and $\bar{T}_p$, which are characteristic of the requirement of the drying process, we start with an initail guess on temperature and moisture content of the emulsion gas, that is, x_e and T_e, respectively. The physical constraints, namely,

$$T_{p0} < T_e < \max(T_0, T_w)$$

and

$$x_0 \leq x_e \leq \theta_1(T_e)$$

are helpful in determining the values for the initial guess. Integration of eqns. (27-a) and (58-a), subject to eqns. (27-b) and (58-b), gives $x_p(t_s)$ and $T_p(t_s)$ respectively. Then $\bar{x}_p$, $\bar{T}_p$, and $\bar{T}_b$ are evaluated from eqns. (28), (59), (3), (33-a) and (33-b). With $\bar{x}_p$, $\bar{T}_p$ and $\bar{T}_b$ known, x_e and T_e are calculated from eqns. (17) and (46), and the resultant values are compared with the respective initial guesses. The fact that a set of non-linear integro-differential equations (integration is involved in determining $\bar{x}_p$, $\bar{T}_p$ and $\bar{T}_b$) is contained in the model renders the procedure cumbersome.

For simplification, first we seek to reduce these integro-differential equations to a set of first order differential equations. This is achieved by introducing three new intermediate variables.

$$X_p^* = \frac{1}{\bar{t}_s} \int_0^{t_s} x_p^* \exp\left(\frac{-t_s}{\bar{t}_s}\right) dt_s \qquad (64\text{-a})$$

or

$$\frac{dX_p^*}{dt_s} = \frac{x_p^*}{\bar{t}_s} \exp\left(-\frac{t_s}{\bar{t}_s}\right) \qquad (64\text{-b})$$

with the boundary condition

$$X_p^* = 0 \qquad \text{at } t_s = 0; \tag{64-c}$$

$$T_p^* = \frac{1}{\bar{t}_s} \int_0^{t_s} T_p \exp\left(-\frac{t_s}{\bar{t}_s}\right) dt_s \tag{65-a}$$

or

$$\frac{dT_p^*}{dt_s} = \frac{T_p}{\bar{t}_s} \exp\left(-\frac{t_s}{\bar{t}_s}\right) \tag{65-b}$$

with the boundary condition

$$T_p^* = 0 \qquad \text{at } t_s = 0; \tag{65-c}$$

and

$$T_b^* = \frac{1}{H_f} \int_0^z T_b \, dz \tag{66-a}$$

or

$$\frac{dT_b^*}{dz} = \frac{T_b}{H_f} \tag{66-b}$$

with the boundary condition

$$T_b^* = 0 \qquad \text{at } z = 0 \tag{66-c}$$

Now $\bar{x}_p^*$, $\bar{T}_p$ and $\bar{T}_b$ can be expressed as

$$\bar{x}_p^* = \lim_{t_s \to \infty} X_p^* \tag{67}$$

$$\bar{T}_p = \lim_{t_s \to \infty} T_p^* \tag{68}$$

$$\bar{T}_b = T_b^*\Big|_{z=H_f} \tag{69}$$

When t_s exceeds a certain value, e.g., t_s^0, x_p^* and T_p in eqns. (64-a) and (65-a), respectively, remain constant; then, we have

$$\begin{aligned}\bar{x}_p^* &= \frac{1}{\bar{t}_s} \int_0^\infty x_p^* \exp(-\frac{t_s}{\bar{t}_s})\, dt_s \\ &= \frac{1}{\bar{t}_s} \int_0^{t_s^0} x_p^* \exp(-\frac{t_s}{\bar{t}_s})\, dt_s + \frac{1}{\bar{t}_s} \int_{t_s^0}^\infty x_p^* \exp(-\frac{t_s}{\bar{t}_s}) dt_s \\ &= X_p^*\Big|_{t_s=t_s^0} + x_p^*\Big|_{t_s=t_s^0} \exp(-\frac{t_s^0}{\bar{t}_s})\end{aligned} \tag{70}$$

Similarly,

$$\bar{T}_p = T_p^*\Big|_{t_s=t_s^0} + T_p\Big|_{t_s=t_s^0} \exp(-\frac{t_s^0}{\bar{t}_s}) \tag{71}$$

Thus, the solution of eqns. (3)., (17), (33-a), (46) and (58-a) can be obtained by solving only a set of first order differential equations along with several algebric equations. The calculation procedure is described below.

1. Input data
2. Assume the inital values x_e' for x_e and T_e' for T_e
3. Choose t_s^0, which depends on the speed of convergence and usually is in the range of $1/3\ \bar{t}_s - 2\bar{t}_s$.
4. Evaluate

$$X_p^* \Big|_{t_s=t_s^0}, \quad T_p^* \Big|_{t_s=t_s^0} \text{ and } T_b^* \Big|_{z=H_f}$$

through eqns. (64-b), (65-b) and (66-b) with corresponding boundary conditions by using the Runge-Kutta method.

5. Calculate $\bar{x}_p^*$, $\bar{T}_p$ and $\bar{T}_b$ using eqns. (70), (71) and (69).
6. Evaluate x_e and T_e from eqns. (17) and (46).
7. Compare x_e and T_e calculated in step 6 with the initially guessed values x_e' and T_e'. If they are not identical, determine a new pair of initial values of x_e and T_e and repeat steps 1 through 7.
8. Stop when x_e', T_e' and x_e, T_e are identical.

The stopping criteria used in the present study are

$$\left|x_e' - x_e\right| < 10^{-4} \text{ and } \left|T_e' - T_e\right| < 10^{-2}$$

For illustration, the following data are considered (Palancz, 1983);

$U_0 = 1\ \text{m s}^{-1}$

$T_0 = 250^{\circ}\text{C}$

$x_0 = 0.015$

$\rho_g = 1\ \text{kg m}^{-3}$

$\rho_s = 2500\ \text{kg m}^{-3}$

$\rho_w = 1000\ \text{kg m}^{-3}$

$\mu_g = 2 \times 10^{-5}\ \text{kg m}^{-1}\ \text{s}^{-1}$

$k_g = 2.93 \times 10^{-2}\ \text{J m}^{-1}\ \text{s}^{-1}\ {}^{\circ}\text{C}^{-1}$

$c_g = 1.06\ KJ\ kg^{-1}\ °C^{-1}$

$c_p = 1.26\ KJ\ kg^{-1}\ °C^{-1}$

$c_{wv} = 1.93\ KJ\ kg^{-1}\ °C^{-1}$

$c_w = 4.19\ KJ\ kg^{-1}\ °C^{-1}$

$\gamma_0 = 2.5 \times 10^3\ kJkg^{-1}$

$x_{p0} = 0.35$

$\bar{t}_s = 300\ s$

$H_f = 0.5\ m$

$D_c = 0.15m$

$d_b = 2 \times 10^{-2} m$

$D_g = 2.10^{-5}\ m^2\ s^{-1}$

$T_{p0} = 20°C$

$T_w = 105°C$

$x_{pc} = 0.2$

$n = 3$

$K = 1 \times 10^{-2}$

RESULTS AND DISCUSSION

Tables 1 through 5 present the performance characteristics of the dryer in terms of the average moisture content and temperature of particles at the exit and the moisture content and temperature of outlet gas. A comparison is given in Table 6 of the performance characteristics of the dryer under the adiabatic condition with those under the dryer-wall heating condition. Table 7 compares the performance characteristics of the dryer based on the present model with those based on Palancz's model under identical operating conditions.

The average moisture content or temperature of particles at the exit is related to the inlet-gas temperature in Fig. 5. Figures 6 through 11 show the effects of various operating parameters on variations of the temperature and moisture content of a single particle as functions of time. In Figure 12, the temperature and moisture content of a particle based on Palancz's model are compared with those based on the present model. The three stages of drying can be clearly identified in the $x_p(t_s)$ and $T_p(t_s)$ curves in Figs. 6 through 11. The rather short initial stage of the $T_p(t_s)$ curves, each with a steep positive slope, involves preheating of a particle, resulting in a sharp rise in its temperature from the inlet value. This value is lower than the dew-point temperature of the emulsion gas, thereby inducing condensation of moisture on the particle. This gives rise to a rapid increase in the $x_p(t_s)$ curve, which is immediately followed by a linearly declining section representing the constant-rate drying period. The corresponding portion of the $T_p(t_s)$ curve is horizontal since the temperature of the particle stays at the wet-bulb temperature. The remaining portion of each of the two curves represents the falling-rate drying period in which the temperature and moisture content of the particle approach gradually to their respective values.

Effects of the Operating Parameters

The performance characteristics of the dryer under various T_0 are given in Table 1. The higher the temperature of the inlet-gas, the higher the temperature of the gas in the bubble and emulsion phases, thus enhancing the rate of evaporation. This, in turn, results in an increase in the average temperature and a decrease in the moisture content of particles at the exit. Note that the $\bar{T}_p$ curve in Fig. 5 with T_0 less than 250°C has a relatively small gradient with respect to T_0. This implies that the dryer is not highly sensitive to the change in T_0 if it is less than 250°C. To prevent burning or cracking of particles, the drying operation need be conducted within this range, where moderate fluctuations in T_0 will not cause overdrying.

The influence of the superficial gas velocity on the performance characteristics of the dryer can be discerned in Table 2. When U_0 increases, the average temperature of particles at the exit increases appreciably while their average moisture content reduces sharply. This can be attributed to the intensified mass and heat transfer among bubbles, emulsion gas and solids. The expressions of eqns. (18) and (19) are indicative of a strong dependence of the heat and mass transfer coefficients between the drying gas and particles on U_0; an increase in U_0 accelerates the evaporation of moisture, thereby quickening the drying of an individual particle. This can be seen from the fact that the gradients of the $T_p(t_s)$ and $x_p(t_s)$ curves in Fig. 6 are substantially increased in the constant-rate drying period. It is worth noting that these gradients are not affected as significantly by the change in U_0 in

the falling-rate drying period as they are in the constant-rate drying period. This phenomenon suggests that the fluidized-bed dryer is effective in enhancing the drying rate mainly in the constant-rate drying period. It is possible that an effective drying system can be contrived in which a fluidized-bed dryer precedes a conventional moving-bed or packed-bed dryer, with the latter drying particles with bound moisture content.

Figure 7 demonstrates the relationship between the superficial gas velocity and the length of the constant-rate drying period. This relationship can be roughly approximated by the expression

$$t_s = 4.8 \times 10^4 e^{-6.2U_0}$$

which should be of practical use in the design of the fluidized-bed dryer.

The effect of the dryer-wall temperature on the variations of the moisture content and temperature of an individual particle as functions of time can be observed in Fig. 8. Naturally, a rise of wall temperature increases the rate of heat transfer to the emulsion gas. This leads to an increase in temperature of the emulsion gas, thereby enlarging the driving force for evaporation of moisture from the particle. Consequently, the average temperature of particles at the exit increases while their average moisture content decreases as illustrated in Table 3.

Table 4 gives the performance characteristics of the dryer under different inlet-gas moisture contents. Increasing x_0 increases only slightly the average moisture content of particles at the exit. As can be seen from the $x_p(t_s)$ and $T_p(t_s)$ curves in Fig. 9, the increase in x_o elevates the wet-bulb temperature (temperature of a particle in the constant-rate drying period) as well as the moisture content of the

emulsion gas. The former tends to enhance the rate of drying while the latter tends to lower it; consequently, the overall effect of x_0 on the drying rate is small.

The effect of the mean residence time of particles on the dryer performance is summarized in Table 5. With bed height fixed, the smaller the mean residence time, the larger the feed flow rate of solids and shorter the contact time between particles and drying gas. This results in a relatively low average temperature and high moisture content for the particles at the exit. As illustrated in Fig. 10, a relatively large feed flow rate of solids leads to reduction in the temperature of the emusion gas, thereby lowering the rate of drying of an individual particle.

Table 6 compares the performance characteristics of the dryer under the adiabatic condition with those under the dryer-wall heating condition. Note that under the latter condition, the average moisture content of particles at the exit is reduced while their average temperature is increased. This is due to the fact that additional heat influx from the dryer wall increases the temperature of the emulsion gas; thus enhancing the rate of drying of a particle as shown in Fig. 8.

Comparison with Existing Models

As stated in the introduction, various models have been proposed for the design of a continuous fluidized-bed dryer. In developing these models, different assumptions have been imposed for simplicity.

A model suggested by Vaněček *et al.* (1966) considers solids to be one phase and drying gas to be the other. Unlike the present model, the effect of bubbling is not incorporated into it. The design procedure resorts mainly to the residence time distribution function for solids and the drying curve,

$x_p(t_s)$, obtainable from solving the overall energy balance equation. Some models (see, e.g., Nonhebel and Moss, 1971) assume that the bed temperature is uniform and that the exit streams are in equilibrium. These models also assume that the drying gas remains in one phase; all these models are essentially empirical in nature.

Several investigators (see, e.g., Kato et al., 1981) have developed models which are fairly elaborate in expressing relationships of the mass and heat transfer between solids and drying gas in different drying periods; nevertheless, none of these models is sufficiently mechanistic in that the bubbling behavior is not taken into account.

A mechanistic model proposed by Palancz (1983) gives a comprehensive description of the heat and mass transfer among gaseous and solid phases in a continuous fluidized-bed dryer. It is free of the assumptions that the drying gas is homogeneous and that exit streams are in equilibrium. Palancz's model appears to be the only existing model comparable to the present one. In fact, the present work is an amendment and extension of that by Palancz. The major differences between the two models are as follows:

1. Palancz's model assumes that specific heat of the drying gas remains constant throughout the entire drying process. In other words,

$$c_g + x_e c_{wv} = \text{constant}$$

and

$$c_g + x_b c_{wv} = \text{constant}$$

The second expression implies that the moisture content of gas bubbles, x_b, remains constant, which is contradictory to the plug flow postulate for the bubble phase. Moreover, when moisture evaporates into the drying gas from solids, an appreciable amount of moisture migrates from the emulsion gas

to the bubbles; it is not plausible that its accompanying thermal energy can be neglected. A consequence of this assumption is that in Palancz's model, the energy conservation equation for the bubble phase, which corresponds to eqn. (33-a), is linear and only contains the first term on the right hand side of the equation. Subsequently, in his energy conservation equation for the emulsion gas, the term designating the energy transfer accompanied by the evaporation of moisture contains only T_e instead of $\bar{T}_p - T_e$. This means that the energy conservation equation depends on the choice of reference temperature, which is impossible.

2. To evaluate the equilibrium moisture content of the drying gas on the surface of a particle, Palancz's model resorts to the approximate expression

$$x_p^* = \phi_1(T_p)\ \phi_2(x_p)$$

with

$$\phi_1(T_p) = 0.622\ \frac{P_w}{760 - P_w}$$

and

$$\phi_2(x_p) = \begin{cases} 1 & \text{if } x_p > x_c \\ \dfrac{x_p^n}{x_p^n(x_p^n + K)} & \text{if } x_p \leq x_c \end{cases}$$

Note that a discontinuity occurs at $x_p = x_{pc}$ in the expression for $\phi_2(x_p)$; this is illogical. In contrast, the corresponding expression of the present model, eqn. (23), does not contain such a discontinuity.

The $x_p(t_s)$ and $T_p(t_s)$ curves of the present model are compared with those of Palancz's model in Fig. 12. The values of $T_p(t_s)$ and $x_p(t_s)$ of the

latter obviously are much higher than those of the former. As mentioned earlier, the latter neglects the net outflow of moisture from the emulsion phase to the bubble phase and its accompanying thermal energy transfer. This is tantamount to including extra mass and thermal energy in the emulsion gas in establishing mass and energy balances around it. As a result, relatively high values of x_e and T_e are expected as shown in Table 7, which in turn leads to an overestimation of the values of $\bar{x}_p$ and $\bar{T}_p$.

NOTATION

A_t cross-sectional area of the bed, m^2

A_b cross-sectional area of the bubble phase, m^2

a_w specific heat transfer surface of the dryer wall, m^{-1}

c_g specific heat of dry gas, kJ kg^{-1} $°C^{-1}$

c_p specific heat of particles (dry basis), kJ kg^{-1} $°C^{-1}$

c_w specific heat of water (liquid state), kJ kg^{-1} $°C^{-1}$

c_{wv} specific heat of water vapor, kJ kg^{-1} $°C^{-1}$

D_c diameter of bed column, m

D_g molecular diffusion coefficient of the drying gas, m^2 s^{-1}

D_{geff} effective diffusion coefficient of the drying gas, m^2 s^{-1}

d_b effective bubble diameter, m

d_p particle diameter, m

g gravitational acceleration, m s^{-2}

H_f expanded bed height, m

H_{mf} bed height at minimum fluidizing conditions, m

$(H_{ce})_b$ volumetric heat transfer coefficient between the bubble and cloud-wake regions based on the volume of bubbles, J s^{-1} m^{-3} $°C^{-1}$

$(H_{be})_b$ volumetric heat transfer coefficient between the bubble and emulsion phases based on the volume of bubbles, j s^{-1} m^{-3} $°C^{-1}$

$(H_{ce})_b$ volumetric heat transfer coefficient between the cloud-wake region and the emulsion phase based on the volume of bubbles, J s^{-1} m^{-3} $°C^{-1}$

h_p heat transfer coefficient between the drying gas and solids, J s^{-1} m^{-2} $°C^{-1}$

h_w heat transfer coefficient between the drying gas and the dryer wall, J s^{-1} m^{-2} $°C^{-1}$

i_0 enthalpy of inlet gas (dry basis), kJ kg^{-1}

i_b enthalpy of gas bubbles (dry basis), kJ kg^{-1}

i_e enthalpy of the emulsion gas (dry basis), kJ kg^{-1}

i_{ws} enthalpy of water vapor on the surface of a particle, kJ kg^{-1}

$\bar{i}_{ws}$ average enthalpy of water vapor on the surface of particles, kJ kg^{-1}

i_{we} enthalpy of water vapor contained in the emulsion gas, kJ kg^{-1}

i_p enthalpy of a particle (wet basis), kJ kg^{-1}

j_p Colburn-factor

$(K_{bc})_b$ coefficient of gas interchange between the bubble and cloud-wake regions based on the volume of bubbles, s^{-1}

$(K_{be})_b$ coefficient of gas interchange between the bubble and emulsion phases based on the volume of bubbles, s^{-1}

$(K_{ce})_b$ coefficient of gas interchange between the cloud-wake region and the emulsion phase based on the volume of bubbles, s^{-1}

k_g thermal conductivity of the drying gas, J m^{-1} $°C^{-1}$

L_e Lewis number, dimensionless

N_m Nusselt number, dimensionless

P_r Prantle number, dimensionless

P_w pressure of saturated water vapor, mm Hg

q_s conductive heat flux inside a particle, J s^{-1} m^{-2}

R_{e_p} particle Reynolds number, dimensionless

S_w heat transfer surface area of the dryer wall, m^2

T_0 temperature of the inlet gas, °C

T_b temperature of gas bubbles, °C

$\bar{T}_b$ bed-height average temperature of gas bubbles, °C

T_e temperature of the emulsion gas, °C

T_p temperature of a particle, °C

$\bar{T}_p$ average temperature of particles, °C

T_{p0} temperature of inlet particles, °C

T_{ref} reference-state temperature, °C

T_w dryer-wall temperature, °C

t_s time, s

$\bar{t}_s$ mean residence time of particles in the dryer, s

U_0 superficial gas velocity (measured on an empty bed basis) through a bed of solids, m s^{-1}

U_b superficial gas velocity in the bubble-phase, based on total cross-sectional area of the bed, m s^{-1}

U_{br} linear velocity of a single bubble, m s^{-1}

U_{mf} superficial gas velocity at minimum fluidizing conditions, m s^{-1}

V_t volume of the bed, m^3

x_0 moisture content of inlet gas (dry basis), dimensionless

x_b moisture content of gas bubbles (dry basis), dimensionless

$\bar{x}_b$ bed-height average moisture content of gas bubbles (dry basis), dimensionless

x_e moisture content of the emulsion gas (dry basis), dimensionless

x_p moisture content of a particle (dry basis), dimensionless

$\bar{x}_p$ average moisture content of particles (dry basis), dimensionless

x_p^* moisture content of the drying gas on the surface of a particle (dry basis), dimensionless

$\bar{x}_p^*$ average moisture content of the drying gas on the surface of a particle (dry basis), dimensionless

x_{p0} miosture content of inlet particles (dry basis), dimensionless

x_{pc} critical moisture content of a particle (dry basis), dimensionless

z elevation, m

GREEK LETTERS

γ_0 heat of vaporization, kJ kg^{-1}

δ_b fraction of the fluidized bed consisting of bubbles, dimensionless

ϵ_e void fraction in the emulsion phase, dimensionless

ϵ_{mf} void fraction at minimum fluidizing conditions, dimensionless

μ_g viscosity of gas, kg m^{-1} s^{-1}

ρ_g density of gas, kg m^{-3}

ρ_w density of water, kg m^{-3}

ρ_{ws} density of wet solids, kg m^{-3}

σ evaporation coefficient, kg m^{-2} s^{-1}

ϕ_s sphericity of a particle, dimensionless

LITERATURE CITED

Babu, S. P., B. Shah and A. Talwalkar, Fluidization Correlation for Coal Gasification Materials - Minimum Fluidization Velocity and Fluidized Bed Expansion Ratio, AIChE Symp. Ser. 74, 176-186(1978).

Broadhurst, T. E. and H. A. Becker, Onset of Fluidization and Slugging in Beds of Uniform Particles, AIChE J., 21, 238-247(1975).

Davidson, J. F. and D. Harrison, Fluidized Particles, Chapter 1, pp. 19-20, Cambridge University Press, 1963.

Kato, K., S. Omura, D. Taneda, I. Onozania and A. Iijima, Drying Characteristics in a Packed Fluidized Bed Dryer, J. Chem. Eng. Japan, 14, 365-371(1981).

Kunii, D. and O. Levenspiel, Fluidization Engineering, Chapter 7, Wiley, New York, 1969.

Li, C. H. and B. A. Finlayson, Heat Transfer in Packed Beds - A Reevaluation, Chem. Eng. Sci. 38, 147-153(1977).

Nonhebel, G. and A. A. H. Moss, Drying Solids in the Chemical Industry, Chapter 11, Butterworth, London, 1977.

Palancz, B., A Mathematical Model for Continuous Fluidized-bed Drying, Chem. Eng. Sci. 38, 1045-1059(1983).

Vanecek, V., M. Markvart and R. Drbohlav, Fluidized Bed Drying, Translated by J. Landau, Leonard Hill, London, 1966.

Wen, C. Y. and Y. H. Yu, A Generalized Method for Predicting the Minimum Fluidization Velocity, AIChE J. 12, 610-612(1966).

APPENDIX A. DERIVATION OF EQN. (2-a)

Consider the controlled volume element with a size of $A_b \Delta z$ shown in Fig. 1. A steady-state moisture balance around this volume element gives

$$0 = \begin{pmatrix}\text{rate of moisutre in}\\ \text{by convection}\end{pmatrix} - \begin{pmatrix}\text{rate of moisture out}\\ \text{by convection}\end{pmatrix} + \begin{pmatrix}\text{rate of moisture in through}\\ \text{gas exhange with the emulsion}\\ \text{phase}\end{pmatrix} \qquad (A\text{-}1)$$

The various contributions to the moisture balance are

$$\begin{pmatrix}\text{rate of moisture in}\\ \text{by convection at } z\end{pmatrix} = (U_b A_t)\, \rho_g\, x_b\big|_z$$

$$\begin{pmatrix}\text{rate of moisture out}\\ \text{by convection}\\ \text{at } z+\Delta z\end{pmatrix} = (U_b A_t)\, \rho_g\, x_b\big|_{z+\Delta z}$$

$$\begin{pmatrix}\text{rate of moisture in}\\ \text{through gas exchange}\\ \text{with the emulsion}\\ \text{phase}\end{pmatrix} = (A_b \Delta z)\rho_g\, (\bar{K}_{be})_b\, (x_e - x_b)$$

By substituting these expressions into eqn. (A-1), dividing the resultant expression by $A_b \Delta z \rho_g$ and taking the limit as Δz goes to zero, we obtain

$$\frac{U_b}{\delta_b}\left(\lim_{\Delta z \to 0} \frac{x_b\big|_{z+\Delta z} - x_b\big|_z}{\Delta z}\right) = (K_{be})_b (x_e - x_b) \qquad (A\text{-}2)$$

The expression within the braces on the left-hand side of eqn. (A-2) is the first derivative of x_b with respect to z; thus,

$$\frac{U_b}{\delta_b}\frac{dx_b}{dz} = (K_{be})_b (x_e - x_b) \qquad (A\text{-}3)$$

This is eqn. (2-a) in the text.

APPENDIX B. DERIVATION OF EQN. (15)

Under the assumption of complete mixing, the moisture content of the emulsion gas is constant throughout the emulsion phase. At steady state, a moisture balance around the emulsion gas gives

$$0 = \begin{pmatrix}\text{rate of moisture in}\\ \text{by convection}\end{pmatrix} - \begin{pmatrix}\text{rate of moisture out}\\ \text{by convection}\end{pmatrix} + \begin{pmatrix}\text{rate of moisture in}\\ \text{through gas exchange}\\ \text{with the bubble}\\ \text{phase}\end{pmatrix} + \begin{pmatrix}\text{rate of moisture in}\\ \text{by evaporation}\\ \text{of moisture in solids}\end{pmatrix} \qquad \text{(B-1)}$$

The individual terms in eqn. (B-1) are

$$\begin{pmatrix}\text{rate of moisture in}\\ \text{by convection}\\ \text{at } z=0\end{pmatrix} = (U_{mf}A_t)\,\rho_g x_0$$

$$\begin{pmatrix}\text{rate of moisture out}\\ \text{by convection}\\ \text{at } z = H_f\end{pmatrix} = (U_{mf}A_t)\rho_g x_e$$

$$\begin{pmatrix}\text{rate of moisture in}\\ \text{through gas exchange}\\ \text{with the bubble}\\ \text{phase}\end{pmatrix} = \int_0^{H_f} A_b\rho_g(K_{be})_b(x_b-x_e)dz$$

$$\begin{pmatrix}\text{rate of moisture in}\\ \text{by evaporation}\\ \text{of moisture in solids}\end{pmatrix} = (H_f A_t)\cdot(1-\delta_b)(1-\varepsilon_{mf})\cdot\left(\frac{6}{d_p}\right)\cdot\sigma(\bar{x}_p^{*}-x_e)$$

total volume of the bed — *volume fraction of solids* — *specific surface of solids* — *average evaporation rate per unit surface area of solids*

Substituting these individual terms into Eq. (B-1) gives

$$0 = (U_{mf}A_t)\rho_g(x_0-x_e) + \int_0^{H_f} A_b\rho_g(K_{be})_b(x_b-x_e)dz$$

$$+ (H_fA_t) \cdot (1-\delta_b)(1-\varepsilon_{mf}) \cdot (\frac{6}{d_p})\sigma(\bar{x}_p^*-x_e) \qquad \text{(B-2)}$$

This is eqn. (15) in the text.

APPENDIX C. DERIVATION OF EQN. (27-a)

The moisture content of a particle in the dryer decreases with time due to evaporation. Applying moisture balance around the particle gives

$$\begin{pmatrix}\text{rate of accumulation}\\ \text{of moisture}\end{pmatrix} = \begin{pmatrix}\text{rate of moisture}\\ \text{in}\end{pmatrix} - \begin{pmatrix}\text{rate of moisture}\\ \text{out by evaporation}\end{pmatrix} \quad \text{(C-1)}$$

The three terms in eqn. (C-1) are

$$\begin{pmatrix}\text{rate of accumulation}\\ \text{of moisture}\end{pmatrix} = \left(\frac{\pi d_p^3}{6}\right) \cdot \rho_{ws} \cdot \left(\frac{1}{1+x_{pc}}\right) \cdot \frac{dx_p}{dt_s}$$

volume of a particle — *density of wet particles* — *ratio of mass of a dry particle to that of a wet particle* — *rate of change of moisture content of a particle*

$$\begin{pmatrix}\text{rate of moisture}\\ \text{in}\end{pmatrix} = 0$$

$$\begin{pmatrix}\text{rate of moisture out}\\ \text{by evaporation}\end{pmatrix} = (\pi d_p^2)\sigma(x_p^* - x_e)$$

The density of wet solids, ρ_{ws}, is related to the moisture contained in the void of solids, M_w, and the mass of dry particles, M_s, through:

$$\rho_{ws} = \frac{M_{ws}}{V_{ws}} = \frac{M_w + M_s}{V_w + V_s}$$

$$= \left(\frac{M_s}{V_s}\right) \frac{1+\frac{M_w}{M_s}}{1+\frac{V_w}{V_s}\frac{M_s}{M_w}}$$

$$= \rho_s \frac{1+\frac{M_w}{M_s}}{1+\frac{V_w}{V_s}\frac{M_s}{M_w}} \quad \text{(C-2)}$$

or

$$\rho_{ws} = \rho_s \frac{1+\frac{M_w}{M_s}}{1+\frac{\rho_s}{\rho_w}\frac{M_w}{M_s}} \qquad (C-3)$$

The moisture content in excess of x_{pc} exists only as a liquid film surrounding solids and thus should not be considered as a part of the water contained in solids. Therefore, we have

$$x_{pc} = \frac{M_w}{M_s} \qquad (C-4)$$

and correspondingly, eqn. (C-3) becomes

$$\rho_{ws} = \rho_s \frac{1+x_{pc}}{1+\frac{\rho_s}{\rho_w}x_{pc}} \qquad (C-5)$$

Substitution of the three individual terms into eqn. (C-1) and rearrangement of the resultant equation give

$$\rho_s \frac{dx_p}{dt_s} = -\left(1+\frac{\rho_s}{\rho_w}x_{pc}\right)\frac{6}{d_p}\,\sigma(x_p^*-x_e) \qquad (C-6)$$

This is eqn. (27-a) in the text.

APPENDIX D. DERIVATION OF EQN. (29)

For the controlled volume element with a size of $A_b \Delta z$ shown in Fig. 2, a steady-state energy balance leads to

$$0 = \begin{pmatrix}\text{rate of thermal energy}\\ \text{in by convection}\end{pmatrix} - \begin{pmatrix}\text{rate of thermal energy}\\ \text{out by convection}\end{pmatrix} + \begin{pmatrix}\text{rate of thermal energy}\\ \text{in through bubble-emulsion}\\ \text{interphase exchange}\end{pmatrix} + \begin{pmatrix}\text{rate of thermal energy}\\ \text{in accompanied by net mois-}\\ \text{ture influx at bubble-}\\ \text{emulsion interface}\end{pmatrix} \quad \text{(D-1)}$$

The individual terms are

$$\begin{pmatrix}\text{rate of thermal energy}\\ \text{in by convection at } z\end{pmatrix} = (U_b A_t)\, \rho_g i_b \big|_z$$

$$\begin{pmatrix}\text{rate of thermal energy}\\ \text{out by convection at}\\ z + \Delta z\end{pmatrix} = (U_b A_t) \rho_g i_b \big|_{z+\Delta z}$$

$$\begin{pmatrix}\text{rate of thermal energy}\\ \text{in through bubble-}\\ \text{emulsion interphase}\\ \text{exchange}\end{pmatrix} = (A_b \Delta z)(H_{be})_b\, (T_e - T_b)$$

$$\begin{pmatrix}\text{rate of thermal energy}\\ \text{in accompanied by net}\\ \text{moisture influx at}\\ \text{bubble-emulsion inter-}\\ \text{face}\end{pmatrix} = (A_b \Delta z) \rho_g (K_{be})_b (x_e - x_b) i_{we}$$

By substituting the above expressions into eqn. (D-1), dividing the resultant expression by $A_b \Delta z \rho_g$ and taking the limit as Δz goes to zero, we have

$$\rho_g \frac{U_b}{\delta_b} \frac{di_b}{dz} = (H_{be})_b\, (T_e - T_b) + \rho_g (K_{be})_b\, (x_e - x_b)\, i_{we} \qquad \text{(D-2)}$$

This is eqn. (29) in the text.

APPENDIX E. DERIVATION OF EQN. (37)

Referring to Fig. 3, a steady-state energy balance around the entire emulsion gas is

$$0 = \begin{pmatrix}\text{rate of thermal energy}\\ \text{in by convection}\end{pmatrix} - \begin{pmatrix}\text{rate of thermal energy}\\ \text{out by convection}\end{pmatrix} + \begin{pmatrix}\text{rate of thermal energy}\\ \text{in by evaporation of}\\ \text{moisture in solids}\end{pmatrix} + \begin{pmatrix}\text{rate of thermal energy}\\ \text{in through bubble-emul-}\\ \text{sion interphase ex-}\\ \text{change}\end{pmatrix} + \begin{pmatrix}\text{rate of thermal}\\ \text{energy in from}\\ \text{the bed wall}\end{pmatrix} - \begin{pmatrix}\text{rate of thermal energy}\\ \text{out accompanied by mois-}\\ \text{ture flux at bubble-}\\ \text{emulsion interface}\end{pmatrix} - \begin{pmatrix}\text{rate of thermal energy}\\ \text{transfer to solids}\end{pmatrix} \qquad \text{(E-1)}$$

The various contributions to eqn. (E-1) are

$$\begin{pmatrix}\text{rate of thermal energy}\\ \text{in by convection at } z = 0\end{pmatrix} = (U_{mf}A_t)\rho_g \cdot i_0$$

$$\begin{pmatrix}\text{rate of thermal energy}\\ \text{out by convection at}\\ z = H_f\end{pmatrix} = (U_{mf}A_t)\rho_g \cdot i_e$$

$$\begin{pmatrix}\text{rate of thermal energy}\\ \text{in by evaporation of}\\ \text{moisture in solids}\end{pmatrix} = (H_f A_t) \cdot [(1-\delta_b)(1-\varepsilon_{mf})] \cdot \left(\frac{6}{d_p}\right) \cdot \sigma(\bar{x}_p^* - x_e) \cdot \bar{i}_{ws}$$

total volume of the bed — *volume fraction of solids* — *specific surface of solids* — *average evaporation rate per unit surface area of solids* — *average enthalpy of moisture on the surface of solids*

$$\begin{pmatrix}\text{rate of thermal energy in through bubble-emulsion interphase exchange}\end{pmatrix} = \int_0^{H_f} A_b (H_{be})_b (T_b - T_e) dz$$

$$\begin{pmatrix}\text{rate of thermal energy in from the bed wall}\end{pmatrix} = S_w h_w (T_w - T_e)$$

$$\begin{pmatrix}\text{rate of thermal energy out accompanied by mass flux at bubble-emulsion interface}\end{pmatrix} = \int_0^{H_f} A_b \rho_g (K_{be})_b (x_e - x_b) i_{we} dz$$

$$\begin{pmatrix}\text{rate of thermal energy transfer to solids}\end{pmatrix} = (H_f A_t) \cdot [(1-\delta_b)(1-\varepsilon_{mf})] \cdot \left(\frac{6}{d_p}\right) \cdot \dot{h}_p (T_e - \bar{T}_p)$$

total volume of bed · *volume fraction of solids* · *specific surface of solids* · *heat transfer rate per unit surface of solids*

Substituting these individual terms into eqn. (E-1) yields

$$0 = (U_{mf} A_t) \rho_g (i_0 - i_e) + (H_f A_t)(1-\delta_b)(1-\varepsilon_{mf}) \frac{6}{d_p} \sigma (\bar{x}_p^* - x_e) \bar{i}_{w\ell}$$

$$+ \int_0^{H_f} A_b (H_{be})_b (T_b - T_e) dz + S_w h_w (T_w - T_e)$$

$$- \int_0^{H_f} A_b \rho_g (K_{be})_b (x_e - x_b) i_{we} dz$$

$$- (H_f A_t)(1-\delta_b)(1-\varepsilon_{mf}) \frac{6}{d_p} h_p (T_e - \bar{T}_p) \qquad \text{(E-2)}$$

This is eqn. (37) in the text.

APPENDIX F. DERIVATION OF EQN. (48)

An energy balance around a particle in Fig. 3 yields

$$\begin{pmatrix}\text{rate of accumulation}\\ \text{of thermal energy}\end{pmatrix} = \begin{pmatrix}\text{rate of thermal energy}\\ \text{in by conduction}\end{pmatrix} - \begin{pmatrix}\text{rate of thermal energy}\\ \text{out by evaporation}\end{pmatrix} \qquad \text{(F-1)}$$

The individual terms are

$$\begin{pmatrix}\text{rate of accumulation}\\ \text{of thermal energy}\end{pmatrix} = \left(\frac{\pi d_p^3}{6}\right) \cdot \left(\rho_s \frac{1+x_{pc}}{1+\frac{\rho_s}{\rho_w} x_{pc}}\right) \cdot \left(\frac{1}{1+x_{pc}}\right) \cdot \frac{di_p}{dt_s}$$

volume of a solid particle — *density of wet particles* — *ratio of mass of a dry particle to that of a wet particle* — *rate of change of enthalpy of a particle*

$$\begin{pmatrix}\text{rate of thermal energy}\\ \text{in by conduction}\end{pmatrix} = (\pi d_p^2) q_s$$

$$\begin{pmatrix}\text{rate of thermal energy}\\ \text{out by evaporation}\end{pmatrix} = (\pi d_p^2)\sigma(x_p^* - x_e) i_{ws}$$

Substituting these individual terms into eqn. (F-1) and rearrangement of the resultant equation give

$$\rho_s \frac{di_p}{dt_s} = \frac{6}{d_p}\left(1+\frac{\rho_s}{\rho_w} x_{pc}\right)\left[q_s - \sigma(\bar{x}_p^* - x_e) i_{ws}\right] \qquad \text{(F-2)}$$

This is eqn. (48) in the text.

Table 1. Performance characteristics of the dryer under various T_0

(T_w=105°C, T_{p0}=20°C, U_0=1m/sec., x_{p0}=0.35, x_0=0.015, T_s=300sec.)

T_0[°C]	T_e[°C]	x_e[-]	$\bar{x}_p$ [-]	$\bar{T}_p$[°C]	$\bar{T}_b$[°C]	x_{out}[-]	T_{out}[°C]
50°C	45.9	0.055	0.250	44.8°C	46.7	0.054	45.9
100°C	51.6	0.068	0.218	50.2	61.3	0.067	51.8
150°C	58.0	0.085	0.195	56.4	76.5	0.084	58.4
200°C	64.8	0.092	0.166	62.9	91.9	0.091	65.5
250°C	72.0	0.100	0.143	69.9	107.7	0.099	72.9

Table 2. Performance characteristics of the dryer under various U_0

(T_0=250°C, T_{p0}=20°C, T_w=50°C, x_{p0}=0.35, x_0=0.015, T_s=300sec.)

U_o[m/sec.]	T_e[°C]	x_e[-]	$\bar{x}_p$[-]	$\bar{T}_p$[°C]	$\bar{T}_b$[°C]	x_{out}[-]	T_{out}[°C]
0.80	51.0	0.075	0.271	49.9	85.5	0.060	51.8
1.0	55.3	0.075	0.199	53.8	94.4	0.074	56.2
1.2	63.7	0.075	0.153	61.9	105.5	0.074	64.6

Table 3. Performance characteristics of the dryer under various T_w

(T_0=250°C, T_{p0}=20°C, U_0=1m/sec., x_{p0}=0.35, x_0=0.015, T_s=300sec.)

T_w[C]	T_e[°C]	x_e[-]	$\bar{x}_p$[-]	$\bar{T}_p$[°C]	$\bar{T}_b$[°C]	x_{out}[-]	T_{out}[°C]
50	55.3	0.075	0.199	53.8	94.4	0.074	57.1
75	63.0	0.092	0.174	61.2	100.5	0.090	63.9
105	72.0	0.100	0.143	69.9	107.7	0.099	72.9

Table 4. Performance characteristics of the dryer under various x_0

(T_w=150°C, T_0=250°C, T_{p0}=20°C, U_0=1m/sec., x_{p0}=0.35, T_s=300sec.)

x_0[0]	T_e[°C]	x_e[-]	$\bar{x}_p$[-]	$\bar{T}_p$[°C]	$\bar{T}_b$[°C]	x_{out}[-]	T_{out}[°C]
0.015	72.0	0.100	0.143	69.9	107.7	0.099	72.9
0.050	75.5	0.135	0.148	73.4	112.5	0.134	76.6
0.100	79.6	0.180	0.150	77.5	118.6	0.179	78.1

Table 5. Performance characteristics of the dryer under various $\bar{t}_s$

(T_0=250°C, T_w=105°C, T_{p0}=20°C, U_0=1m/sec., x_{p0}=0.35, x_0=0.015)

$\bar{t}_s$[sec]	T_e[°C]	x_e[-]	$\bar{x}_p$[-]	$\bar{T}_p$[°C]	$\bar{T}_b$[°C]	x_{out}[-]	T_{out}[°C]
150	57.9	0.093	0.239	55.5	96.5	0.092	58.8
300	72.0	0.100	0.143	69.9	107.7	0.099	72.9
450	86.0	0.090	0.092	84.3	118.9	0.089	86.8

Table 6. Comparison of performance characteristics of the dryer under adiabatic condition with those under bed-wall heating condition.

(T_0=250°C, T_{p0}=20°C, U_0=1 m/sec., x_{p0}=0.35, x_0=0.015, T_s=300 sec.)

Case	T_w[°C]	T_e[°C]	x_e[-]	$\bar{x}_p$[-]	$\bar{T}_p$[°C]	$\bar{T}_b$[°C]	x_{out}[-]	T_{out}[°C]
Adiabatic	58.0	58.0	0.083	0.193	56.4	96.5	0.082	58.9
Bed-wall Heating	105.0	72.0	0.100	0.143	69.9	107.7	0.099	72.9

Table 7. Comparison of the performance characteristics of the dryer based on present model with those based on Palancz's model

(T_0=250°C, T_w=50°C, T_{p0}=20°C, U_0=1m/sec., x_{p0}=0.35, x_0=0.015, $\bar{t}_s$=300sec.)

Model	T_e[°C]	x_e[-]	$\bar{x}_p$[-]	$\bar{T}_p$[°C]	$\bar{T}_b$[-]	x_{out}[-]	T_{out}[°C]
Present	55.3	0.075	0.199	53.8	94.4	0.074	56.2
Palancz's	66.3	0.159	0.228	66.3	102.8	0.158	67.2

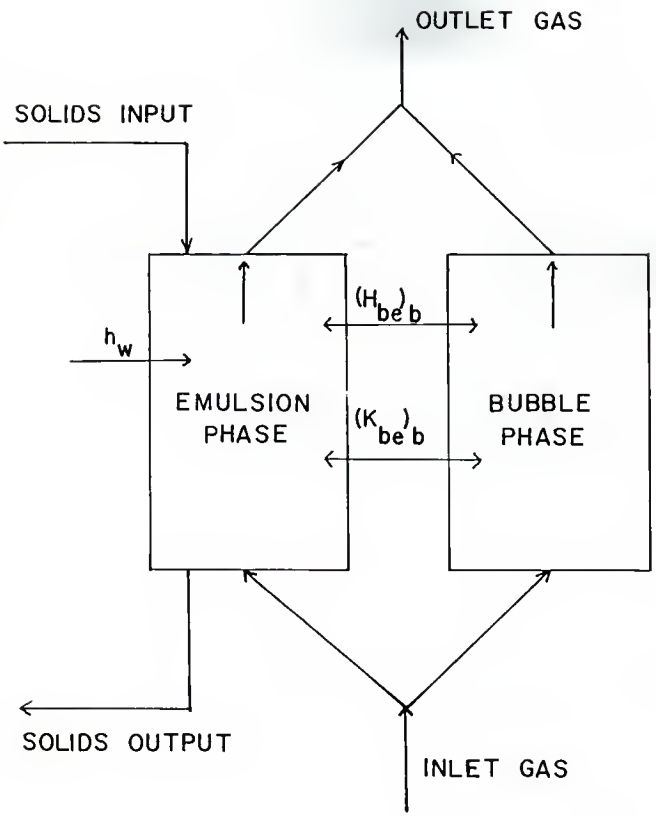

Fig. I. Schematic diagram of continuous drying in the fluidized bed.

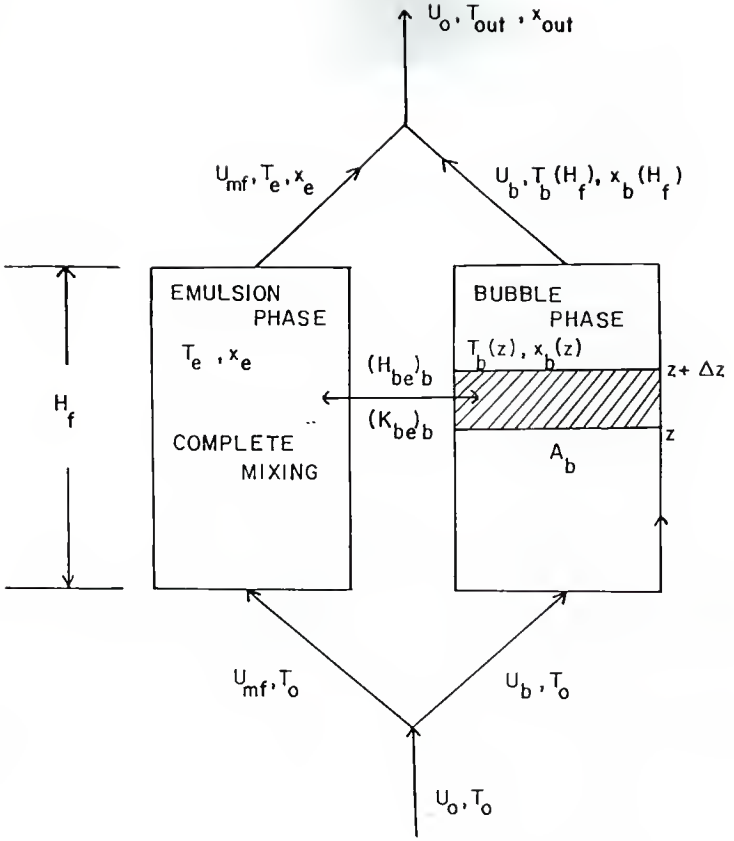

Fig. 2. Mass and energy transfer between the bubbles and emulsion gas.

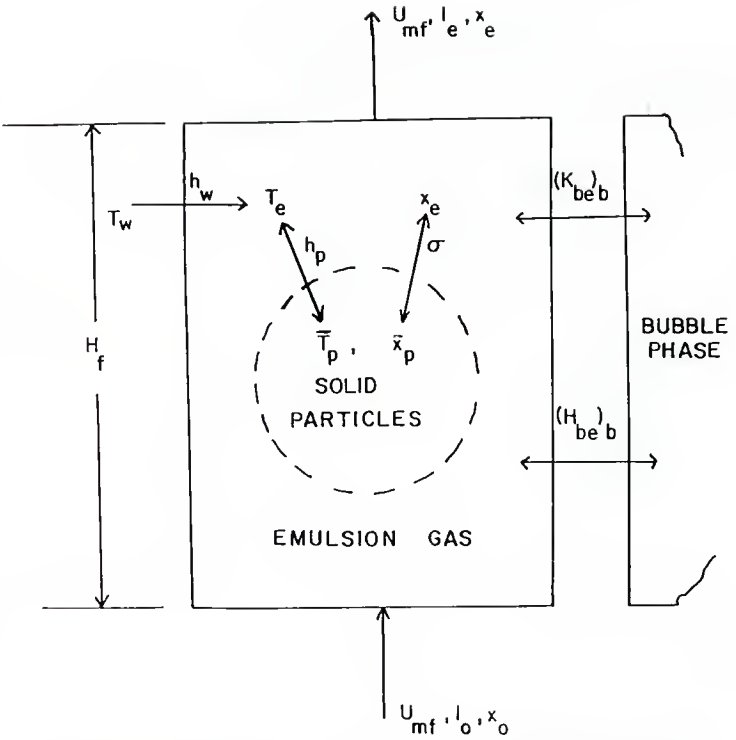

Fig. 3. Mass and energy transfer between solid particles and emulsion gas.

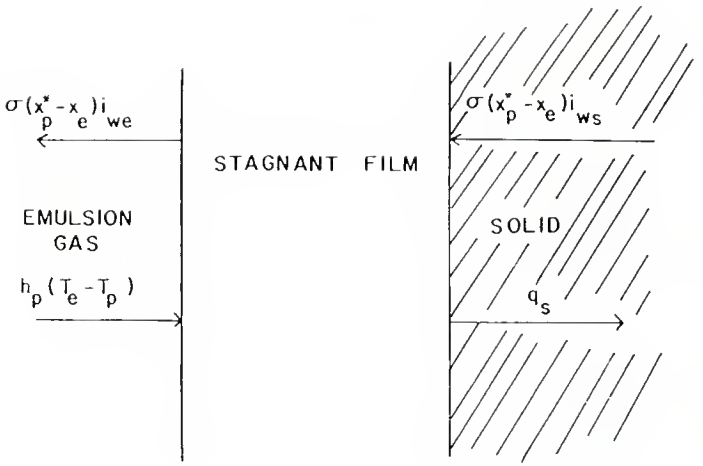

Fig. 4 Energy balance around the stagnant film surrounding a solid particle.

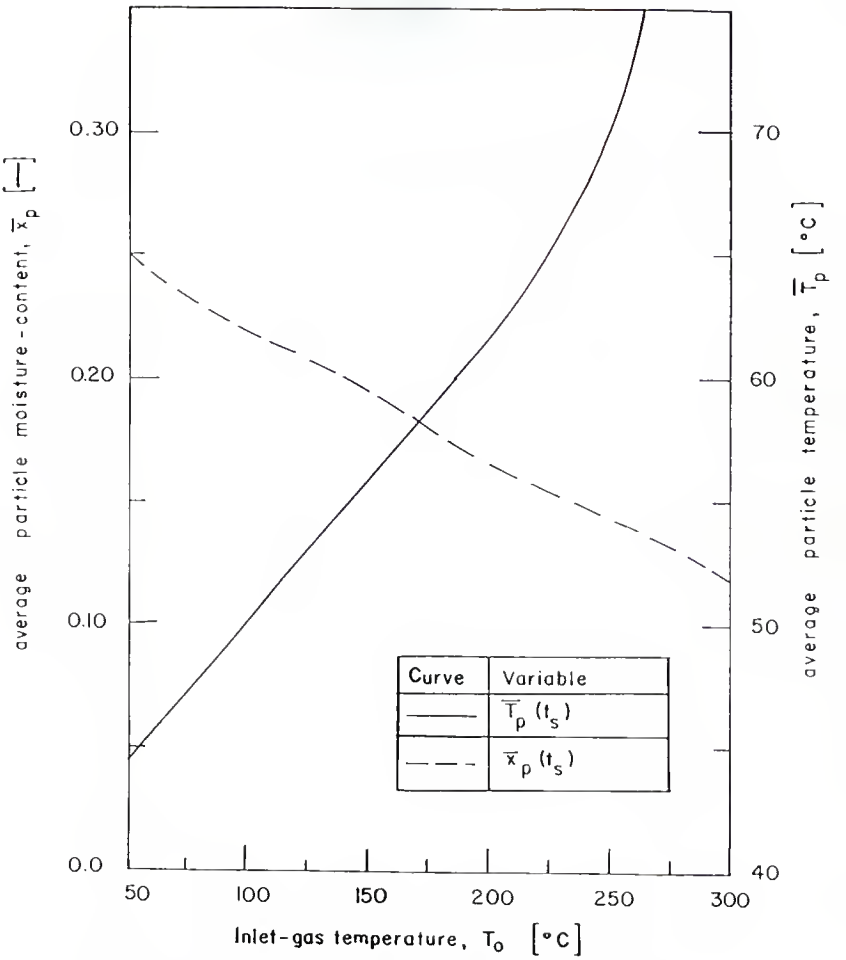

Fig. 5. Effect of the inlet-gas temperature: $T_w = 105\,°C$, $T_{p_o} = 20\,°C$, $U_o = 1\,m/sec.$, $x_{p_o} = 0.35$, $x_o = 0.015$, $\overline{t}_s = 300\,sec.$

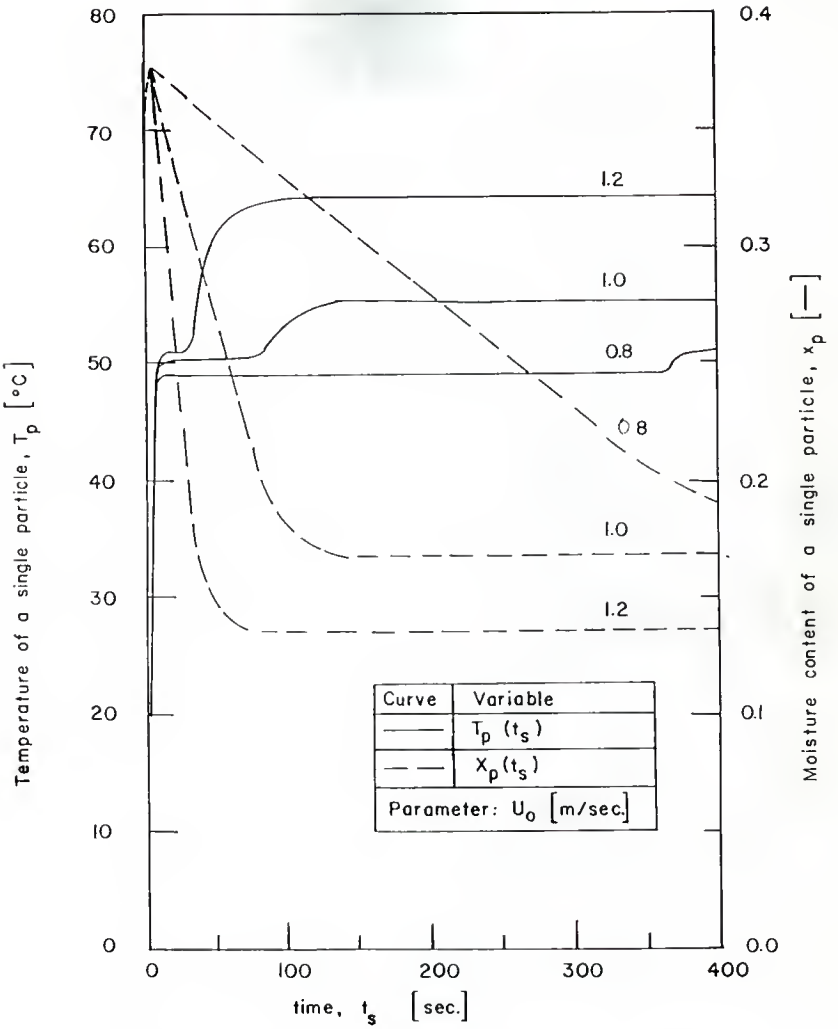

Fig. 6 Effect of the superficial gas velocity: $T_a = 250°C$, $T_{p_0} = 20°C$, $T_w = 50°C$, $x_{p_a} = 0.35$, $x_a = 0.015$, $\bar{t}_s = 300$ sec.

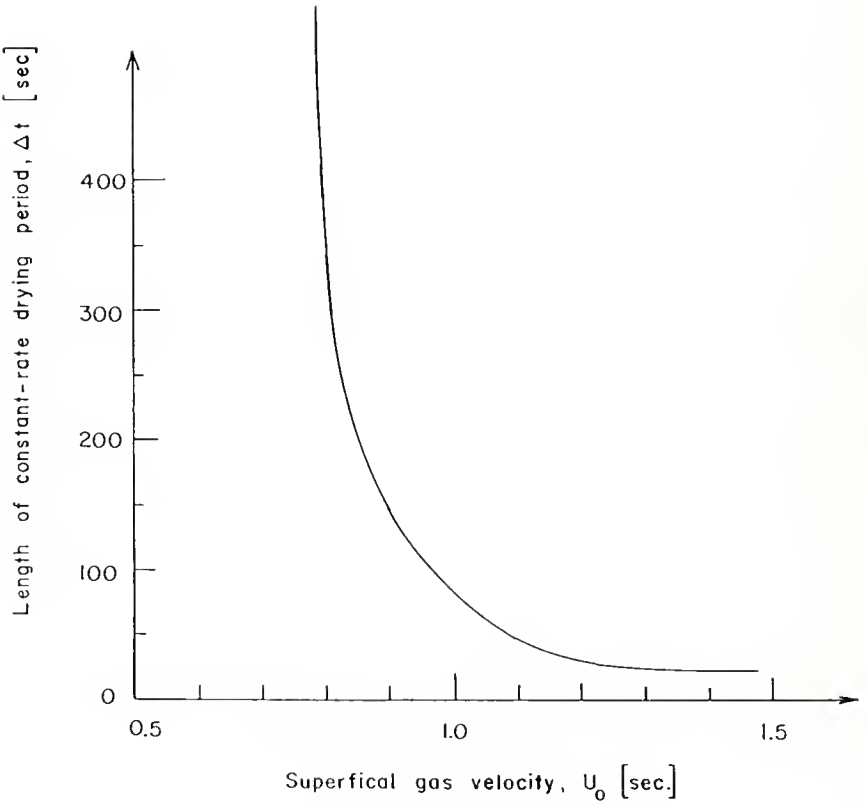

Fig. 7. Plot of length of the constant-rate drying period against the superficial gas velocity: $T_o = 250°C$, $T_{po} = 20°C$, $T_w = 50°C$, $x_{po} = 0.35$, $x_o = 0.015$, $\bar{t}_s = 300$ sec.

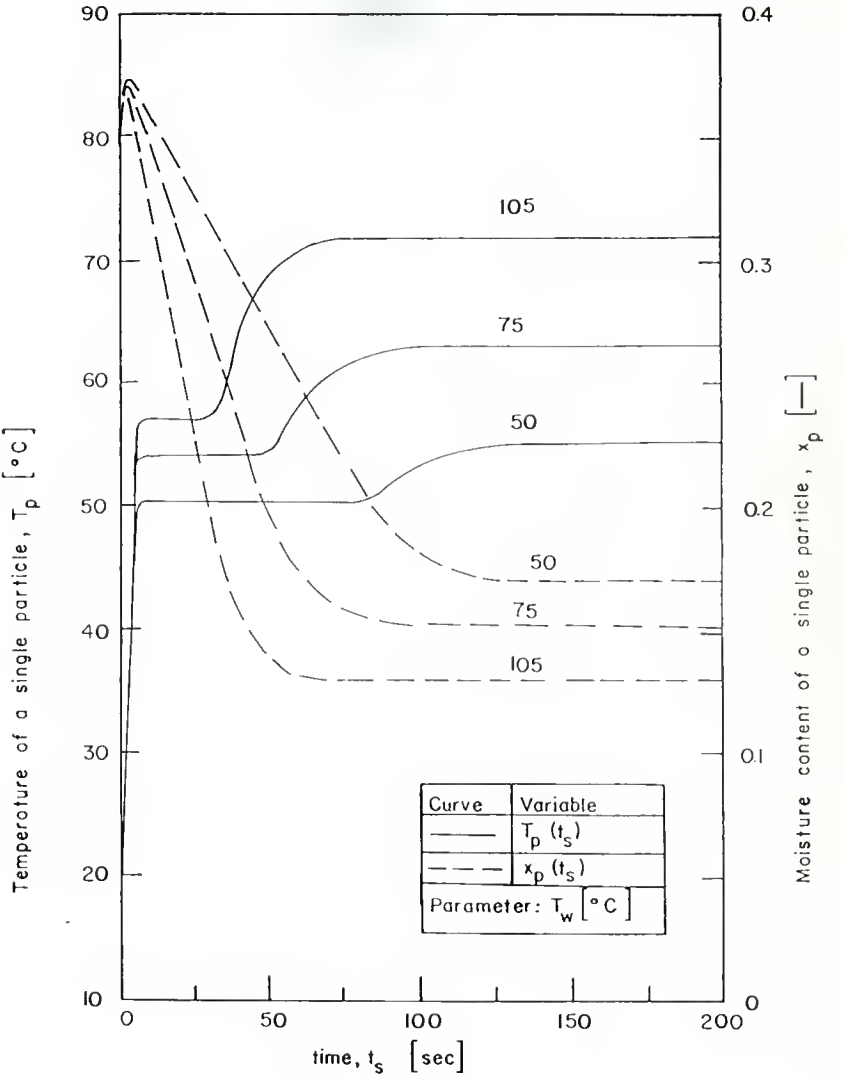

Fig.8. Effect of the dryer-wall temperature: $T_o = 250°C$, $T_{po} = 20°C$, $U_o = 1 m/sec$, $x_{p_o} = 0.35$, $x_o = 0.015$, $\bar{t}_s = 300$ sec.

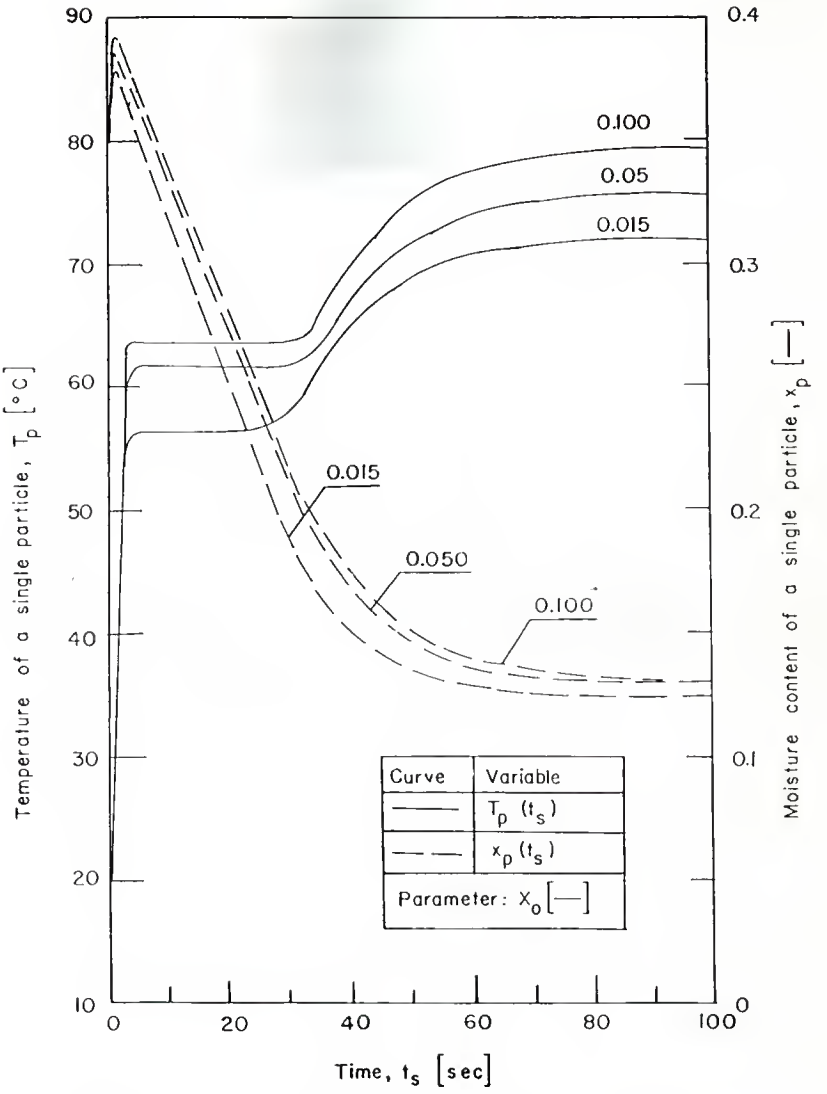

Fig.9. Effect of the inlet-gas moisture content: T_w=105°C, T_o=250°C, T_{p_o}=20°C, U_a=1m/sec, x_{p_o}=0.35, $\bar{t}_s$=300 sec.

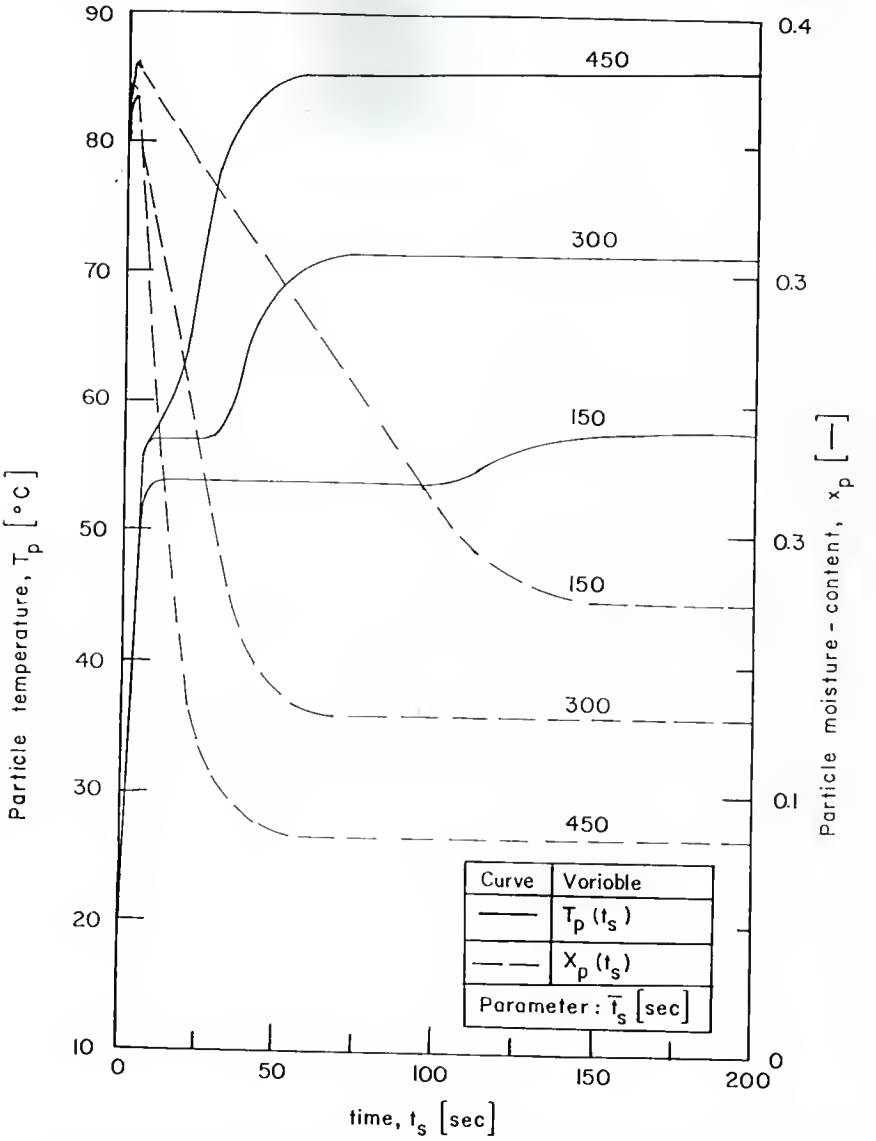

Fig. 10. Effect of the mean residence time of particles: $T_0 = 250°C$, $T_w = 105°C$, $T_{p_0} = 20°C$, $U_0 = 1\ m/sec$, $x_{p_0} = 0.35$, $x_0 = 0.015$.

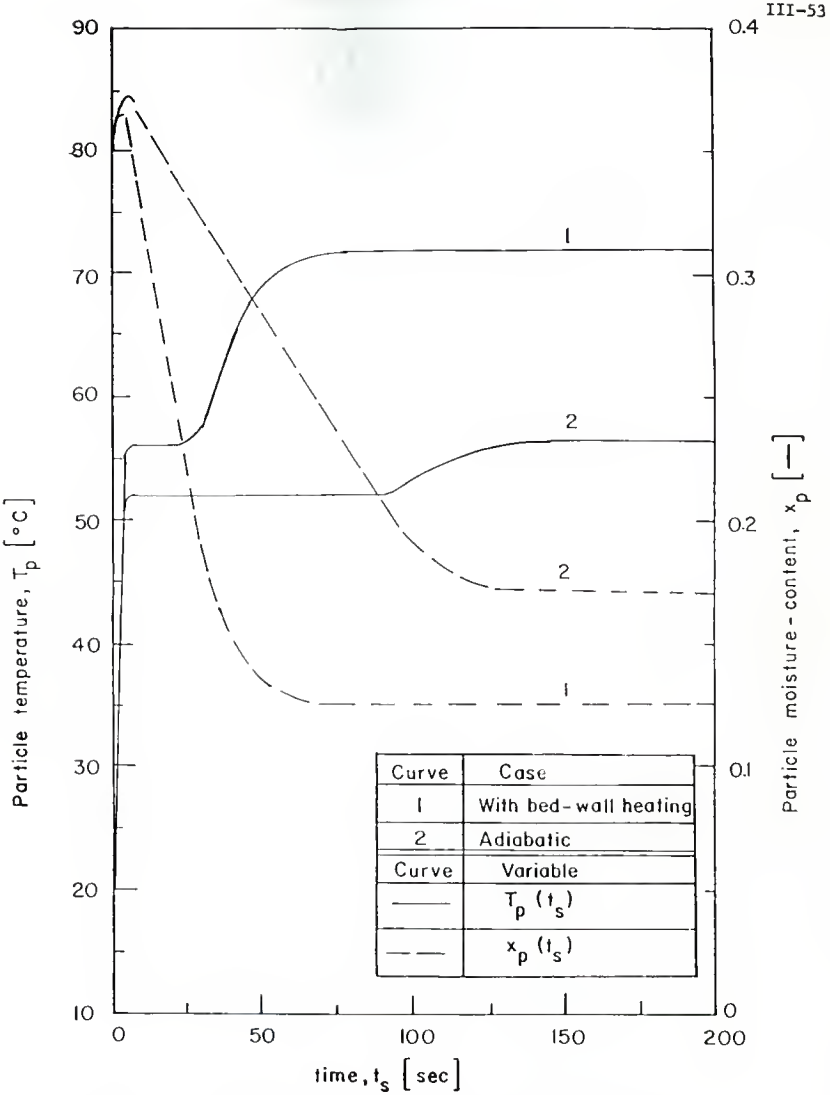

Fig.11. Comparison between adiabatic and bed-wall heating cases: $T_a = 250°C$, $T_w = 105°C$, $T_{p_o} = 20°C$ $U_a = 1$ m/sec, $x_{p_o} = 0.35$, $x_a = 0.015$, $\overline{t_s} = 300$ sec.

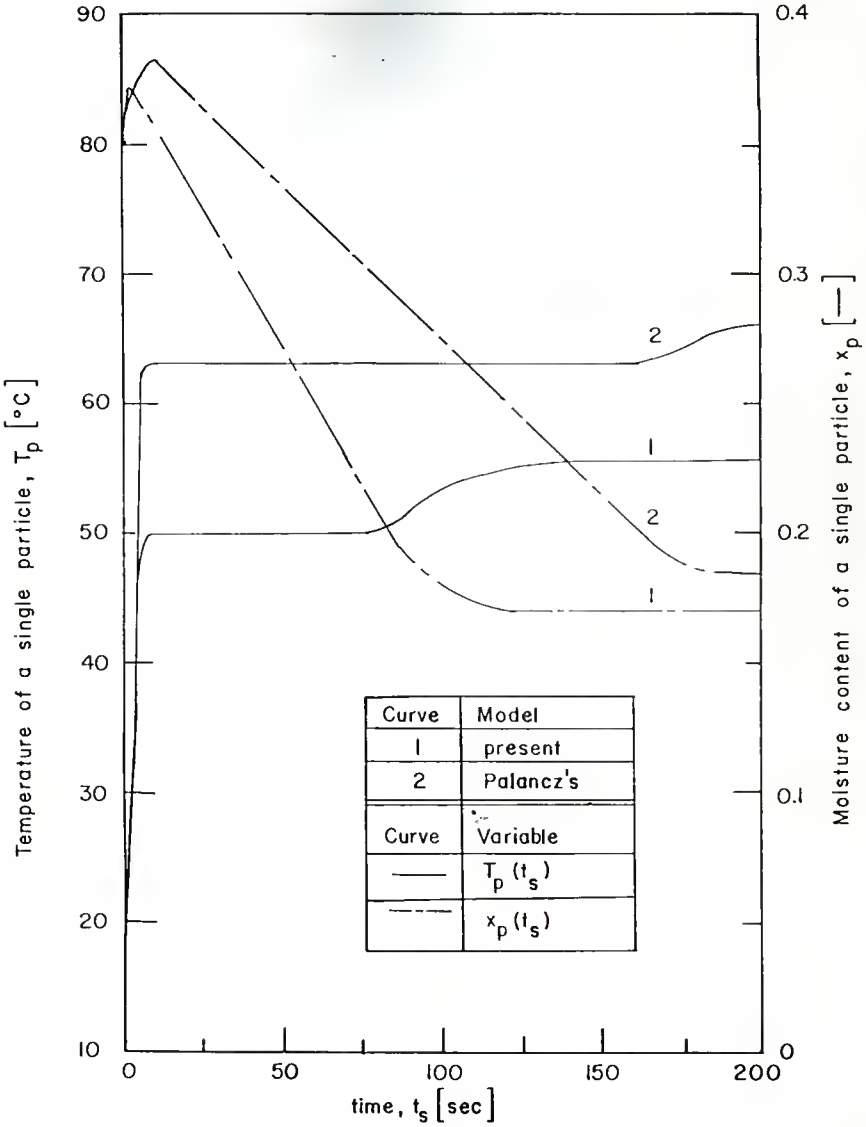

Fig.12. Comparison of the present model with Palancz's model: $T_0 = 250°C$, $T_w = 50°C$, $T_{po} = 20°C$, $U_0 = 1$ m/sec, $x_{p_0} = 0.35$, $x_0 = 0.015$, $\bar{t}_s = 300$ sec.

CHAPTER IV

CONCLUSIONS AND RECOMMENDATIONS

CONCLUSIONS AND RECOMMENDATIONS

An extensive and critical review of the fluidized-bed drying has been performed. It has given rise to a fairly rigorous mechanistic model for a continuoua fluidized-bed dryer. Based on the model, the numerical simulation has been conducted for the purpose of investigating the influence of the various operating parameters. The results indicate that the performance characteristics of the dryer are affected significantly by the superficial gas velocity, inlet temperature of the drying gas, mean residence time of the solids and dryer-wall temperature.

In drying, the moisture content of the drying gas is appreciably increased by evaporation of moisture from the solids. Consequently, a substancial amount of energy is transfered through this moisture migration. This factor is taken into account in the present model. In contrast, the exiating comparable model propoaed by Palancz assumes that the specific heat of the drying gas remains invariant. Results of simulation have proved that this assumption leads to an over-estimation of the temperature and moisture content of the solids.

It is unlikely that the moisture content of the drying gas on the surface of a particle can undergo a discontinuity as suggested by the existing model. The preaent model does not contain such a discontinuity, and thus is more rational in expressing the heat and mass transfer relationships between the drying gas and solids.

In the modeling, it has been assumed that cloud does not exist around the bubble. This is often true in the case wbere bubbles are small as they leave the distributor and move slowly to the top. When

the bubble has grown sufficiently large to have cloud, three-phase model should be employed to include the transport processes occuring in the cloud. It is worth pointing out that even though particles in both the emulsion and cloud-wake phases are commonly assumed to have residence time distribution of the completely mixed type, they should be treated differently because of their different moisture contents and mean residence times.

When small bubbles leave the distributor, they tend to grow rapidly by coalescence as they rise through the bed. Consequently, humidification of the bubble gas may occur primarily in the lower portions of the bed. It would be of interest to couple the bubble growth model (with changing bubble size) with the two-phase model employed in the present work.

Results of numerical simulation show that the fluidized-bed dryer is effective mainly in the constant-rate drying period. Thus, it appears advisable that a fluidized-bed dryer be used in series with a conventional moving-bed or packed-bed dryer; the latter serves to dry particles with bound moisture content.

MODELING AND SIMULATION OF A CONTINUOUS FLUIDIZED-BED DRYER

by

YIMING CHEN

B.E. ChE. Zhejiang University, Hangzhou, China. 1982

AN ABSTRACT OF A MASTER'S THESIS

submitted in partial fulfillment of the

requirements for the degree

MASTER OF SCIENCE

Department of Chemical Engineering

KANSAS STATE UNIVERSITY

Manhattan, Kansas

1986

An extensive and critical review of the fluidized-bed drying has been performed. It has given rise to a fairly rigorous mechanistic model for a continuous fluidized-bed dryer. The model depicts the interactions between gaseous and solid phases in detail. Performance of the dryer has been simulated numerically based on the model. The effects of the operating parameters on performance characteristics of the dryer have been investigated. These include the superficial gas velocity, inlet temperature and moisture content of the drying ing gas, mean residence time of the solids and dryer-wall temperature. Results of numerical simulation indicate that the performance characteristics of the dryer are affected significantly by the superficial gas velocity, inlet temperature of the drying gas, mean residence time of the solids and dryer-wall temperature. These results have also been compared with those based on an existing model. The comparison shows that the present model is a significant improvement over the the existing model.